Received by OSTI

OCT 0 9 1990

IS-T--1448

DE91 000743

Magnetic and Thermal Properties of High T*c* Superconductors

by

Lee, Wonchoon

PHD Thesis submitted to Iowa State University

Ames Laboratory, U.S. DOE

Iowa State University

Ames, Iowa 50011

Date Transmitted: September 21, 1990

PREPARED FOR THE U.S. DEPARTMENT OF ENERGY

UNDER CONTRACT NO. W-7405-Eng-82.

MASTER

DISTRIBUTION OF THIS DOCUMENT IS UNLIMITED

DISCLAIMER

This report was prepared as an account of work sponsored by an agency of the United States Government. Neither the United States Government nor any agency thereof, nor any of their employees, makes any warranty, express or implied, or assumes any legal liability or responsibility for the accuracy, completeness or usefulness of any information, apparatus, product, or process disclosed, or represents that its use would not infringe privately owned rights. Reference herein to any specific commercial product, process, or service by trade name, trademark, manufacturer, or otherwise, does not necessarily constitute or imply its endorsement, recommendation, or favoring by the United States Government or any agency thereof. The views and opinions of authors expressed herein do not necessarily state or reflect those of the United States Government or any agency thereof.

Magnetic and thermal properties
of high T_c superconductors

Wonchoon Lee

Under the Supervision of David C. Johnston
From the Department of Physics
Iowa State University

Measurements of the normal state magnetic susceptibility $\chi(T)$ of $YBa_2Cu_3O_7$, $Bi_{1.8}Pb_{0.2}Sr_2CaCu_2O_{8+\delta}$, and $Bi_{2-x}Pb_xSr_2Ca_2Cu_3O_{10+\delta}$ ($x = 0.2$ and 0.25) were carried out. All $\chi(T)$ data show negative curvature below $\sim 2T_c$. The data for $YBa_2Cu_3O_7$ are in excellent agreement with a new calculation of the superconducting fluctuation diamagnetism. From the analysis, we infer s-wave pairing and microscopic parameters are obtained. For $\chi(T)$ of $YBa_2Cu_3O_7$, part of the negative curvature is inferred to arise from the normal state background. We find a strong temperature dependent anisotropy $\Delta\chi \equiv \chi_c - \chi_{ab}$ and estimate the normal state spin contributions to $\chi(T)$. The heat capacity $C(T)$ of $YBa_2Cu_3O_7$ is reported for $0.4\ K < T < 400\ K$ in zero and 70 kG magnetic fields. In addition to the feature associated with the onset of the superconductivity at T_c, two anomalies in $C(T)$ were observed near 74 K and 330 K, with another possible anomaly

near 102 K; the temperatures at which they occur correlate with anomalies in $\chi(T)$ and ultrasonic measurements. The occurrence of the anomaly at $\approx$ 330 K is found to be sample-dependent. The influences of a magnetic field and the thermal and/or magnetic field treatment history dependence of a pellet sample on C(T), the entropy and the influence of superconducting fluctuations on C(T) near T_c, and the possible source of the observed intrinsic nonzero $\gamma(0)$ at low T are discussed.

Magnetic and thermal properties of high T_c superconductors

by

Wonchoon Lee

A Dissertation Submitted to the
Graduate Faculty in Partial Fulfillment of the
Requirements for the Degree of
DOCTOR OF PHILOSOPHY

Department: **Physics**
Major: **Solid State Physics**

Approved:

In Charge of Major Work

For the Major Department

For the Graduate College

Iowa State University
Ames, Iowa

1990

TABLE OF CONTENTS

	Page
I. INTRODUCTION	1
II. THEORETICAL REVIEW	12
A. Bulk Superconductor	12
B. Layered Superconductor	16
a. One layer case	16
b. Multi-layer case	18
III. EXPERIMENTAL DETAILS	23
A. Sample Preparations	23
a. $YBa_2Cu_3O_{7-\delta}$	23
b. $Bi_{2-x}Pb_xSr_2CaCu_2O_{8+\delta}$ and $Bi_{2-x}Pb_xSr_2Ca_2Cu_3O_{10+\delta}$	24
B. Grain Alignment of $YBa_2Cu_3O_{7-\delta}$	27
C. DC Resistivity Measurements	33
D. Magnetic Susceptibility Measurements	33
E. Heat Capacity Measurements	34
IV. RESULTS	37
A. DC Resistivity	37
B. Magnetic Susceptibility	37
a. Polycrystalline pellet $YBa_2Cu_3O_{7-\delta}$	37
b. Grain-aligned $YBa_2Cu_3O_{7-\delta}$	41
c. $Bi_{2-x}Pb_xSr_2CaCu_2O_{8+\delta}$ and $Bi_{2-x}Pb_xSr_2Ca_2Cu_3O_{10+\delta}$	53

C. Heat Capacity 62

V. ANALYSIS AND DISCUSSION 74

A. Superconducting Fluctuation Diamagnetism above T_c 74

a. $YBa_2Cu_3O_{7-\delta}$ 74

b. $Bi_{2-x}Pb_xSr_2CaCu_2O_{8+\delta}$, $Bi_{2-x}Pb_xSr_2Ca_2Cu_3O_{10+\delta}$, and $La_{1.8}Sr_{0.2}CuO_{4-\delta}$ 80

B. Superconducting and Normal State Magnetic Susceptibility Anisotropy 91

C. DC Resistivity 98

D. Heat Capacity 99

a. Near T_c 99

b. Between 0.4 K and 10 K 106

c. Above 120 K 113

VI. CONCLUSIONS 115

VII. REFERENCES 121

VIII. APPENDIX 132

IX. ACKNOWLEDGMENTS 138

I. INTRODUCTION

The discoveries of high T_c superconductors which show superconducting transition temperatures (T_c) below [Bednorz and Muller, 1986] and well above [Wu et al., 1987] liquid nitrogen temperature in layered copper oxides have prompted a lot of experimental and theoretical researches towards elucidating the microscopic mechanism for the unusual high transition temperatures. Some of the unusual properties of the new high T_c superconductors compared with the old conventional ones are: large T_c, large anisotropy in electronic transport [Crommie et al., 1988; Dinger et al., 1987; Hagen et al., 1988a and 1988b; Tozer et al., 1987] and thermodynamic properties [Bauhofer et al., 1989; Collins et al., 1989; Enomoto et al., 1987; Forro et al., 1988; Farrell et al., 1989; Gray et al., 1988; Nakao et al., 1989; Welp et al., 1989], short zero temperature Ginzburg-Landau coherence length [Inderhees et al., 1988; Kanoda et al., 1988a and 1988b; Lee et al., 1989], heat capacity behavior around T_c in magnetic fields [Lee et al., 1990d; Phillips et al., 1987; Salamon et al., 1988], linear term in low temperature heat capacity [Junod et al., 1989; Kato et al., 1988; Phillips et al., 1989 and 1990; Reeves et al., 1989; Stupp and Ginsberg, 1989], broad behavior in magnetoresistance below T_c [Iye et al., 1987; Palstra et al., 1988a and 1988b; Sun et al.,

1987], and normal state properties [Iye et al., 1988; Penny et al., 1988; Wang et al., 1987].

To explain the large T_c, a lot of new and modified microscopic models [Anderson, 1987; Anderson and Zou, 1988; Chen and Goddard, 1988; Kresin, 1987; Prelovsek et al., 1987; Schrieffer et al., 1988; Varma et al., 1987] instead of the conventional Bardeen-Cooper-Schrieffer (BCS) electron-phonon theory [Bardeen et al., 1957] were proposed. But still there is no consensus regarding the microscopic mechanism for the superconductivity. From the measurements of electronic transport and thermodynamic properties with single crystals, unusually large anisotropy above and below T_c was reported, which has important implications for the many applications. Also, due to the very short zero-temperature Ginzburg-Landau(LD) coherence length in the CuO_2 plane $\xi_{ab}(0)$ of ~ 20 Å [Inderhees et al., 1988; Kanoda et al., 1988a and 1988b; Lee et al., 1989], weak flux pinning was observed [Yeshurun and Malozemoff, 1988], which reduced the critical current. Such a short coherence length is expected to result in the flux melting also [Gammel et al., 1988; Yeshurun and Malozemoff, 1988]. Another effect associated with the short coherence length is that small volumes of size ~ $\xi^3(T)$ exhibit noticeable superconducting behavior even above T_c by the fluctuation effect [Dubson et al., 1987; Freitas et al., 1987; Friedmann et al., 1989; Goldenfeld et al., 1988; Hagen

et al., 1988b; Inderhees et al., 1988; Lee et al., 1989 and 1990a; Oh et al., 1988; Ong et al., 1988; Vidal et al., 1988].

First, let's consider some of the crystal structures of the new high T_c superconductors briefly which were studied in this work (see appendix). $La_{2-x}A_xCuO_4$ (A = Ba, Sr, Ca) has the K_2NiF_4 structure and there are two CuO_2 layers in the unit cell. The mobile holes due to the doping of A^{+2} ions for La^{+3} for $x > 0$ are essentially restricted to being on the oxygen sublattice within the CuO_2 planes [Nücker et al., 1988; Stassis et al., 1988]. The structure of the most widely studied compound $YBa_2Cu_3O_{7-\delta}$ is similar to the above one in some respects: both are layered structures, with some similarity to perovskite in a sense that Cu could be octahedrally coordinated in the formally filled structure of $YBa_2Cu_3O_9$. But due to oxygen vacancy ordering, it has two CuO_2 layers which are separated by a Y layer and there is also one CuO chain in the unit cell. The distance from a CuO layer to the nearest CuO layer is ~ 3.4 Å and to the next nearest one is ~ 8.4 Å [Le Page et al., 1987]. A great deal of work has been done on the roles of those layers and chains and it is known that CuO layers play the major role in superconductivity, while the chains behave as electron carrier reservoirs which are filled or empty depending on the oxygen deficiency δ [Maeno et al., 1987; Tarascon et al.,

1987 and 1988a; Tokura et al., 1988; Xiao et al., 1988]. Other structures of $Bi_2Sr_2Ca_{n-1}Cu_nO_{2n+4+\delta}$ (n = 1, 2, 3) are shown in Appendix. In these materials, there is no CuO chain at all and the number of CuO_2 layers are equal to n. For the case of n = 2 and 3, two CuO_2 layers are separated by a Ca layer and in $Bi_2Sr_2CaCu_2O_{8+\delta}$ (n = 2), the distances between the CuO_2 layers are ~ 3 Å and ~ 15 Å for nearest and next nearest CuO_2 layers, respectively [Tarascon et al., 1988b].

In superconductors, there are several fundamental microscopic parameters, which are the penetration depth λ, coherence length ξ, critical field H_c, order parameter $\psi(r)$, and superconducting energy gap 2Δ. From magnetic penetration depth measurements [Krusin-Elbaum et al., 1989; Mitra et al., 1989; Uemura et al., 1988], the nature of the pairing mechanism of the superconducting electrons and of the order parameter can be inferred from the temperature dependence of $\lambda(T)$ and low temperature behavior. Also, upper critical field [$H_{c2}(T)$] measurements [Bauhofer et al., 1989; Enomoto et al., 1987; Forro et al., 1988; Iye et al., 1987; Nakao et al., 1989; Palstra et al., 1988b; Welp et al., 1989] can provide information about the coherence length and superpair mass anisotropy. But due to broadness in the magnetoresistance [Iye et al., 1987; Palstra et al., 1988a and 1988b; Sun et al., 1987] in the high T_c superconductors near T_c, the determination of $H_{c2}(T)$ from these measurements

is ambiguous. On the other hand, the measured effects of superconducting fluctuation on the magnetic susceptibility and heat capacity can provide important information about the order parameter, coherence length and mass anisotropy directly. In addition, the dimensionality of the microscopic interactions between the carriers can be inferred directly from the temperature dependences of the fluctuation effects. Especially, for the layered structures such as high T_c superconductors, direct determinations of dimensionality and related microscopic parameters will be definitely useful and can be determined easily from $\chi(T)$ measurements with different magnetic field directions with respect to the crystal axis on high purity grain-aligned samples.

We know that the superconducting transition is a second order phase transition for which the order parameter is continuous cross the transition temperature [Tinkham, 1975]. In Ginzburg-Landau (GL) theory [Ginzburg and Landau, 1950], the free energy density (f) in the absence of a magnetic field and a gradient in the complex-order parameter, $\psi(\mathbf{r})$, can be expanded as

$$f_s = f_n + \alpha(T)|\psi(\mathbf{r})|^2 + \frac{\beta}{2}|\psi(\mathbf{r})|^4 , \qquad (1)$$

where f_s and f_n are the superconducting and normal state free energy density, respectively, and $\alpha(T)$ depends on whether the

superconducting ($\alpha < 0$) or normal ($\alpha > 0$) state. The superconducting transition temperature, T_c, is defined as the temperature at which the coefficient $\alpha(T)$ changes sign. Therefore below T_c, f_s has the minimum value for $\langle|\psi|\rangle \neq 0$, but above T_c it is minimum when $\langle|\psi|\rangle = 0$. However, due to the finite temperature, thermal fluctuations of ψ raise the total free energy density by an amount of order k_BT. In other words, even above T_c, the minimum can be obtained at $\langle|\psi|^2\rangle \neq 0$. This phenomenon is called superconducting fluctuation effect above T_c in superconductors, which leads to the existence of a dynamic fluctuation-induced superconducting state above T_c. Since the total energy density increase by thermal fluctuations is only $\sim k_BT$, the fluctuation effects are largest in amplitude if confined to a small correlation volume. The old conventional superconductors have zero-temperature GL coherence lengths, $\xi(0)$ (which characterizes the size of a Cooper pair) of order 10^3 Å. But in new high T_c superconductors, $\xi(0) \sim 20$ Å [Inderhees et al., 1988; Kanoda et al., 1988a and 1988b; Lee et al., 1989], which allows much larger fluctuation effects than in the old superconductors.

So far, there have been several reports for superconducting fluctuation effects in high T_c copper oxide superconductors from low-frequency [Dubson et al., 1987; Freitas et al., 1987; Friedmann et al., 1989; Goldenfeld et

al., 1988; Hagen et al., 1988b; n et al., 1988; Ong et al., 1988; Vidal et al., 1988] and microwave [Porch et al., 1988] conductivity data above $T_c \approx 91$ K as well as heat capacity [Fisher et al., 1988a; Gordon et al., 1989; Inderhees et al., 1988; Laegreid et al., 1989] data near T_c for $YBa_2Cu_3O_7$; these indicate that superconducting fluctuations are strong at temperatures in the vicinity of T_c and above, and that the superconductivity is three-dimensional. In these measurements, a strong temperature dependent background is present and must be subtracted, subject to strong assumptions about the background, in order to extract the fluctuation contributions, leading to ambiguities in the derived microscopic parameters. On the other hand, these fluctuations are also observable as a diamagnetic contribution to the magnetic susceptibility $\chi(T)$ above T_c [Freitas et al., 1987; Johnston et al., 1988; Kanoda et al., 1988a and 1988b; Lee et al., 1989], which is otherwise nearly independent of temperature [Johnston et al., 1988; Kanoda et al., 1988a and 1988b] (see below).

The bismuth-based high T_c superconductors such as $Bi_2Sr_2CaCu_2O_{8+\delta}$ (Bi2212) and $Bi_2Sr_2Ca_2Cu_3O_{10+\delta}$ (Bi2223) are similar to $YBa_2Cu_3O_7$ (Y123) in that each has conducting CuO_2 layers and shows strong anisotropy in the structure [Koyama et al., 1988; Matsui et al., 1988; Tarascon et al., 1988b] and in the electronic transport and thermodynamic properties

[Farrell et al., 1989; Martin et al., 1989; Naughton et al., 1988]. Therefore, one might expect superconducting fluctuation effects in the bismuth-based high T_c superconductors similar in magnitude to those observed in $YBa_2Cu_3O_7$. However, as yet no well-defined sharp heat capacity feature near T_c has been observed in the bismuth-based superconductors, presumably due to chemical inhomogeneities in the samples; this precludes analysis of the influence of superconducting fluctuations on C(T) near T_c. Further, to our knowledge there is no convincing evidence for fluctuation effects in other measurements on these Bi-based materials.

Besides the fluctuation effects, there have been many studies of the normal state anisotropy [Crommie et al., 1988; Dinger et al., 1987; Hagen et al., 1988a; Tozer et al., 1987] and heat capacity behavior [Butera, 1988; Fisher et al., 1988a and 1988b; Fossheim et al., 1988; Inderhees et al., 1988; Ishikawa et al., 1988; Junod et al., 1988 and 1989; Kato et al., 1988; Phillips et al., 1987; Reeves et al., 1989; Salamon et al., 1988; Stupp and Ginsberg, 1989]. But resistivity measurements of single crystals have not led to an unambiguous identification of the nature of the quasiparticles excitations in the metallic state of the high T_c cuprates, because these anisotropies should depend in detail on the nature of these excitations. And still there

exist some controversies about (i) anomalies around T_c (~ 91 K) and ~ 220 K - 240 K in the heat capacity C(T) of $YBa_2Cu_3O_7$ which may arise from possible phase transitions [Butera, 1988; Fossheim et al., 1988; Ishikawa et al., 1988; Junod et al., 1988], (ii) the presence of a linear term in C(T) at low temperature [Phillips et al., 1989 and 1990; Reeves et al., 1989], and (iii) the magnitude of the superconducting fluctuation effect on C(T) around T_c. Also, from sound attenuation measurements, two possible phase transitions around 65 K and around 130 K are reported [Bhattacharya et al., 1988].

In this work, we report $\chi(T)$ data for $YBa_2Cu_3O_7$, $Bi_{2-x}Pb_xSr_2CaCu_2O_{8+\delta}$ ($0.0 \leq x \leq 0.5$), and $Bi_{2-x}Pb_xSr_2Ca_2Cu_3O_{10+\delta}$ ($x = 0.2$ and 0.25) which we believe closely approximate the intrinsic $\chi(T)$. The data increase monotonically with temperature up to at least 400 K and exhibit negative curvature below ~ 200 K. For $YBa_2Cu_3O_7$, we present the results of a new calculation of the angular dependence of the superconducting fluctuation diamagnetism (SFD) and compare the predictions with our $\chi(T)$ data for highly oriented powder with $H \parallel c$ and $H \perp c$. This comparison shows that the data are consistent with s-wave superconducting pairing and that strong SFD exists up to at least 126 K; theoretical fits to the observed SFD provide quantitative estimates of the zero-temperature coherence

lengths and the effective mass anisotropy. We infer that the background $\chi(T)$ exhibits negative curvature above T_c. For the Bi2212 and Bi2223 samples, the Curie-Weiss-type contribution to $\chi(T)$ from impurity phases was found to be absent for the Bi2223 samples and Bi2212 samples with x = 0.1, 0.2 and 0.3. For these samples, above a few K above T_c, the $\chi(T)$ data show two-dimensional fluctuation behaviors. From fits of the static Lawrence-Doniach two-dimensional prediction, as modified by Klemm [1990], for the fluctuation susceptibility to the data, the in-plane GL coherence lengths $\xi_{ab}(0)$ of Bi2212 and Bi2223 are obtained and compared with values derived from published upper critical field measurements.

From the magnetic susceptibility measurements, we find strong anisotropy in $\chi(T)$ for the superconducting as well as normal states of high purity $YBa_2Cu_3O_7$. The origin of anisotropy in $\chi(T)$ will be discussed and we compare our results with previous measurements on single crystals and powders.

Also we carried out extensive high resolution measurements of C(T) for the same high purity batch of $YBa_2Cu_3O_7$. Our primary goals were to (i) determine whether the nonzero Sommerfeld coefficients $\gamma(T = 0) \gtrsim 4$ mJ/mole-K^2 observed in previous low T C(T) studies [Stupp and Ginsberg, 1989] are comparable to or greater than that for our batch

and determine whether our observed $\gamma(T = 0)$ is intrinsic [Stupp and Ginsberg, 1989] or extrinsic [Phillips et al., 1989 and 1990], (ii) document the influence of superconducting fluctuations on C(T) near T_c [Gordon et al., 1989; Fisher et al., 1988a; Inderhees et al., 1988; Laegreid et al., 1989] and (iii) ascertain whether the anomalies sometimes observed in $\chi(T)$ measurements near 240 K [Johnston et al., 1988; Miljak et al., 1988 and 1989] and/or 320 K [Johnston et al., 1988], and in other types of measurements at various temperatures, are also manifested in C(T).

II. THEORETICAL REVIEW

A. Bulk Superconductor

The calculation of the fluctuation-induced diamagnetism within the framework of the Ginzburg-Landau (GL) theory was derived straightforwardly by Schmid [Schmid, 1969]. Considering a superconductor as a collection of independent fluctuating droplets of superconductivity, the linearized GL free energy functional was written as

$$F_{GL}[\psi(\mathbf{r})] = \int d^3\mathbf{r}\left[\frac{1}{2m^*}\left|\left(\frac{\hbar}{i}\nabla + \frac{2e}{c}\mathbf{A}\right)\psi(\mathbf{r})\right|^2 + |\alpha||\psi(\mathbf{r})|^2\right] \quad (2)$$

where $\psi(\mathbf{r})$ is the order parameter, m^* is the pair mass, α is a temperature-dependent coefficient and $\mathbf{A}$ is the vector potential. Here, the $|\psi|^4$ term in the GL free energy was neglected since only temperature outside of the critical region were considered, where the contribution of the quadratic term is very small. The coefficient α is related to the GL coherence length $\xi(T)$ by $\alpha = \hbar/m^*\xi^2(T)$, where $\xi(T) = \xi(0)[T_c/(T-T_c)]^{1/2}$. Expanding the order parameter $\psi(\mathbf{r})$ in terms of the normalized eigenfunctions of a particle in a

uniform magnetic field [Ziman, 1972], the free energy functional can be written as

$$F_{GL} = \sum_{q,k,n} |C(q,k,n)|^2 \left[E(k, n + \frac{1}{2}) + |\alpha|\right] \tag{3}$$

where C(q,k,n) are expansion coefficients of $\psi(r)$, **k** is a wave vector, n is an integer and E(k,n+1/2) is given by

$$E(k, n + \frac{1}{2}) = \frac{\hbar^2 k^2}{2m^*} + (n + \frac{1}{2}) \frac{2e\hbar H}{m^* c} \tag{4}$$

where H is magnetic field. This is similar to the Landau levels of a free particle with mass m^* and charge 2e in a uniform magnetic field. The contribution to the free energy can be obtained from the partition function Z which is generated by summing $\exp[-F_{GL}(\psi)/k_B T]$ over all possible $\psi(r)$. Using the thermodynamic relations $F = - k_B T \ln Z$ and magnetic susceptibility $\chi = - \partial^2 F/\partial H^2$, and the Poisson sum rule, Schmid showed that the free energy and diamagnetic susceptibility induced by superconducting fluctuations can be written as

$$F = F_o + \frac{1}{2} V \left[\frac{1}{6\pi}\right] \left[\frac{e}{\hbar c}\right]^2 k_B T H^2 \xi(T) \tag{5}$$

and

$$\chi\ (T) = -\frac{\pi k_B \xi(0)}{6}\ \frac{T}{\phi_o^2}\left[\frac{T_c}{T - T_c}\right]^{1/2} \tag{6}$$

where F_o is the normal state free energy, V is the volume and the GL coherence length $\xi(T)$ is given by $\xi(T) = \xi(0)[T_c/(T-T_c)]^{1/2}$ with zero temperature GL coherence length $\xi(0)$. Therefore, for a bulk superconductor, the fluctuation induced diamagnetism is proportional to the temperature dependent factor $T[T_c/(T-T_c)]^{1/2}$ and the corresponding magnetization is linear in H. Experiment [Gollub et al., 1969] showed that at low magnetic field, the above temperature dependence was correct qualitatively, but the magnetization did not follow the expected linear dependence on H at high magnetic fields. This disagreement at high fields was found due to the approximation that only terms up to order H^2 are present in equation (3). In other words, due to this approximation, the Schmid result holds only at low magnetic fields.

The more detailed calculation in arbitrary magnetic fields was obtained by Prange without any approximation, but still based on GL theory [Prange, 1970]. He found that the magnetization induced by the fluctuations can be written as

$$M = -\sqrt{H}\ T\ g(x) \tag{7}$$

with

$$x = \left[\frac{dH_{c2}}{dT}\right]_{T_c} \frac{T - T_c}{H} \tag{8}$$

where g(x) is a universal function independent of the material (see Prange, 1970) and H_{c2} is the upper critical magnetic field. This result explained the experimental results well around T_c and in low magnetic fields. But comparing this expression with several experiments, the theoretical universal curve g(x) fell well above the experimental data systematically, especially for high magnetic fields. The reason was due to the fact that the GL theory is rigorous only close to T_c.

To improve the agreement in high magnetic fields, a microscopic theory was proposed [Kurkijärvi et al., 1972; Lee and Payne, 1971], based on phenomenological theory [Patten et al., 1969] and on the microscopic Gorkov theory in the clean limit, where GL coherence length is much smaller than the mean free path. Considering that the GL theory is valid only for slow variations in space of $\psi(r)$, they corrected the Prange calculation by cutting off the short-wavelength fluctuations. With that correction, the fluctuation induced magnetization in the Prange result was modified to

$$M = -\sqrt{H}\ T\ g(x,\ H/H_s) \tag{9}$$

where $g(x,H/H_s)$ is a universal function (see Lee and Payne, 1971) and H_s is a certain scaling magnetic field depending on the material. This result gave good agreement with experimental results, especially for the clean limit where nonlocal electrodynamic effects play an important role. But in the case of the dirty limit, where the GL coherence length is much larger than the mean free path such as for the In-16%Tl superconductor, strong large dynamic effects are expected and there was disagreement between the above equation (9) and experimental results due to locality. Maki and Takayama improved the above calculation by including dynamic corrections for the dirty limit [Maki and Takayama, 1971] and found that such corrections gave good agreement with experimental results for dirty limit superconductors.

B. Layered Superconductor

a. One layer case

In 1971, Lawrence and Doniach [Lawrence and Doniach, 1971] developed a model for superconducting fluctuation effects for the case of a one layer structure in the layer repeat distance s, based on the static Ginzburg-Landau theory. In their model, only the magnetic field perpendicular to the layer was considered and the

superconducting order parameter in adjacent layers is coupled by Josephson tunneling. Therefore, the single particle state consisted of two parts, a free electron form for motion parallel to the layer and a tight binding one for motion perpendicular to the layer. Then the energy of single particle is given by

$$E(k) = \frac{\hbar^2}{2m} k_{||}^2 + \zeta [1 - \cos(sk_{\perp})] \tag{10}$$

where m is the in-layer effective mass, $k_{||}$ and $k_{\perp}$ are the components of the wave vector parallel and perpendicular to the layer, respectively, s is the distance between layers, ζ is the Josephson tunneling parameter given by $\zeta = \hbar^2/Ms^2$ and M is the out-of-layer effective mass. Then the fluctuation-induced diamagnetism for H perpendicular to the layer is given by

$$\chi_c(T) = -\frac{\pi k_B T \xi_{ab}^2(T)}{3\phi_o^2 s} \left[1 + \frac{4m\xi_{ab}^2(T)}{Ms^2} \right]^{-1/2} \tag{11}$$

where $\xi_{ab}(T)$ is the in-layer coherence length, ϕ_o is the flux quantum and the coherence length $\xi_c(T)$ perpendicular to the layer is given by $[m/M]^{1/2}\xi_{ab}(T)$. $\xi_{ab}(T)$ can be expressed as $\xi_{ab}(0)[T_c/(T-T_c)]^{1/2}$, where $\xi_{ab}(0)$ is the zero temperature Ginzburg-Landau coherence length. If $\xi_c(T) >> s/2$, then the

temperature dependence of $\chi_c(T)$ is given by $T[T_c/(T-T_c)]^{1/2}$ which is 3 dimensional behavior, while $T[T_c/(T-T_c)]$ if $\xi_c(T) << s/2$, which is 2 dimensional behavior. The dimensional crossover temperature T_o is given by $T_c[1 + 4m\xi_{ab}^2(0)/ms^2]$. For the case of a magnetic field parallel to the layer in the scheme of the Lawrence-Doniach model, the superconducting fluctuation-induced diamagnetism can be written as [Klemm, 1990]

$$\chi_{ab}(T) = -\frac{\pi k_B}{6\phi_o^2}\left[\frac{m}{M}\right]^{1/2}\xi_{ab}(0)\,T\left[\frac{T_c}{T - T_c}\right]^{1/2} . \qquad (12)$$

In this case, no dimensional crossover occurs. Most known high T_c superconductors except $Ba_{0.6}K_{0.4}BiO_3$ and $La_{1.85}Sr_{0.15}CuO_4$ contain more than one conducting layer in a layer repeat distance s, which means that the Lawrence-Doniach model should be modified to include several layers in a repeat distance s.

b. Multi-layer case

Recently [Klemm, 1990; Lee et al., 1989], considering the broadening of Landau levels arising from the finite temperature and from the pair phase-coherence lifetime, the importance of including dynamic effects as well as several layers in a repeat distance s is addressed. The Lawrence-

Doniach (LD) model was generalized to a magnetic field H at an arbitrary angle θ with respect to the c-axis of the unit cell, where the influence of local clean limit dynamics has also been accounted for. In that model, there are N conducting CuO_2 layers per repeat distance s, with N-1 equal interlayer spacings d and one different spacing d′ (N = 2 for $YBa_2Cu_3O_7$), and one complex s-wave order parameter per layer; the repeat distance $s = d' + (N - 1)d$. The layers are coupled by Josephson-like tunneling, with parameters ζ_1 and ζ_2, respectively. Since the critical region is less than 1 K [Dubson et al., 1987; Freitas et al., 1987; Friedmann et al., 1989; Goldenfeld et al., 1988; Inderhees et al., 1988; Oh et al., 1988; Porch et al., 1988; Vidal et al., 1988], here we considered only Gaussian fluctuations. The Gaussian fluctuation free energy is diagonalized, yielding N order parameter bands (in terms of their c-axis dispersions), with N distinct T_c values. Just above the highest T_c, the fluctuations are dominated by the three dimensional (3D) regime of a single cellular order parameter. In the 2D regime further above T_c, more of the order parameters contribute to the fluctuations, with their relative contributions depending upon the ζ_1 and ζ_2 values. The weak field regime is defined by $\omega_c\tau_\phi << 1$ and $H < H_o \equiv \phi_o/sv_F\tau_\phi$ [Klemm, 1990], where ϕ_o, ω_c, τ_ϕ and v_F are respectively flux quantum, the pair cyclotron resonance frequency, phase

coherence lifetime and intralayer Fermi velocity. In the limit $H \to 0$, the angular dependence of the SFD above T_c is $\chi(\theta,T) = \chi_c(T)\cos^2\theta + \chi_{ab}(T)\sin^2\theta$, where by the standard techniques [Klemm, 1974; Klemm et al., 1973; Schmid, 1969] for N = 2

$$\chi_c(T) = \frac{-16\xi_{ab}^2(0)}{3\pi^2 s\phi_0^2} \sum_{n=0,1} k_B T_{cn} \int_0^\infty \frac{\omega\, d\omega}{e^\omega - 1} \int_0^\pi \frac{dq}{\omega^2 + [B_n(T) + C_n(T)\bar{\lambda}_n(q)]^2} \tag{13}$$

and

$$\chi_{ab}(T) = \frac{-2m\xi_{ab}^2(0)}{3M\xi_c(0)\phi_0^2\sqrt{\pi}} \sum_{n=0,1} k_B (TT_{cn})^{1/2} \int_0^\infty \frac{d\omega\{[\omega^2 + B_n^2(T)]^{1/2} - B_n(T)\}^{1/2}}{(e^\omega - 1)[\omega^2 + B_n^2(T)]^{1/2}} \tag{14}$$

where

$$B_n(T) = \frac{8T_{cn}}{\pi T} \ln(T/T_{cn}), \tag{15}$$

$$C_n(T) = \frac{16 T_{cn} M \xi_c^2(0)}{\pi T \hbar^2}, \tag{16}$$

and

$$\bar{\lambda}_n(q) = \zeta_1 + \zeta_2 \pm [\zeta_1^2 + \zeta_2^2 + 2\zeta_1\zeta_2\cos(q)]^{1/2} \tag{17}$$

are the order parameter band energies in terms of $q = k_z s$ and the Josephson tunneling parameters ζ_1 and ζ_2, where n = 0 (1) corresponds to − (+) for the two order parameter bands, and where the transition temperature T_{c1} for the upper band is given by

$$(T_{c1}/T_{c0})\ln(T_{c0}/T_{c1}) = 4m\xi_{ab}^2(0)\hbar^{-2}\max\{\zeta_1,\zeta_2\}. \qquad (18)$$

The Ginzburg-Landau coherence lengths $\xi_{ab}(T) = \xi_{ab}(0)[\ln(T/T_{c0})]^{-1/2}$ and $\xi_c = \xi_{ab}\sqrt{\varepsilon}$, where $\varepsilon = m/M$ is the ratio of pair effective masses parallel and perpendicular to the a-b plane, and ϕ_o is the flux quantum hc/2e. M is given by $\hbar^2(1/\zeta_1 + 1/\zeta_2)/s^2$ in terms of the microscopic tunneling parameters. They defined $\gamma \equiv \zeta_1\zeta_2/(\zeta_1 + \zeta_2)^2$, so that $0 \leqslant \gamma \leqslant 1/4$. The above equations are exact in the low-field regime within the framework of the time-dependent Ginzburg-Landau theory, which is accurate in the entire Gaussian fluctuation regime, neglecting scattering effects. The above model is consistent with the Klemm, Luther and Beasley (KLB) [Klemm et al., 1975] form for N = 1, which is an extension of the LD model to an arbitrary local magnetic field **H** direction. Also note that for $\zeta_1 = \zeta_2 = \zeta$, s = 2d and neglecting dynamic effects, the above model reduces to the LD model. For either $\zeta_1 << \zeta_2$ or $\zeta_2 << \zeta_1$, it is again of the LD form with $\zeta = \zeta_1\zeta_2/(\zeta_1 + \zeta_2)$ in equation (10). It should be noticed that with dynamic effects included in the calculation, there is no

distinct dimensional crossover between 2 dimensional and 3 dimensional temperature dependences, in contrast to predictions [Klemm, 1974; Klemm et al., 1973; Lawrence and Doniach, 1971; Schmid, 1969] when these effects are neglected. Indeed, the dynamic effects can yield a temperature dependence similar to that previously expected [Klemm, 1974; Klemm et al., 1973; Lawrence and Doniach, 1971; Schmid, 1969] for dimensional crossover even when dimensional crossover does not occur ($\mathbf{H} \perp \mathbf{c}$) [Klemm, 1990].

III. EXPERIMENTAL DETAILS

A. Sample Preparations

a. $YBa_2Cu_3O_{7-\delta}$

A 15 g master batch of polycrystalline $YBa_2Cu_3O_{7-\delta}$ was prepared from pre-dried Ames Lab Y_2O_3, 99.999% CuO and 99.9% $BaCO_3$. The stoichiometric mixture of starting materials was ground thoroughly in air using an agate mortar and pestle and fired at 940 °C for 1 day in air in an alumina crucible. Twelve g was then pressed into a 1/2 in. dia. pellet and the remaining 3 g was maintained separately as powder. Both pellet and powder were fired at 940 °C for 90 days in air with ten intermediate grindings, followed by heating in O_2 at 640 °C for one day and oven-cooling to room temperature. The final pellet sample had a density of 75% of the theoretical value. From powder x-ray diffraction analysis, the batch of $YBa_2Cu_3O_{7-\delta}$ was single phase with lattice parameters a = 3.712(2) Å, b = 3.895(4) Å and c = 11.685(4) Å, with c/a = 3.061 and $(b - a)/(b + a) = 9.98 \times 10^{-3}$. These values indicate an oxygen deficiency $\delta \sim 0$ [Johnston et al., 1987]. The powder sample was examined with an optical microscope and the grains appeared to be well-formed single crystals with a roughly cubic shape with dimensions ~ 25 $(\mu m)^3$.

The results of a differential thermal analysis (DTA) measurement on the powder sample in oxygen gas using a

Perkin-Elmer 1700 DTA with a System 7/4 controller are shown in Fig. 1a. The small endothermic peak with an onset near 925 °C is the melting transition of the Ba- and Cu-rich Y-Ba-Cu-O eutectic composition impurity [McCallum, 1989]. In order to ascertain the amount of eutectic impurity present in the $YBa_2Cu_3O_7$ powder, a small powder sample consisting of 90 wt.% powder $YBa_2Cu_3O_7$ was mixed with 5 wt.% $BaCuO_2$ and 5 wt.% CuO and the mixture heated to 960 °C in a tube furnace under O_2 gas to form a eutectic mixture plus $YBa_2Cu_3O_7$ majority phase. A DTA scan as in Fig. 1a was then performed, and the results are shown in Fig. 1b. The ratio of the enthalpy under the peak in Fig. 1a to that in Fig. 1b indicates that (0.6 ± 0.2) wt.% of our $YBa_2Cu_3O_7$ powder sample consists of the eutectic impurity mixture.

b. $Bi_{2-x}Pb_xSr_2CaCu_2O_{8+\delta}$ and $Bi_{2-x}Pb_xSr_2Ca_2Cu_3O_{10+\delta}$

Polycrystalline samples of $Bi_{2-x}Pb_xSr_2CaCu_2O_{8+\delta}$ (Bi2212), $0.0 \leqslant x \leqslant 0.5$, and $Bi_{1.8}Pb_{0.2}Sr_2Ca_2Cu_3O_{10+\delta}$ (Bi2223) were prepared by the solid state method from stoichiometric mixtures of 99.99% Bi_2O_3, 99.9% PbO, 99.99% $SrCO_3$, 99.99% $CaCO_3$ and 99.999% CuO. After firing the free powders for one day at 840 °C in air, the samples were pelletized and fired at 840 °C for 3 weeks with five intermediate grindings and then air-quenched. The sample of Bi2223 with x = 0.25 was prepared similarly, but the firing

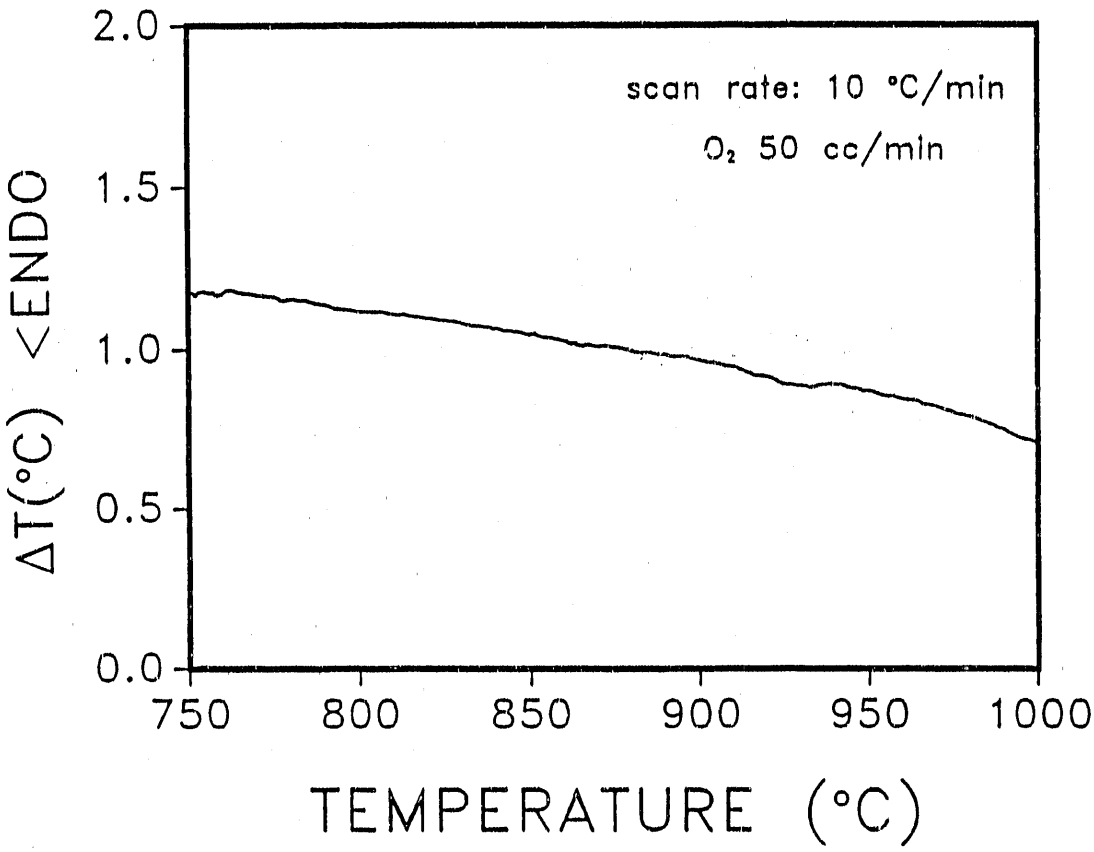

Fig. 1a. Differential thermal analysis scans in O_2 gas for $YBa_2Cu_3O_7$ powder sample

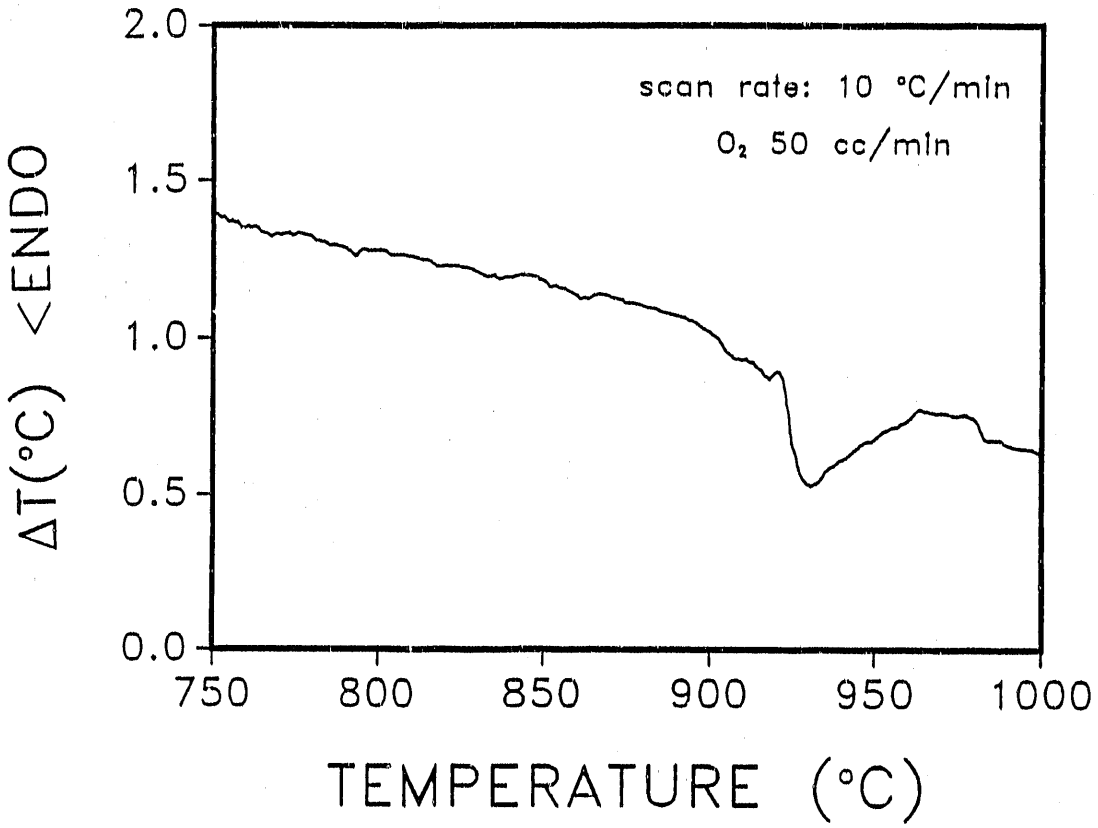

Fig. 1b. Differential thermal analysis scans in O_2 gas for a mixture of 90 wt.% of the $YBa_2Cu_3O_7$ powder sample with 5 wt.% CuO and 5 wt.% $BaCuO_2$

temperature was 850 °C instead of 840 °C. No additional oxygen annealing was done. From powder x-ray analysis, all samples were almost single phase, with lattice parameters in agreement with literature values. The results of DTA measurements on the powder samples in oxygen gas revealed single phase and one of them, the result of Bi2212 (x=0.0), is shown in Fig. 2.

B. Grain Alignment of $YBa_2Cu_3O_{7-\delta}$

As first pointed out by Farrell et al. [Farrell et al., 1987], grain alignment of $YBa_2Cu_3O_7$ powder can be achieved near room temperature by placing a free-flowing powder freshly mixed with epoxy in a strong magnetic field **H**; very good alignment with **c** || **H** is retained once the epoxy has cured. We first utilized this method with H = 80 kG at 300 K using Epotek 301 epoxy. Shown in Fig. 3 are $\chi(T)$ data for the epoxy alone (H = 10 kG), for the grain-aligned powder alone (**c** || **H**, H = 3 kG, see below), and for 27 mg of the aligned powder in 9 mg of epoxy (**c** || **H**, H = 3 kG). The Curie-Weiss contribution [$\chi = C/(T - \Theta)$] evident in the latter data, but not in the former two measurements, indicates that a chemical reaction between the epoxy and the sample occurred which generated paramagnetic species. Indeed, the negative curvature in $\chi(T)$ intrinsic to $YBa_2Cu_3O_7$

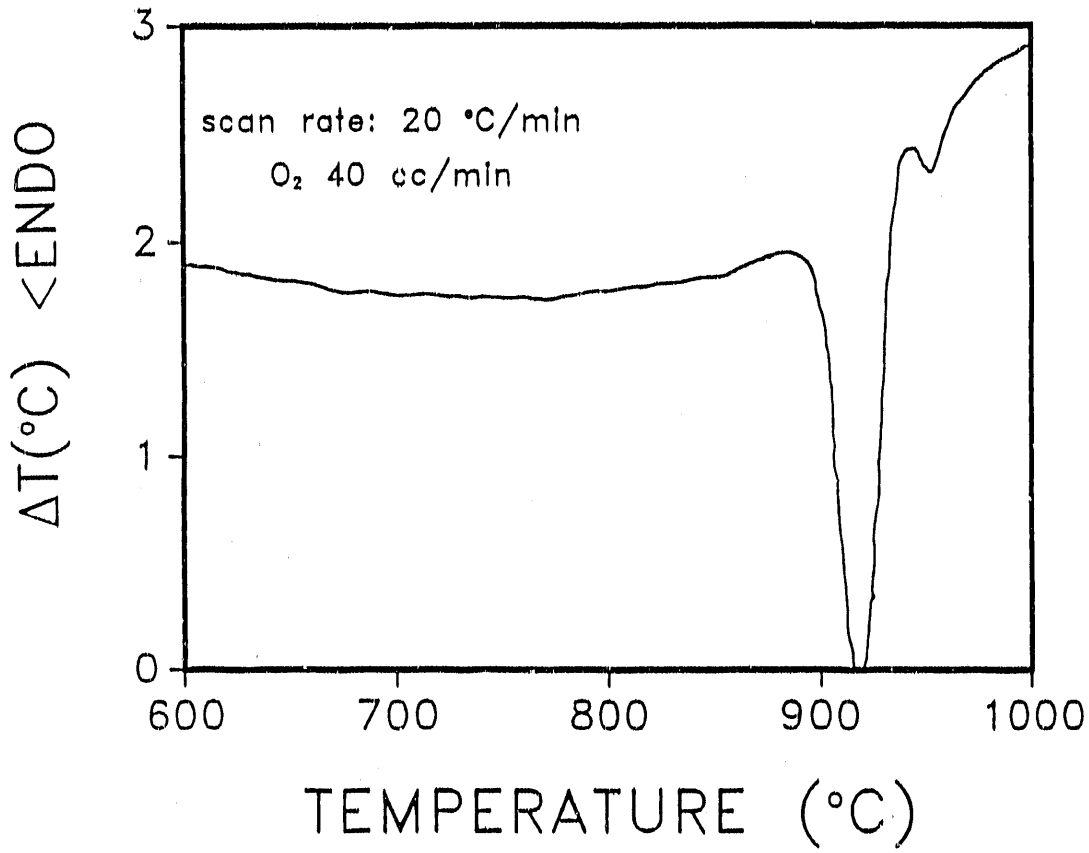

Fig. 2. Differential thermal analysis scans in O_2 gas for $Bi_2Sr_2CaCu_2O_{6+\delta}$ powder sample

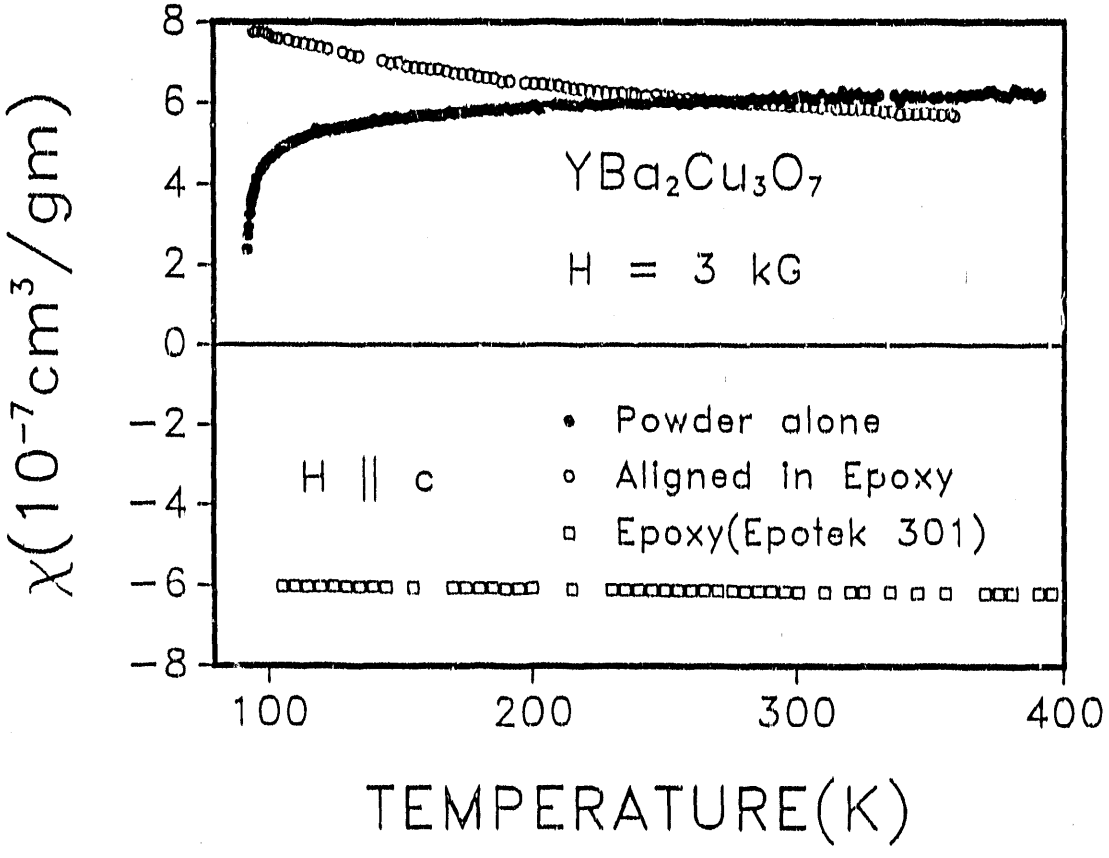

Fig. 3. Magnetic susceptibility χ vs. temperature for grain-aligned $YBa_2Cu_3O_7$ powder (H || c), for Epotek 301 epoxy, and for powder aligned in epoxy with H || c

below ~ 200 K is completely masked by the paramagnetic impurity/defect contribution. We further observed for this aligned sample in epoxy that the screening susceptibility below T_c for H = 50 G was degraded. The deterioration of the superconductivity might be explained, e.g., by an influence of the epoxy on the coupling between grains, but the epoxy-induced Curie tail must originate from a chemical reaction between the sample and epoxy.

We therefore sought a better method of grain alignment. It is known that $\chi(T)$ for **H** || c (χ_c) is larger than that for **H** $\perp$ c near room temperature [Farrell et al., 1987; Fukuda et al., 1988], whereas $\chi_c < \chi_{ab}$ if $T < T_c$ [Solin et al., 1988; Tranquada et al., 1988]. The free energy is minimized for c || **H** above T_c and for c $\perp$ **H** below T_c, and grain alignment will be in these directions in the respective alignment temperature range if the grains are free to rotate. We therefore utilized an in-situ method of grain-alignment of our $YBa_2Cu_3O_7$ powder in the SQUID magnetometer. The free-flowing powder was placed in a quartz tube sample holder rigidly attached to the vertical sample rod. The rod was vibrated with a small 60 Hz buzzer attached to the top of the rod, outside the sample chamber of the magnetometer. The grain alignment was achieved in a field of 50 kG with c || **H** by holding the sample temperature at 300 K (> T_c), or with c $\perp$ **H** at 10 K (< T_c), and vibrating the sample rod overnight.

The amplitude of vibration was then slowly (over minutes) reduced to zero and then the field reduced to zero and essentially complete alignment was achieved. The subsequent magnetization measurements reported below were carried out in fields $H \leq 5$ kG, fields low enough that grain realignment did not occur from 4 K to 400 K for either field alignment direction. The obvious advantages of this alignment method over the above epoxy method are that magnetic impurities are not introduced into the sample upon grain alignment, and that the accuracy of the measured $\chi(T)$ anisotropy is not compromised by removing/handling the sample between measurements of the two field orientations.

We note that excessive grinding of our sample in air using an agate mortar and pestle apparently resulted in the generation of magnetic defects. This is illustrated in Fig. 4, which shows $\chi(T)$ data for powders grain-aligned in situ with $c \parallel H$ before and after heavily grinding the powder. The grain size of the heavily ground sample was measured, as above, to be $\lesssim 1$ μm, much smaller than the above value of 25 μm measured prior to grinding. Although $\chi(T)$ for the heavily ground sample still shows negative curvature above T_c, the slope $d\chi/dT$ becomes negative above about 200 K; this indicates the presence of a Curie-Weiss contribution, presumably originating from magnetic defects generated during grinding.

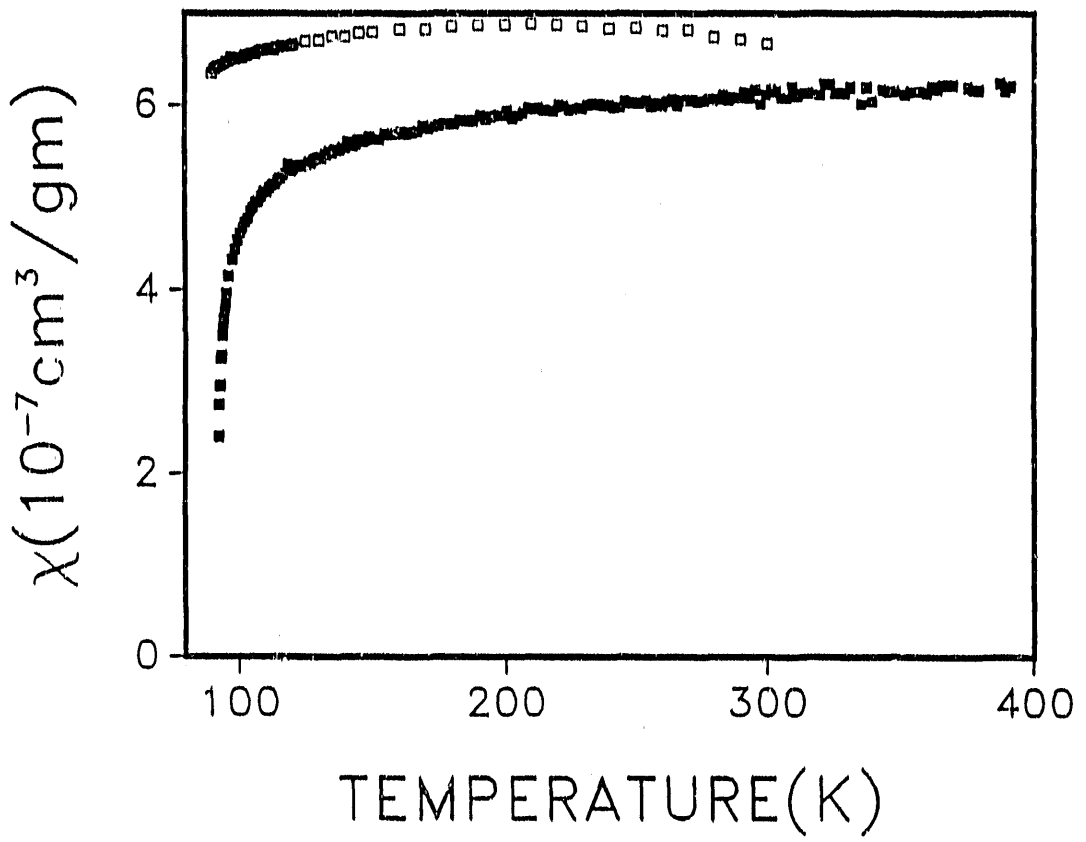

Fig. 4. Magnetic susceptibility χ vs. temperature for grain-aligned $YBa_2Cu_3O_7$ with H || c, before (filled squares) and after (open squares) heavily grinding the powder in air

C. DC Resistivity Measurements

The standard four-probe method was used for a bar-shaped $YBa_2Cu_3O_7$ sample from 300 K down to 77 K. The sample dimensions were 1.0 x 1.0 x 3.8 mm^3. Four parallel fine Platinum wires were attached to the sample with silver paint; the contacts were found to be ohmic. A direct current of 1 mA was used. To eliminate emf's, the voltage was averaged for + and - current directions. The temperature was monitored using a Pt thermometer.

D. Magnetic Susceptibility Measurements

Magnetization data, M(T), were obtained using a commercial Quantum Design superconducting quantum interference device (SQUID) magnetometer for the temperature range from 4 K to 400 K with magnetic fields from 50 G to 50 kG. A commercial dental floss string was used to hold sample at the end of the sample probe for the pellet samples. For a powder sample, a high purity quartz tube with a node in the middle was used instead of string and the final data were corrected for the contribution of the quartz as obtained in a separate experiment. In measuring superconducting properties, such as the Meissner effect, screening

magnetization and transition temperature (T_c), a low magnetic field of 50 G was used.

From a magnetization M versus magnetic field H, M(H), isotherm at 300 K, the ferromagnetic impurity level in the above batch of $YBa_2Cu_3O_7$ was found to be equivalent to ~ 3 ppm of iron metal impurities with respect to copper. This small ferromagnetic impurity contribution to M is corrected for in the data $YBa_2Cu_3O_7$ below. In $Bi_{2-x}Pb_xSr_2CaCu_2O_{8+\delta}$ and $Bi_{2-x}Pb_xSr_2Ca_2Cu_3O_{10+\delta}$, from the magnetization M versus magnetic field H, M(H), isotherms at 300 K, the ferromagnetic impurity levels were found to be equivalent to between ~ 1 ppm and ~ 3 ppm of iron metal impurities with respect to copper. These small ferromagnetic impurity contributions to M are also corrected for in the data for Bi2212 and Bi2223 below.

E. Heat Capacity Measurements

Heat capacity C(T) measurements from 0.4 K to 110 K were carried out on the pellet sample of $YBa_2Cu_3O_7$ using pulse calorimeters at Ames (1.5 K to 105 K, accuracy of 1-2 %, in collaboration with Prof. C. A. Swenson) and at Berkeley (0.4 K to 30 K, in collaboration with Dr. N. E. Phillips). The Berkeley measurements were performed in either zero applied magnetic field or in a field H = 70 kG in order to estimate

the concentration of (nearly) magnetically isolated Cu^{+2} local magnetic moments in the sample, and thereby deduce information about the intrinsic low temperature Sommerfeld heat capacity coefficient $\gamma(T = 0)$. C(T) data for both the powder and pellet samples were obtained between 120 K and 400 K using a Perkin Elmer 7700 Differential Scanning Calorimeter (DSC) at a T ramp rate of 10 °C/min in a search for possible phase transitions. For comparison with these C(T) data, magnetic susceptibility $\chi(T)$ data for the same samples were obtained at Ames using a Quantum Design SQUID magnetometer.

In the Ames pulse C(T) measurements, which were carried out first, we used a small amount of Apiezon N grease to attach the sample to a copper plate, with the thermometer attached to the opposite side of the plate. For the pulse C(T) measurements at Berkeley, the sample was wrapped with silver foil to enhance the thermal contact between sample and addenda and attached to a copper plate with a small amount of GE 7031 varnish. A small thin-film heater was mounted onto the silver foil. In these measurements, the duration of a heat pulse was about 2 min at high temperatures and 30 s below 30 K. The thermal equilibration time was about 5 and 10 min in the respective T ranges.

Additional C(T) measurements, accurate to 0.5%, were made on the pellet sample in Berkeley in H = 0 and H = 70 kG from 68 K to 110 K using a high resolution continuous heating

method and the same sample mounting and addenda as for the pulsed measurements, with a heating rate of ≈ 4 mK/s. A series of four measurements were made, with one in the 70 kG field. Three zero-field measurements were made to determine the reproducibility of the measurements and the possible influence of the thermal and magnetic field history of the sample on its heat capacity.

IV. RESULTS

A. DC Resistivity

The resistivity of the $YBa_2Cu_7O_7$ pellet sample at room temperature was ~ 2 mΩ-cm. The normalized resistance with respect to that at room temperature versus temperature is shown in Fig. 5. We can see the apparent bending down behavior starting around 120 K. The resistance is almost linear with respect to temperature between 150 K and 230 K and there is an anomaly around 250 K. The zero resistance temperature, $T_c(R = 0)$, was observed at 91.5 K and maximum slope in dR/dT was at 93.2 K.

B. Magnetic Susceptibility

a. Polycrystalline pellet $YBa_2Cu_3O_{7-\delta}$

Meissner effect M/H measurements of the polycrystalline pellet sample in H = 50 G gave 48% of $-1/4\pi$ at 10 K with a zero-field-cooled value in the same H of 127%, both uncorrected for demagnetization factors (Fig. 6). The Meissner effect attained 10 and 50% of its maximum value at 91.4 and 88.1 K, respectively. The $\chi(T)$ data of polycrystalline pellet $YBa_2Cu_3O_7$ in H = 50 kG are shown in Fig. 7. This sample shows a clear indication of an anomaly

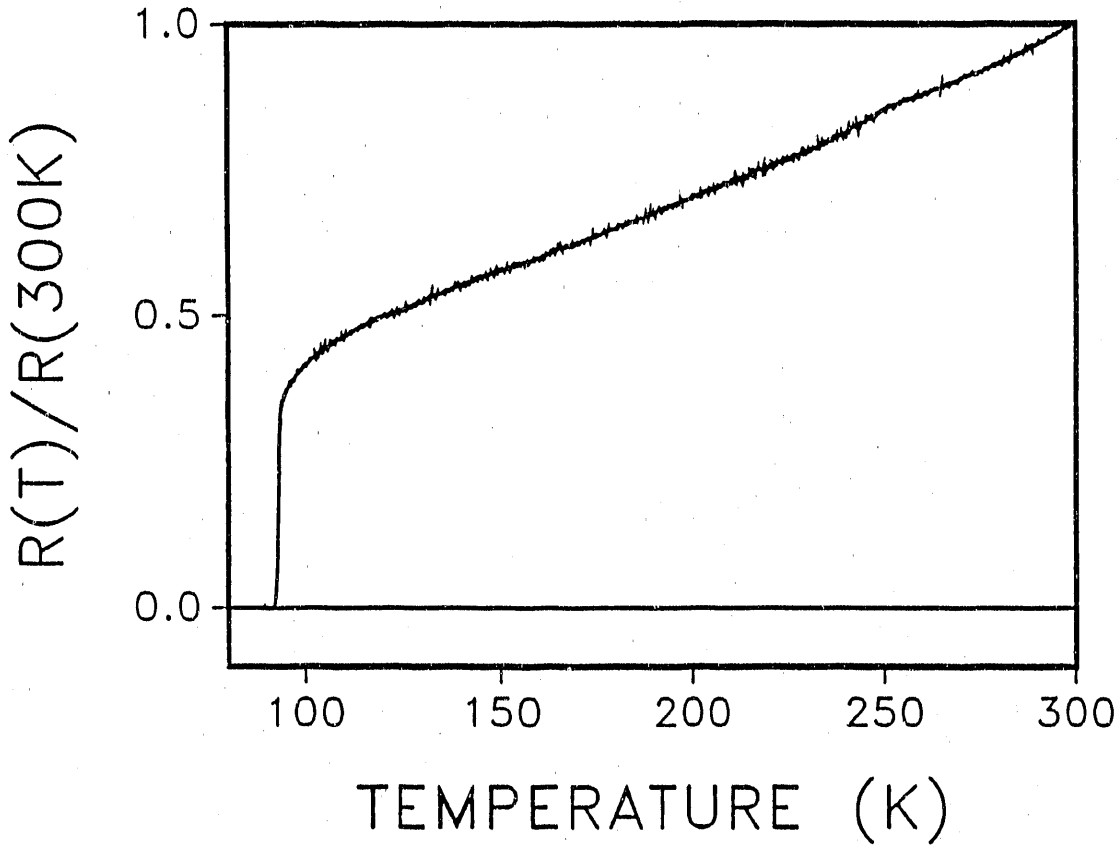

Fig. 5. Normalized resistance with respect to that of 300 K for $YBa_2Cu_3O_7$. At T = 300 K the resistivity is ~ 2 mΩ-cm

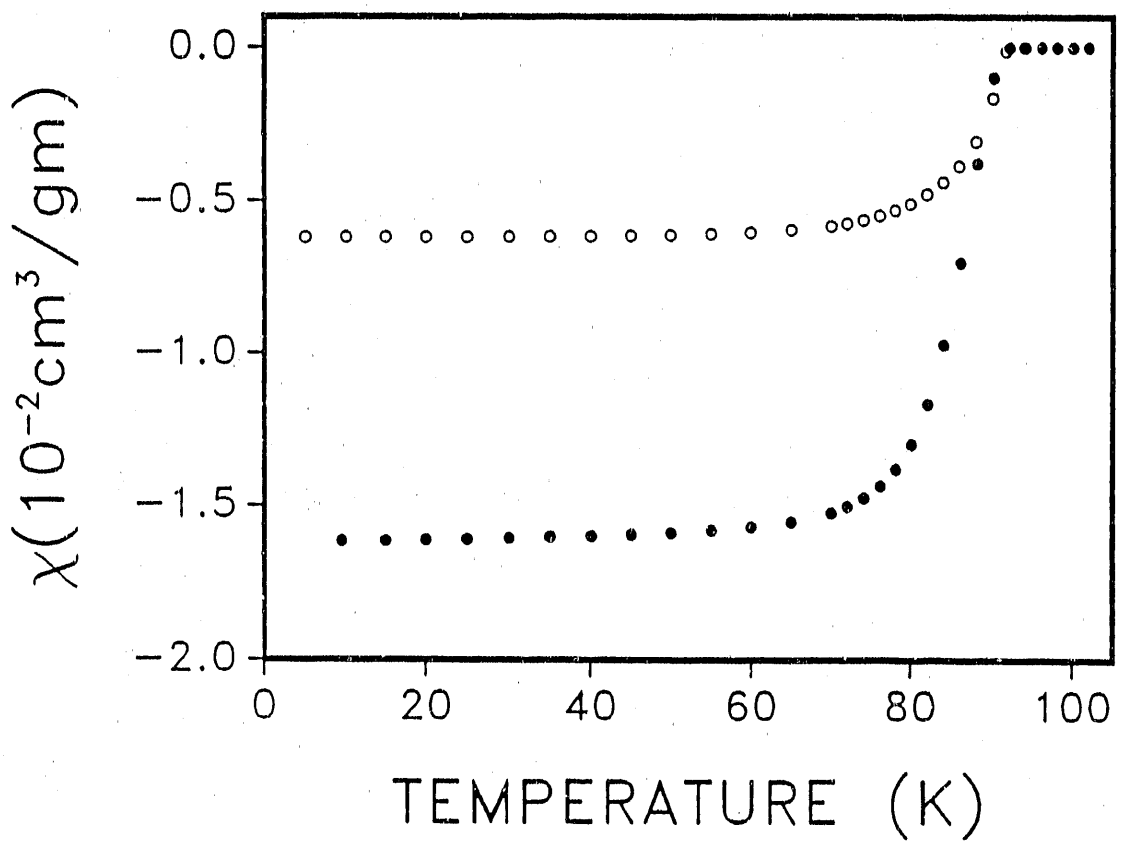

Fig. 6. Screening diamagnetism (filled circles, zero-field-cooled) and Meissner effect (open circles, field-cooled) of the polycrystalline pellet $YBa_2Cu_3O_7$ in a magnetic field of 50 G

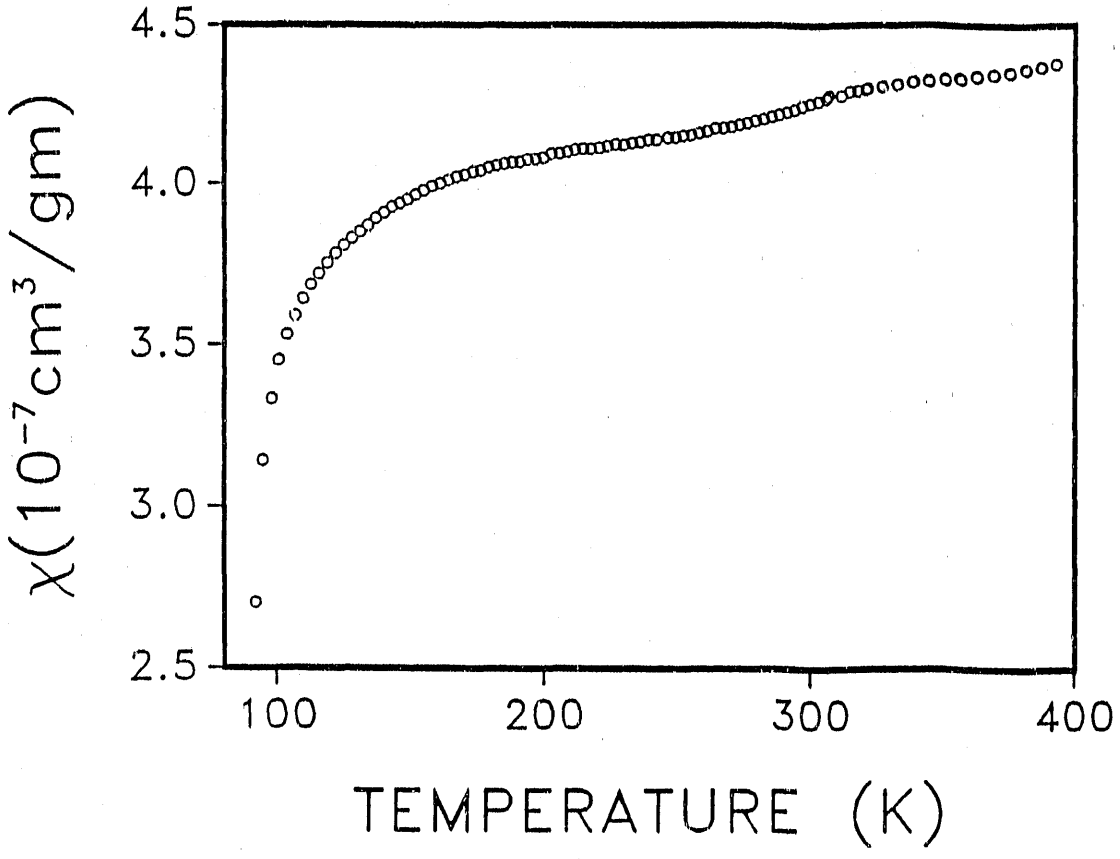

Fig. 7. Magnetic susceptibility χ vs. temperature from 95 K to 400 K for randomly oriented pellet $YBa_2Cu_3O_7$ with H = 50 kG

at T = 310 K which was seen in other studies [Johnston et al., 1987 and 1988] of $YBa_2Cu_3O_7$. The $\chi(T)$ data with H = 50 kG increase monotonically with increasing temperature at least up to 400 K and exhibit negative curvature below ~ 200 K (~ $2T_c$). The region of negative curvature below ~ 200 K in Fig. 7 suggests the onset of either filamentary superconductivity or superconducting fluctuation diamagnetism (SFD) in the sample. The field-cooled (FC) magnetization curves below T_c in H = 50 G, 500 G, 3 kG, 10 kG and 50 kG are shown in Fig. 8. Below T_c, negative curvature in M(T) can be seen for the magnetic fields greater than 3 kG. In Fig. 9 we replot the magnetization data for the superconducting state with the low (H = 50 G) and high (H = 50 kG) magnetic fields. In H = 50 G, we can not see any discontinuous point below T_c, but in H = 50 kG, there is a clear anomaly showing maximum around 70 K, consistent with results of other measurements [Bhattacharya et al., 1988] and the following heat capacity measurements of the same sample.

b. Grain-aligned $YBa_2Cu_3O_{7-\delta}$

M(T) data for $YBa_2Cu_3O_7$ were obtained on grain-aligned free-flowing powder. The screening diamagnetism (zero-field-cooled) and Meissner effect (field-cooled) were measured for our high purity $YBa_2Cu_3O_7$ in a field of 50 G for both **H** || c and **H** $\perp$ c, as well as for the randomly oriented powder. The

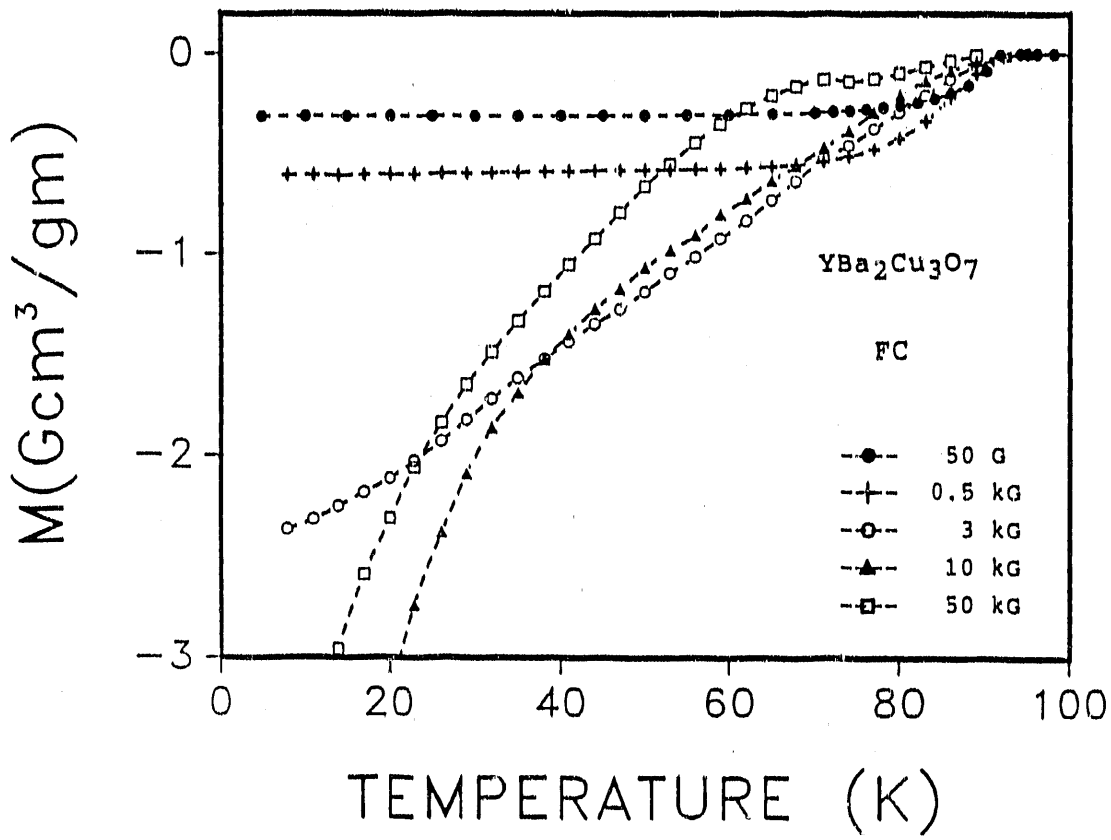

Fig. 8. Field-cooled magnetization vs. temperature of polycrystalline pellet $YBa_2Cu_3O_7$

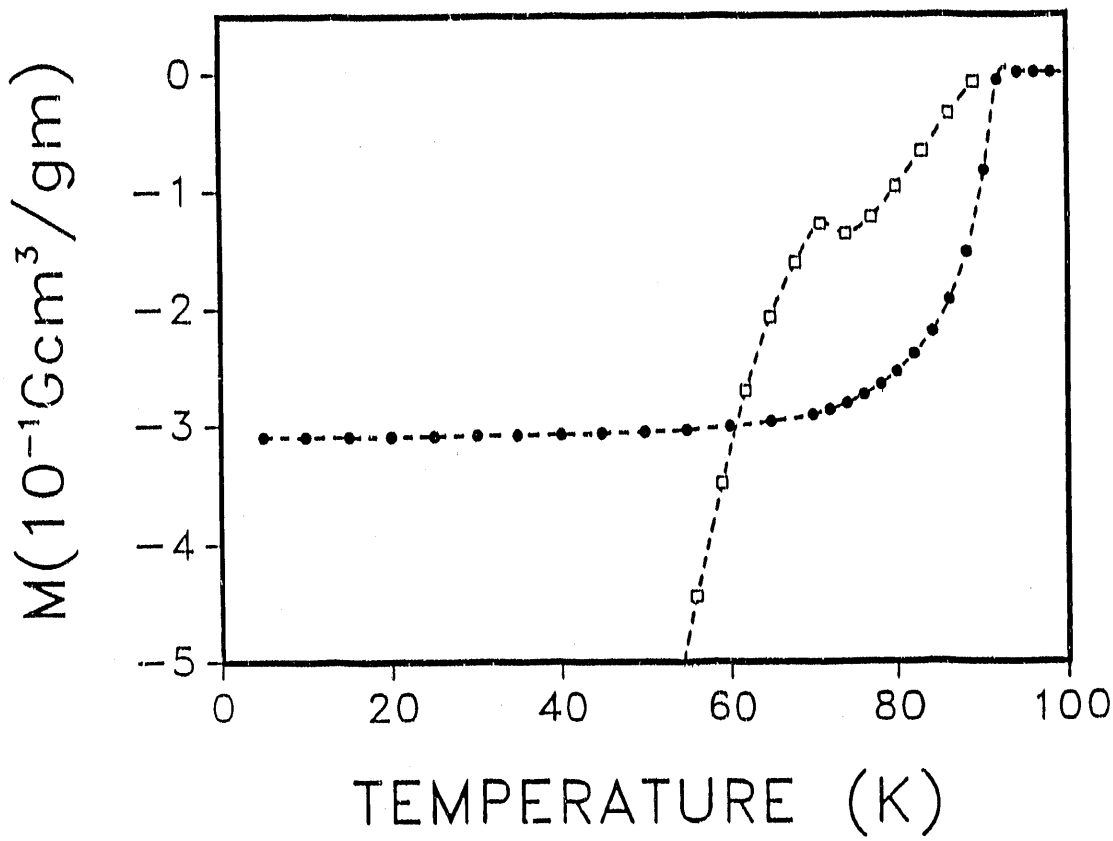

Fig. 9. Magnetization M vs. temperature for a piece of the pellet sample of $YBa_2Cu_3O_7$ in applied fields of 50 G (filled circles) and 50 kG (open squares)

results for $\chi(T) = M(T)/H$ are shown in Fig. 10. Uncorrected for demagnetization factors, the randomly oriented powder shows 165 % of $(-1/4\pi)$ screening susceptibility and a 42 % Meissner effect. From Fig. 10, these measurements depend sensitively on the magnetic field orientation, as expected. The anisotropy in the screening susceptibility is comparable with that found for a single crystal [Rice et al., 1988]; however, because of variabilities associated with shape effects and possible vortex pinning at twins, one does not necessarily expect the Meissner and shielding results to be identical for aligned powders and single crystals. Fig. 11 shows the screening susceptibilities for the three measurements in Fig. 10 normalized to the values at 10 K; for $\mathbf{H} \parallel \mathbf{c}$, the superconducting transition is seen to be narrower than those of the other two measurements. Meissner effect measurements in a field of 3 kG are shown in Fig. 12; the flux expulsion is about an order of magnitude smaller than seen for H = 50 G in Fig. 10, and the apparent transition width is of order T_c.

Magnetic susceptibility $\chi(T)$ data were obtained above T_c = 91 K in fields of 3 or 5 kG on nonaligned and aligned samples of mass 17 to 53 mg. Six different complete sets of data as in Fig. 13 below were obtained on four different samples from the same batch. The largest anisotropy in χ was observed for the sample with the smallest mass (17.6 mg).

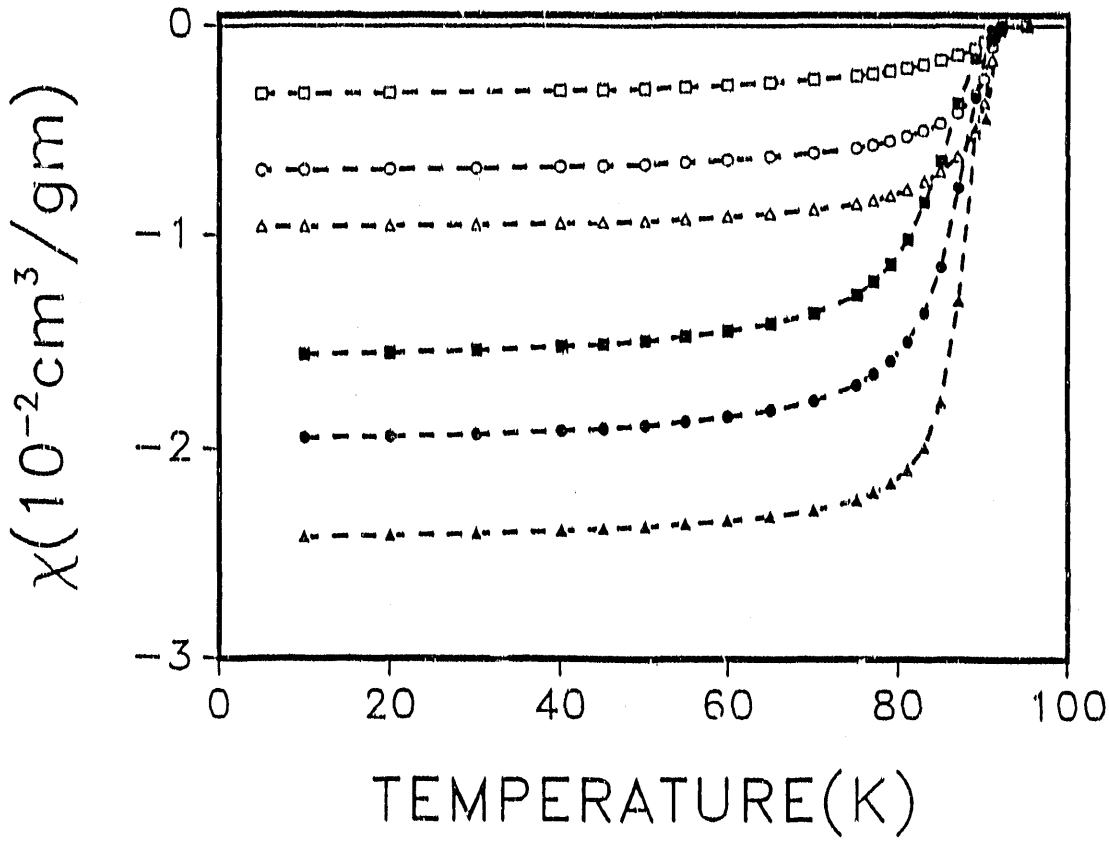

Fig. 10. Screening diamagnetism (filled symbols, zero-field-cooled) and Meissner effect (open symbols, field-cooled) vs. temperature for nonaligned powder (circles) and grain-aligned $YBa_2Cu_3O_7$ in a field of 50 G with H || c (triangles) and H ⊥ c (squares)

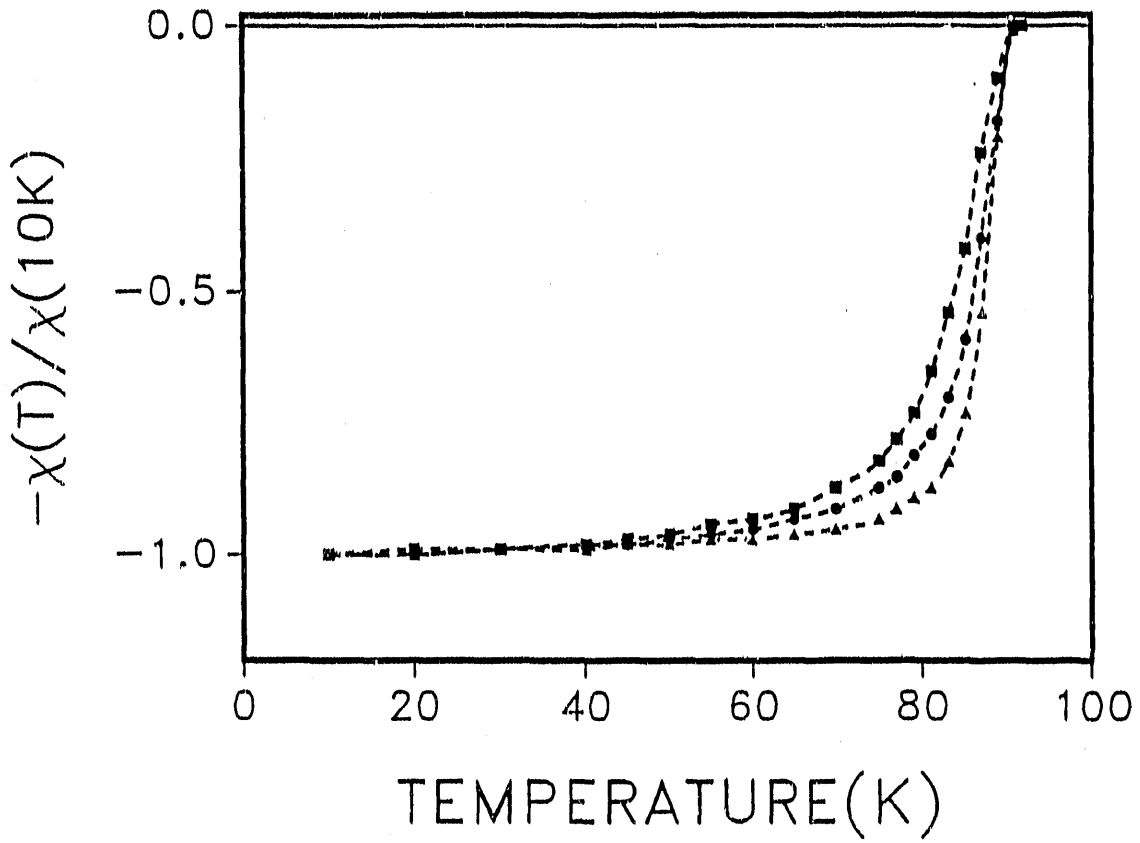

Fig. 11. Normalized magnetic susceptibility $-\chi(T)/\chi(10\ K)$ vs. temperature for the screening measurements of grain-aligned $YBa_2Cu_3O_7$ in Fig. 10

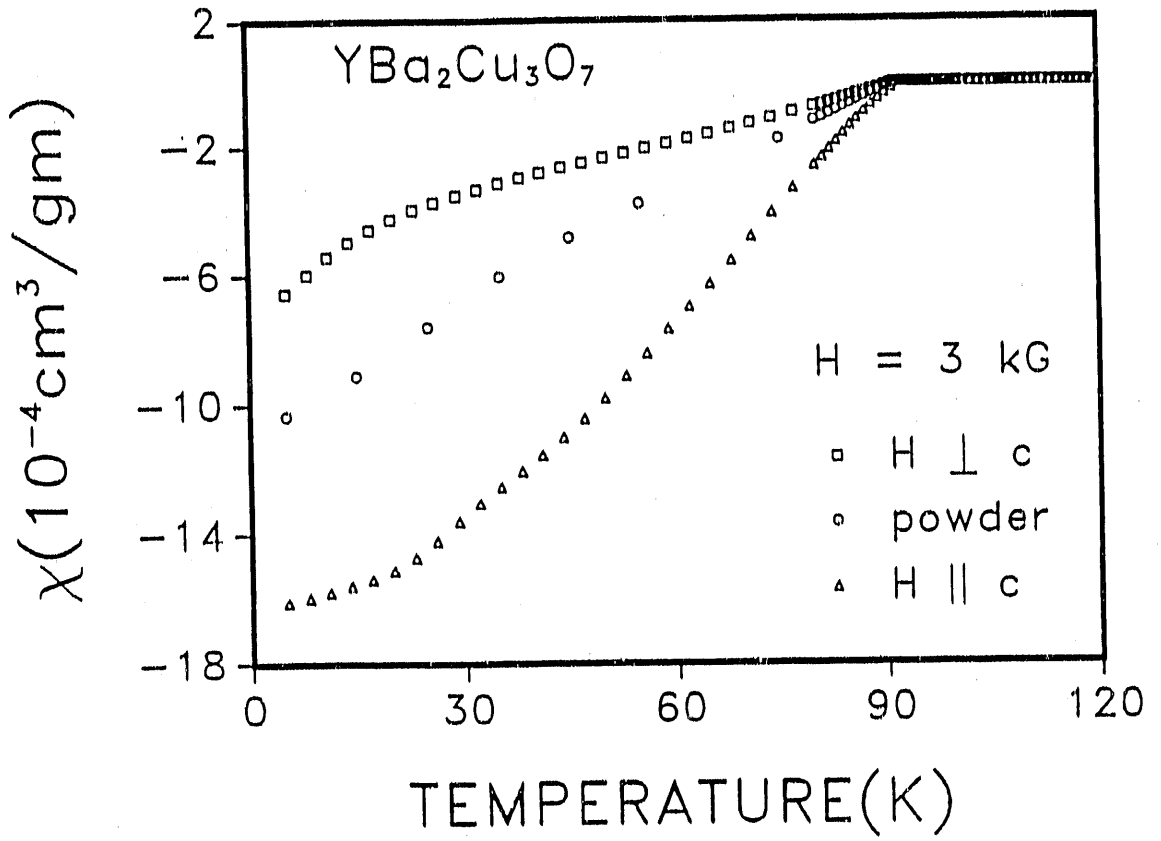

Fig. 12. Meissner effect vs. temperature in H = 3 kG; the symbols are same as in Fig. 10

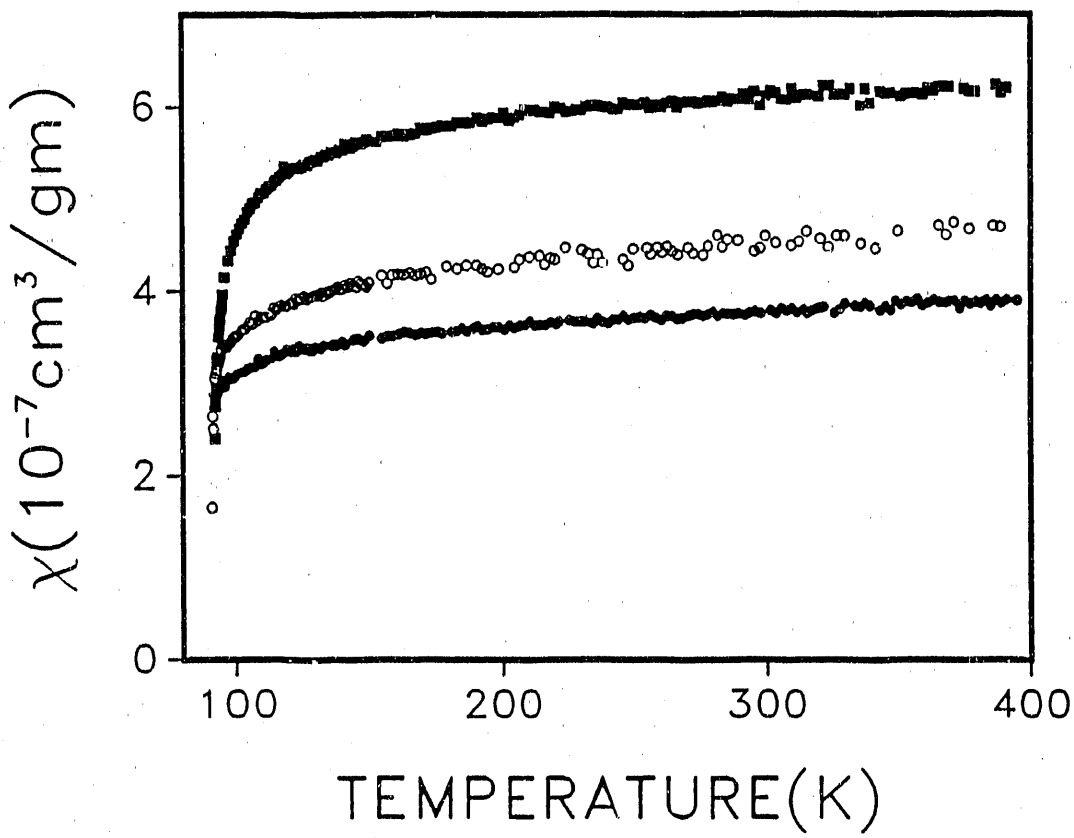

Fig. 13. Magnetic susceptibility χ vs. temperature of the grain-aligned $YBa_2Cu_3O_7$ in H = 3 kG for **H** || c (squares), nonaligned powder (open circles), and for **H** ⊥ c (filled circles)

The $\chi(T)$ data for H = 3 kG are shown in Fig. 13 for this $YBa_2Cu_3O_7$ powder sample before and after grain-alignment. The $\chi(T)$ for the aligned $YBa_2Cu_3O_7$ are shown again in Fig. 14, along with a theoretical fit to the background (solid curve, see below). This powder sample does not show any clear indication of the anomalies at 220 - 240 K and/or 310 K which was seen in other $\chi(T)$ studies such as for our pellet sample above [Cheong et al., 1987; Johnston et al., 1987 and 1988; Miljak et al., 1988 and 1989]. Another complete set of data for this sample closely reproduced the data in Fig. 13. The $\chi(T)$ data for each measurement increase monotonically with increasing temperature and exhibit negative curvature below ~ 200 K (~ $2T_c$). Above 240 K, the data increase approximately linearly with temperature, with slope (1.40 ± 0.08) x 10^{-10} cm^3/gm-K for both χ_c and χ_{ab}. The anisotropy $\Delta\chi \equiv \chi_c - \chi_{ab}$ is plotted in Fig. 15. Above T_c, $\Delta\chi > 0$, whereas below T_c, $\Delta\chi < 0$. That $\Delta\chi$ passes through zero very near to T_c is consistent with the temperature dependent anisotropy obtained from torque magnetometer measurements on single crystals [Miljak et al., 1988 and 1989]. The ratio $\chi_c/\chi_{ab} \simeq 1.63$ at 300 K, and the temperature dependence of this ratio is shown in Fig. 16; for all temperatures except perhaps very close to T_c, $|\chi_c/\chi_{ab}| > 1$.

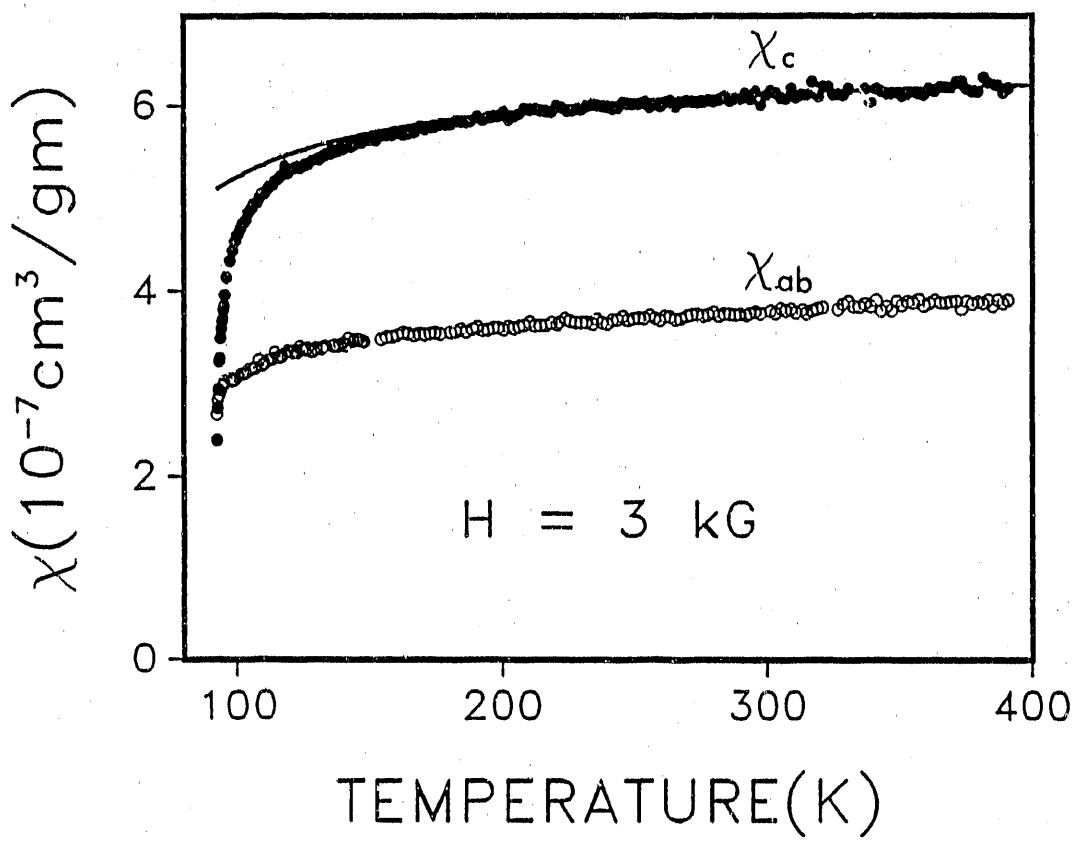

Fig. 14. Magnetic susceptibility χ vs. temperature for grain-aligned $YBa_2Cu_3O_7$ in Fig. 13. The solid curves are normal state backgrounds (see text)

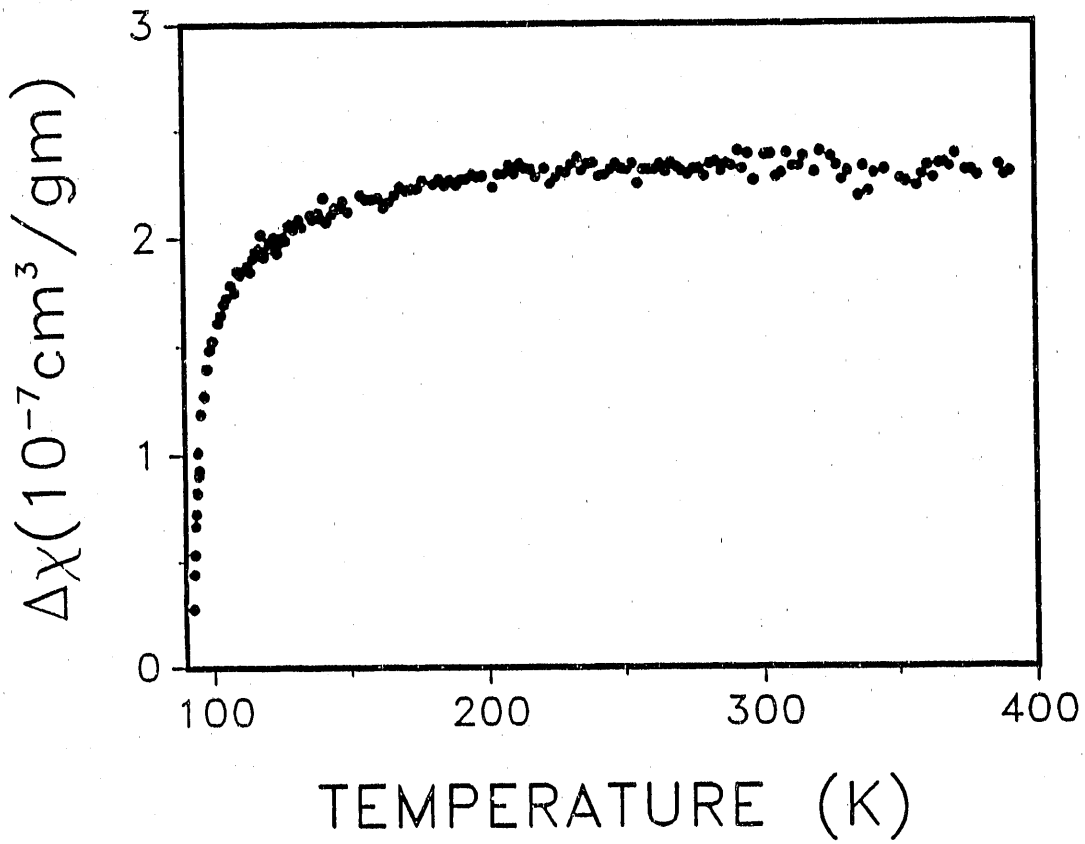

Fig. 15. Magnetic susceptibility anisotropy $\Delta\chi = \chi_c - \chi_{ab}$ vs. temperature for $YBa_2Cu_3O_7$

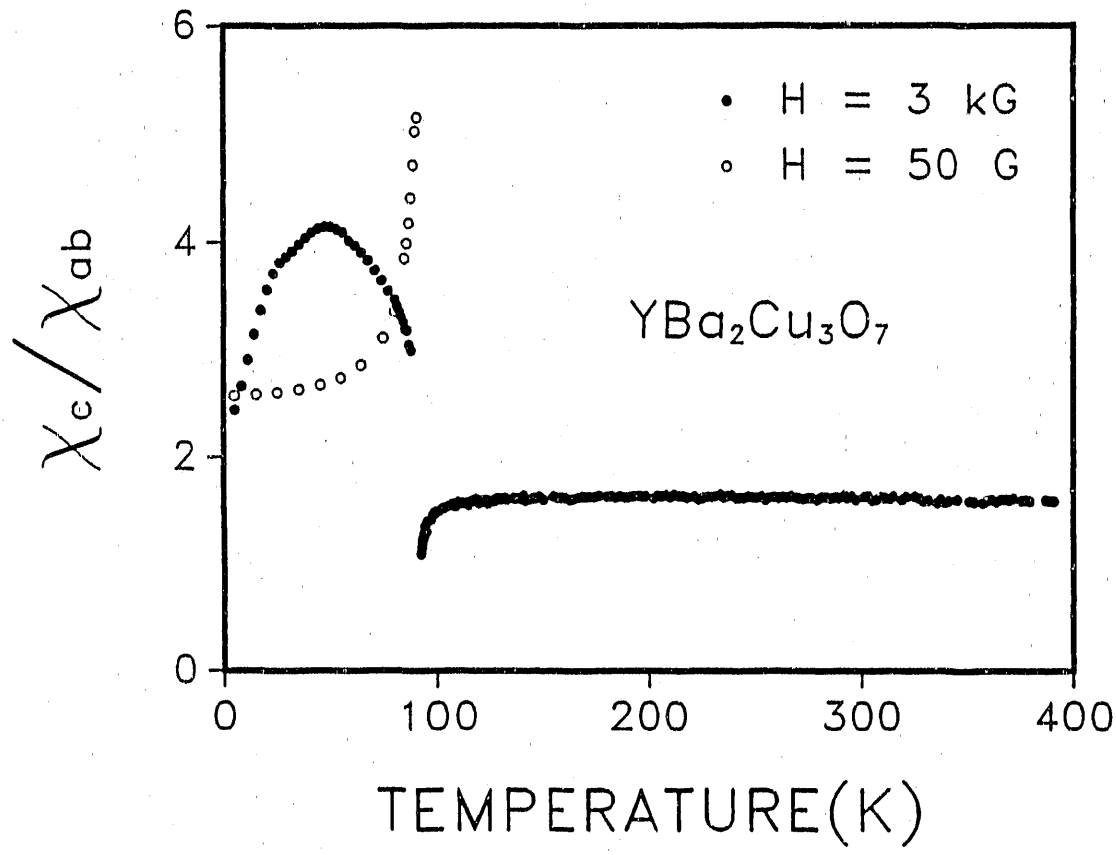

Fig. 16. Ratio of the susceptibility with the field H parallel and perpendicular to the c-axis χ_c/χ_{ab} versus temperature for $YBa_2Cu_3O_7$

c. $Bi_{2-x}Pb_xSr_2CaCu_2O_{8+\delta}$ and $Bi_{2-x}Pb_xSr_2Ca_2Cu_3O_{10+\delta}$

Meissner effect data for the $Bi_{2-x}Pb_xSr_2CaCu_2O_{8+\delta}$ samples with x = 0.0, 0.1, 0.2, 0.3, and 0.5 are shown in Fig. 17. For the x = 0.2 sample, the superconducting onset temperature T_{on} is ≈ 96 K, with a Meissner fraction of 40% of $-1/4\pi$ at 10 K, uncorrected for demagnetization factors. The Meissner effect attained 10 and 50% of its maximum value at 93 K and 89 K, respectively. It is well-known that $Bi_2Sr_2CaCu_2O_{8+\delta}$ has T_{on} ≈ 85 K, whereas T_{on} ≈ 110 K for $Bi_2Sr_2Ca_2Cu_3O_{10+\delta}$ [Koyama et al., 1988; Matsui et al., 1988]. Our value T_{on} ≈ 96 K therefore suggests that a small amount of the Bi2223 phase is present in this sample; this is supported by fits of theory to the data (see below). From Fig. 17, the T_{on} value and magnitude of the Meissner effect depend on the Pb content x. For x = 0.0, 0.1 and 0.2, T_{on} ≈ 96 K, but for x = 0.3, T_{on} shifts down to 92 K. The data for x = 0.5 show two clear transitions, with T_{on} ≈ 107 K and ≈ 89 K, respectively. Defining the superconducting transition width ΔT_c as the difference between the temperatures at which the Meissner effect attains 10% and 50% of its maximum value, we find ΔT_c = 6 K, 4 K, 4 K and 3 K for x = 0.0, 0.1, 0.2 and 0.3, respectively. Since the different samples had different and irregular shapes and therefore different demagnetization factors, comparison of the magnitudes of the respective Meissner effects is not discussed here.

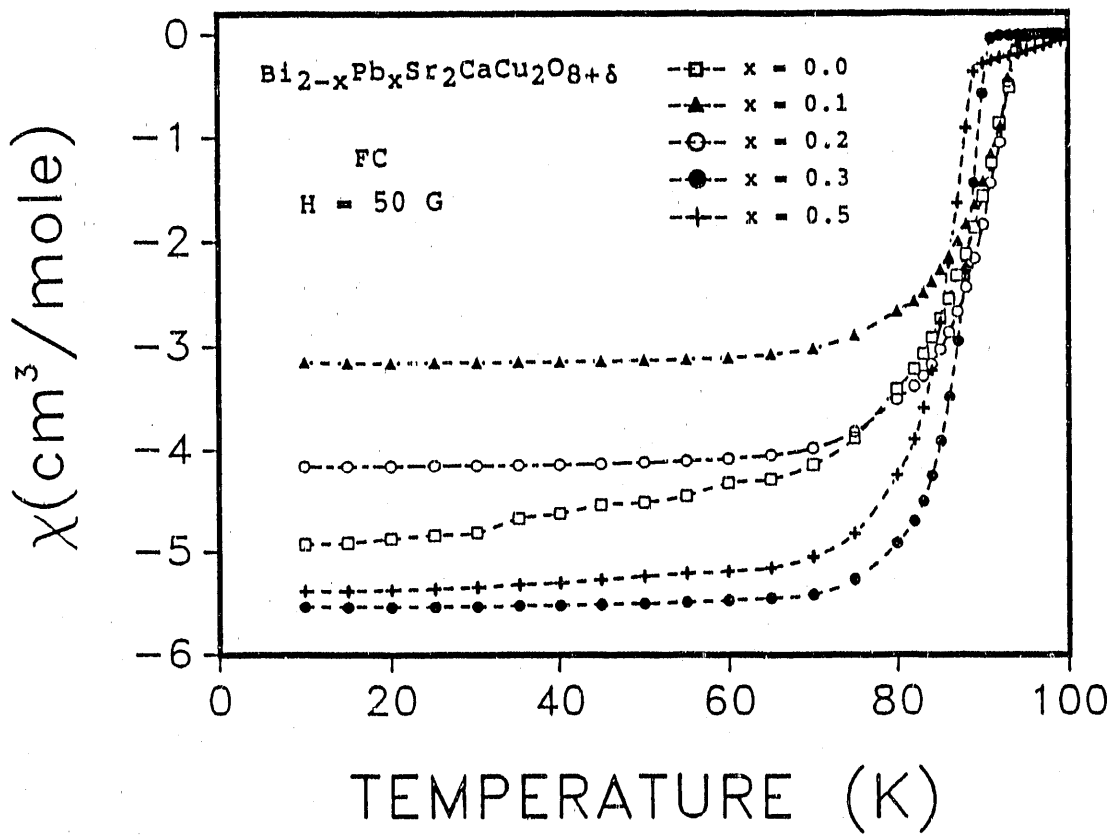

Fig. 17. Meissner effects χ vs. temperature of polycrystalline $Bi_{2-x}Pb_xSr_2CaCu_2O_{8+\delta}$ in H = 50 G

Magnetization M(T) data below T_c for the above polycrystalline Bi2212 samples with $0.0 \leq x \leq 0.5$ in H = 3 kG are shown in Fig. 18. A second derivative maximum in M(T) with respect to T at T ~ 40 - 50 K is observed for each sample. For x = 0.2, field-cooled (FC) magnetization data below T_c in H = 50 G, 3 kG, 10 kG, 20 kG and 30 kG were obtained and are shown in Fig. 19. Between T_c and the second derivative maximum temperature, positive curvature in dM(T)/dT is seen for $H \gtrsim 3$ kG, which is opposite to the behavior observed for $YBa_2Cu_3O_7$ [Lee and Johnston, 1990b and 1990c]; these behaviors are not yet understood.

$\chi(T)$ data above T_c for the Bi2212 samples with $0.0 \leq x \leq 0.5$ in H = 3 kG are shown in Figs. 20 and 21. For $0.1 \leq x \leq 0.3$, $d\chi(T)/dT$ is positive at least up to 400 K. However, for x = 0.0 and 0.5, $d\chi(T)/dT$ is negative above ~ 150 K, indicating the presence of appreciable amounts of magnetic impurity phases with a Curie-Weiss-like susceptibility.

The Meissner effects and screening susceptibilities for our samples of $Bi_{2-x}Pb_xSr_2Ca_2Cu_3O_{10+\delta}$ with x = 0.20 and 0.25 in H = 50 G are shown in Figs. 22a and 22b. The value of T_{on} for x = 0.2 is ~ 108 K; the Meissner effect and screening magnetization data yield M/H = 18% and 34% of $-1/4\pi$ at 10 K, respectively, uncorrected for demagnetization factors; the respective values for the x = 0.25 sample are 109 K, 28%, and 46%. Both the Meissner effect and screening data for the x =

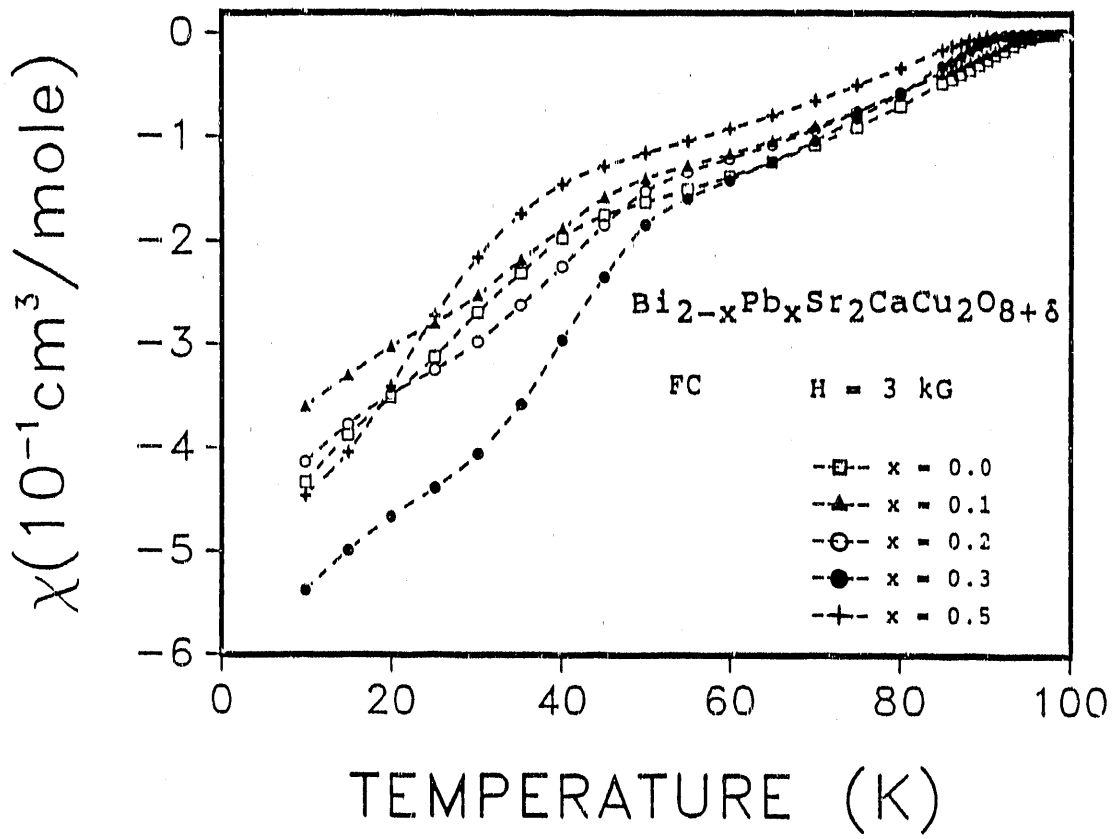

Fig. 18. Meissner effects χ vs. temperature of polycrystalline $Bi_{2-x}Pb_xSr_2CaCu_2O_{8+\delta}$ in H = 3 kG

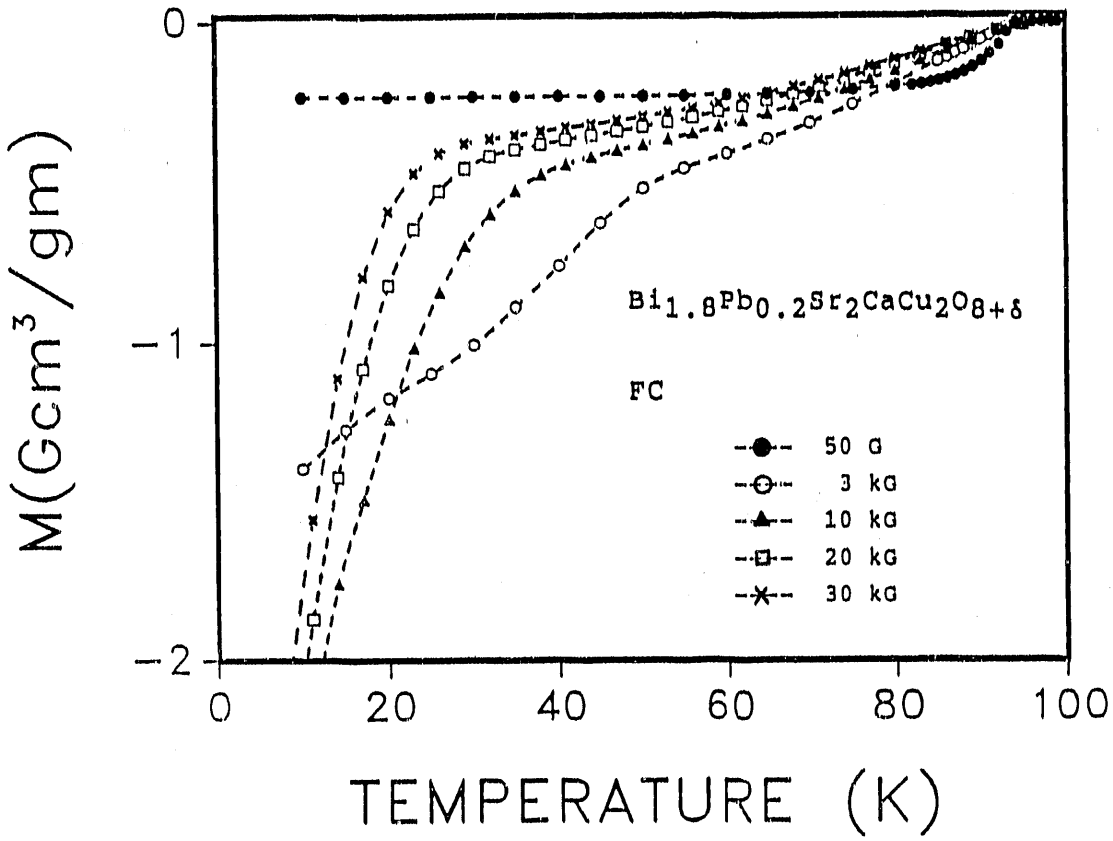

Fig. 19. Meissner effects vs. temperature of polycrystalline $Bi_{1.8}Pb_{0.2}Sr_2CaCu_2O_{8+\delta}$ in various magnetic fields

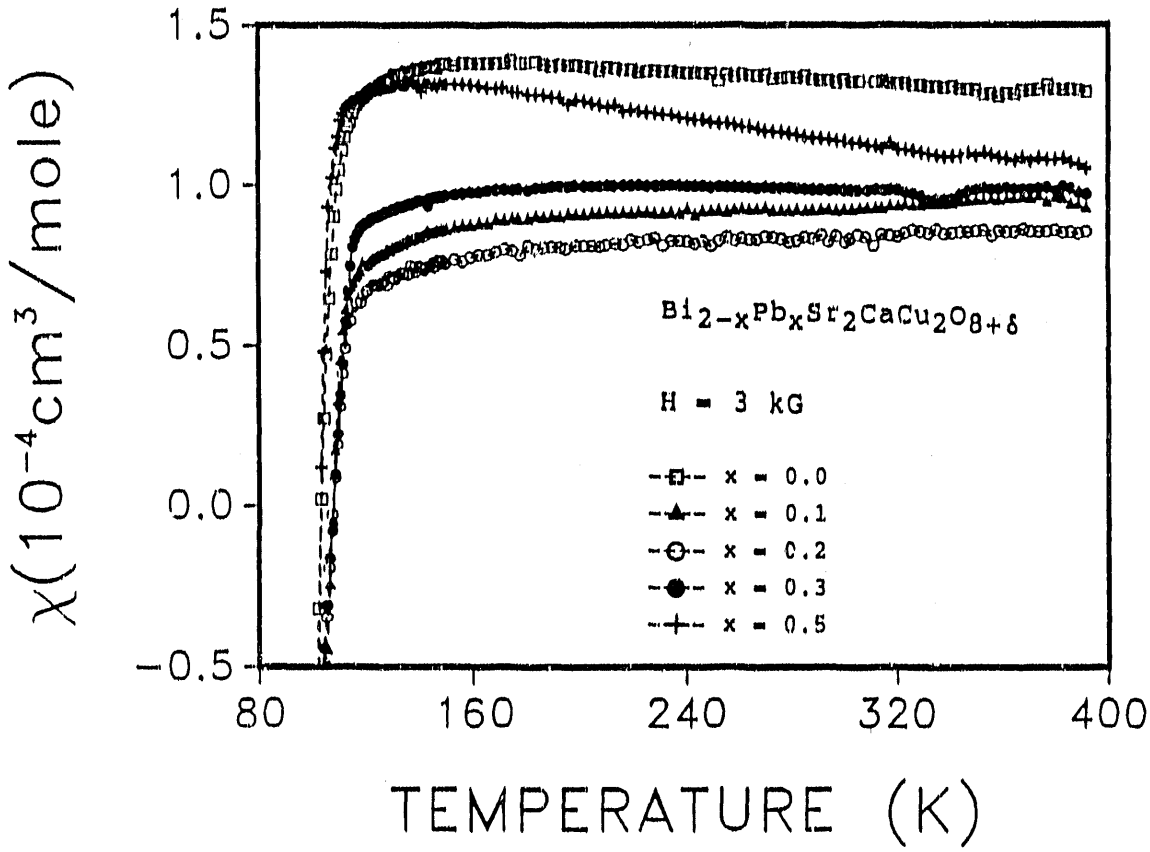

Fig. 20. Magnetic susceptibility χ vs. temperature of the polycrystalline $Bi_{2-x}Pb_xSr_2CaCu_2O_{8+\delta}$ in H = 3 kG

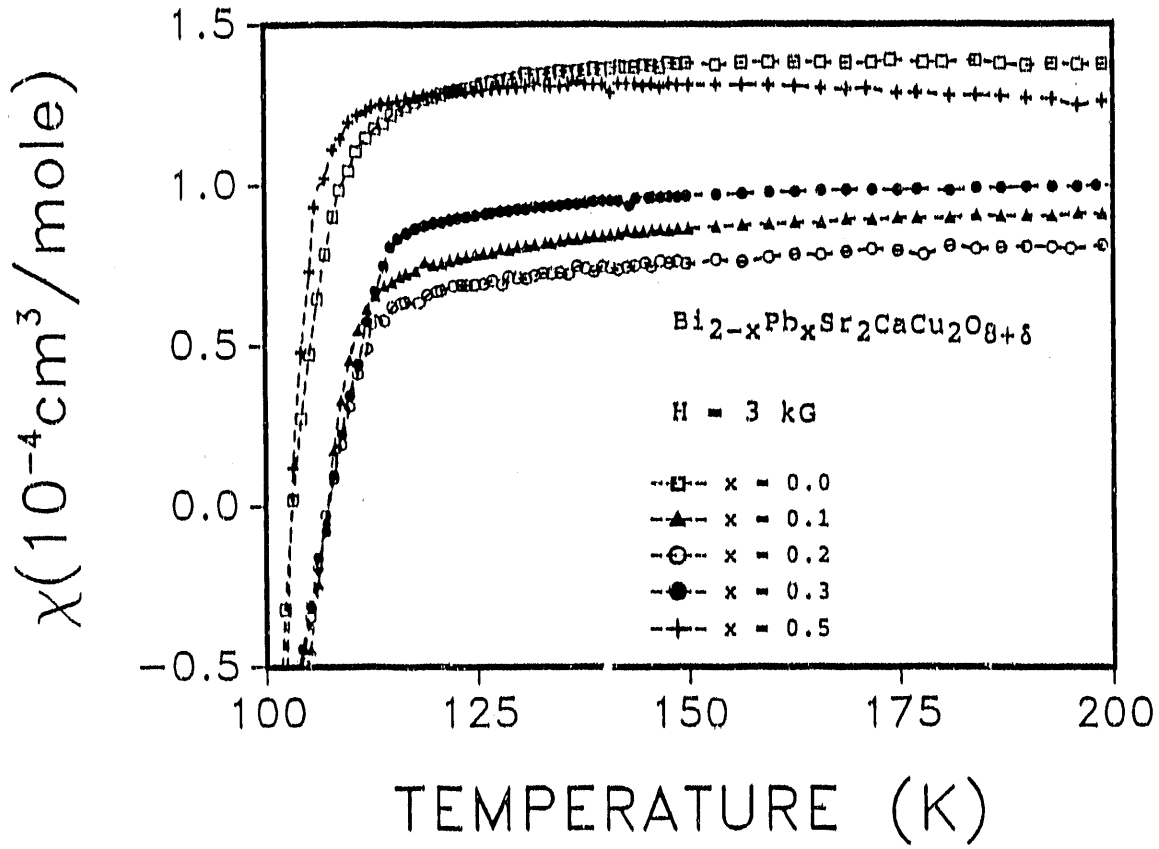

Fig. 21. Expanded magnetic susceptibility χ vs. temperature of the $Bi_{2-x}Pb_xSr_2CaCu_2O_{8+\delta}$ below ~ $2T_c$ from the Fig. 20

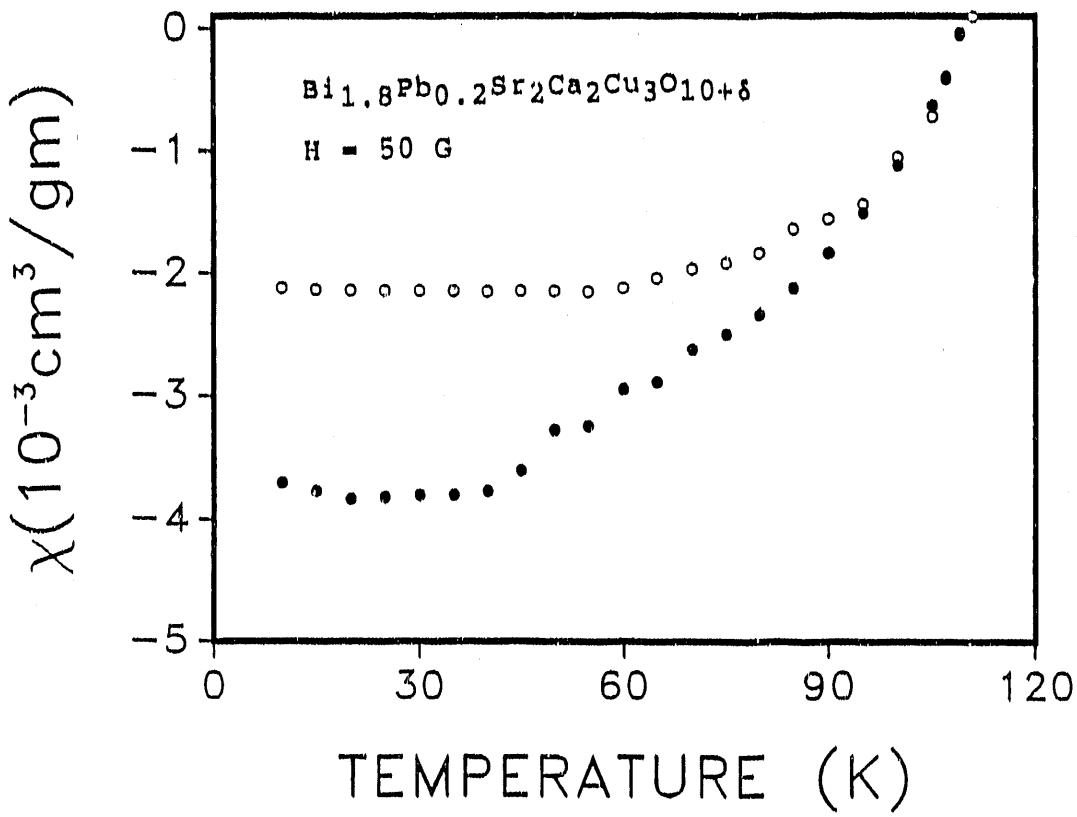

Fig. 22a. Meissner effect (open circles) and screening current (filled circles) vs. temperature of polycrystalline $Bi_{1.8}Pb_{0.2}Sr_2Ca_2Cu_3O_{10+\delta}$ in H = 50 G

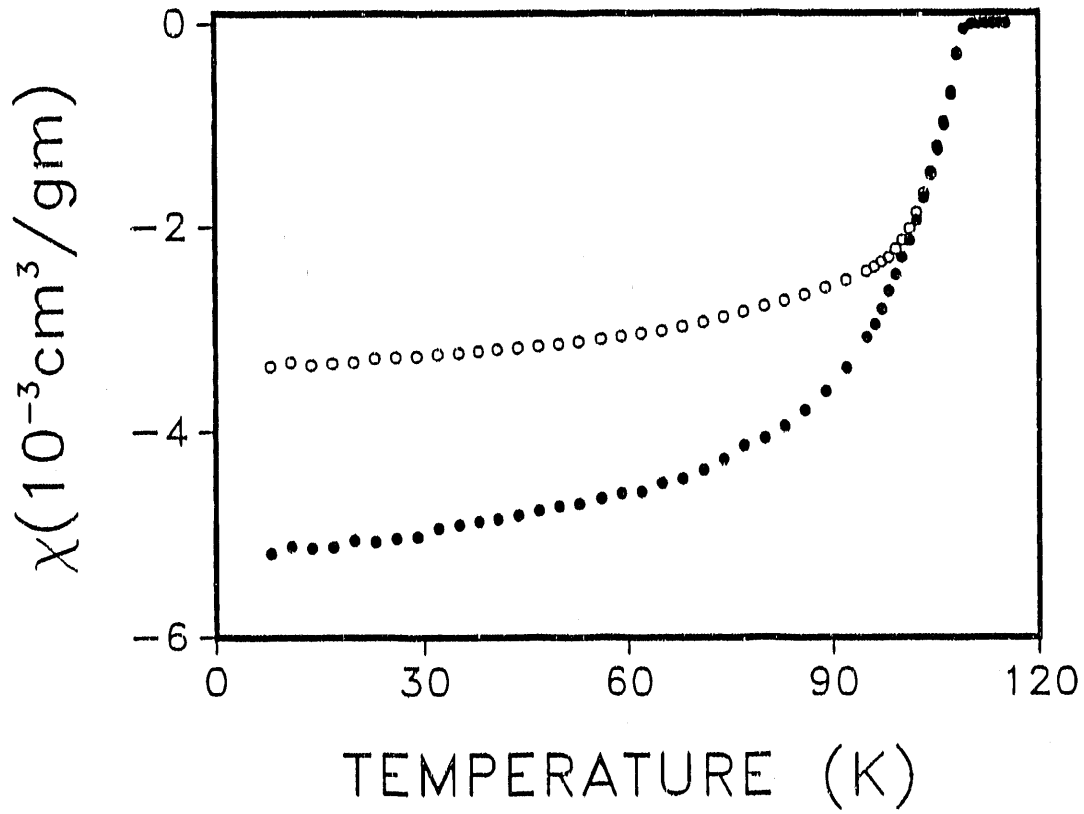

Fig. 22b. Meissner effect (open circles) and screening current (filled circles) vs. temperature of polycrystalline $Bi_{1.75}Pb_{0.25}Sr_2Ca_2Cu_3O_{10+\delta}$ in H = 50 G

0.2 sample show the presence of a small amount of the Bi2212 phase. The Meissner effect attained 10 and 50 % of its maximum value at 106 K and 99 K for x=0.2, and 108 K and 103 K for x = 0.25, respectively.

The $\chi(T)$ data in H = 5 kG are shown in Figs. 23a and 23b. As for $YBa_2Cu_3O_7$ and Bi2212, negative curvature is present in $\chi(T)$ up to at least 200 K.

C. Heat Capacity

An overview of C(T) of our $YBa_2Cu_3O_7$ pellet sample in zero applied magnetic field from 1.5 K to 400 K is shown in Fig. 24 (C vs. T) and Fig. 25 (C/T vs. T). There is good agreement between the C(T) near 120 K measured using the pulsed and continuous heating calorimeters and that measured using the DSC. The magnitude of the heat capacity over the whole temperature range is similar to the results of previous measurements on relatively magnetically pure samples [Fisher et al., 1988b; Junod et al., 1989; Sun et al., 1990].

To ascertain the reproducibility of the heat capacity near T_c, a series of four measurements was carried out using the Berkeley continuous heating calorimeter. Initially, the sample was cooled from room temperature to 65 K and held at that temperature overnight. Curve A in Fig. 26 shows the first measurement (H = 0) up to ≈ 110 K. A feature with a

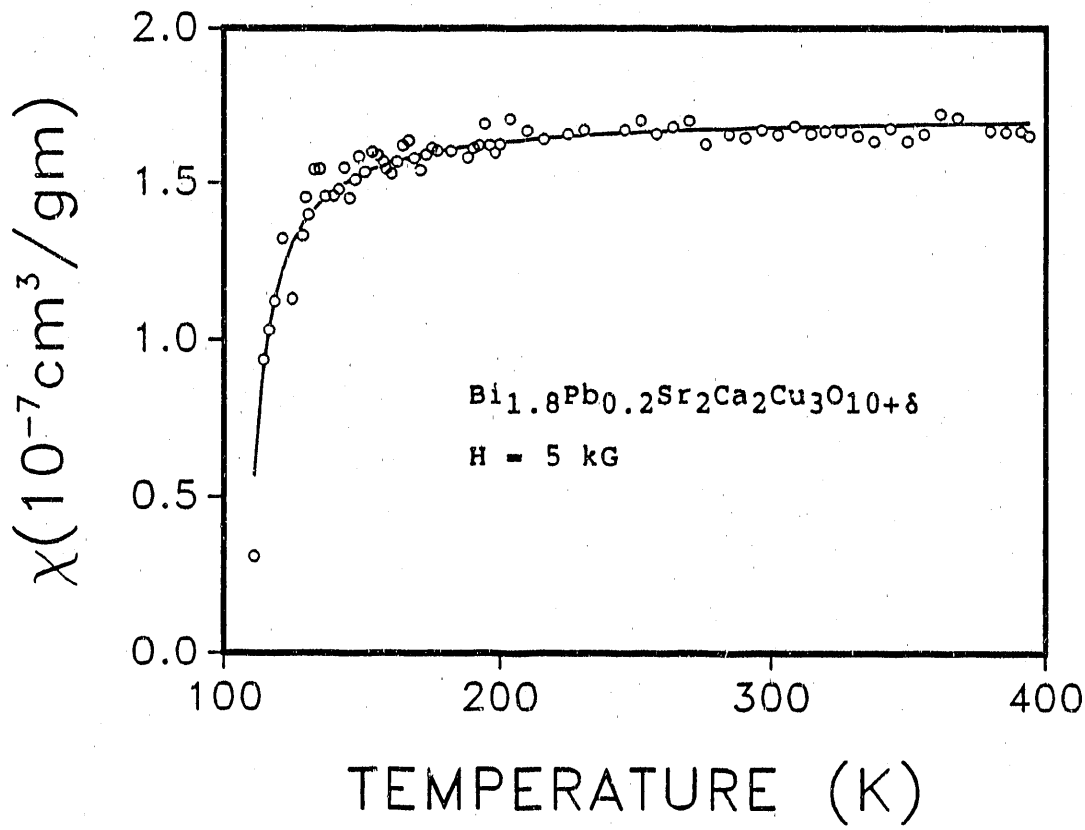

Fig. 23a. Magnetic susceptibility χ vs. temperature of the $Bi_{1.8}Pb_{0.2}Sr_2Ca_2Cu_3O_{10+\delta}$ in H = 5 kG. Solid curve is the LD 2 dimensional theory

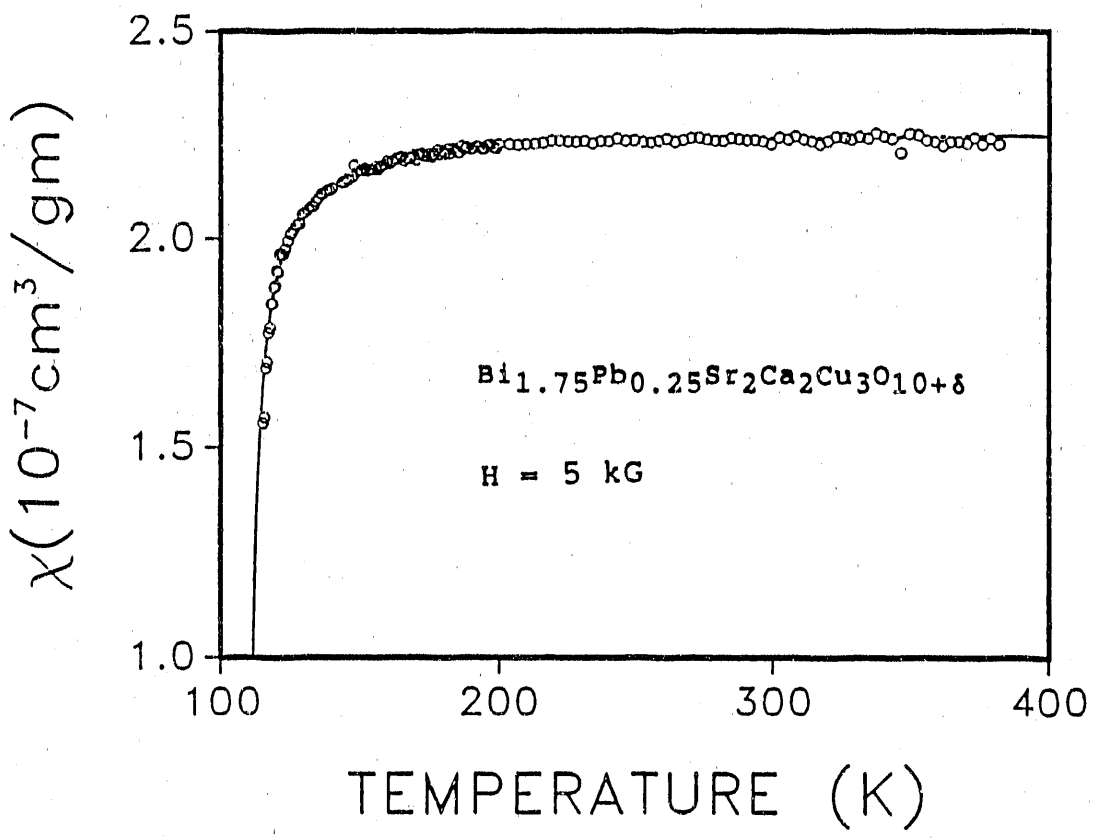

Fig. 23b. Magnetic susceptibility χ vs. temperature of the $Bi_{1.75}Pb_{0.25}Sr_2Ca_2Cu_3O_{10+\delta}$ in H = 5 kG. Solid curve is the LD 2 dimensional theory

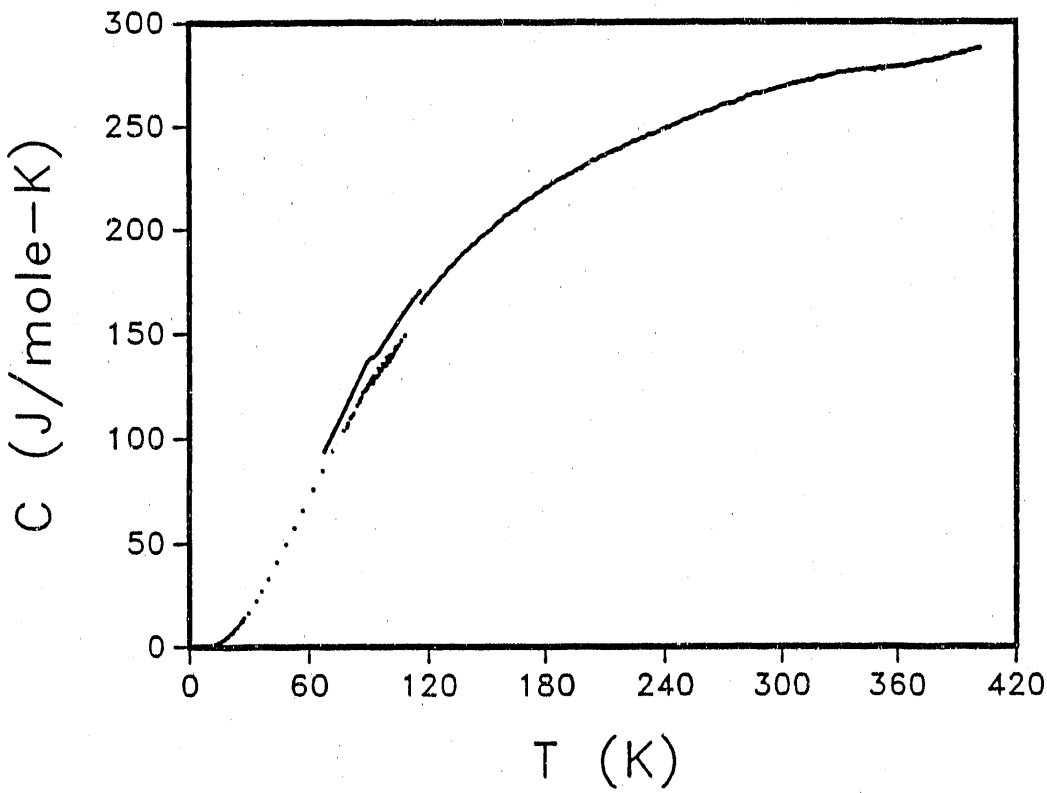

Fig. 24. Overview of heat capacity C(T) vs. temperature T for a polycrystalline $YBa_2Cu_3O_7$ pellet sample in zero applied magnetic field from pulsed calorimeter measurements at Ames (below ~ 120 K), pulsed calorimeter measurements at Berkeley (1 - 30 K), continuous heating calorimeter measurements at Berkeley (68 - 110 K, top data set here, set A in Fig. 26), and differential scanning calorimeter measurements at Ames (120 - 400 K)

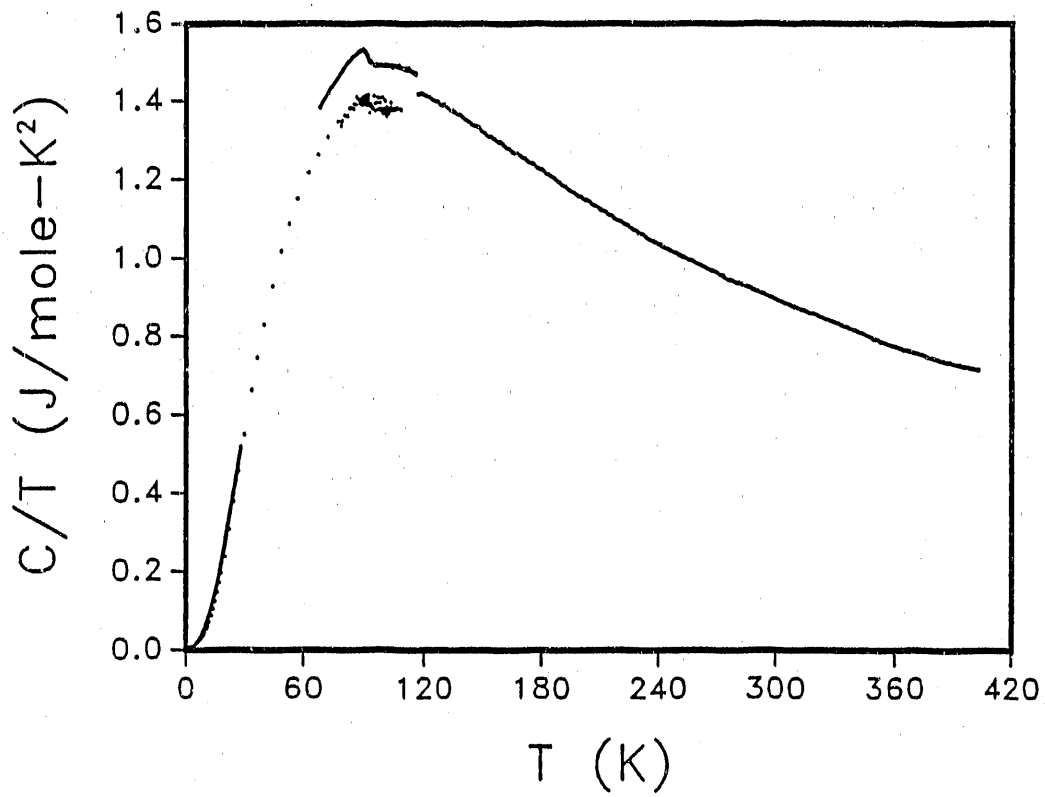

Fig. 25. C/T vs. T data derived from Fig. 24

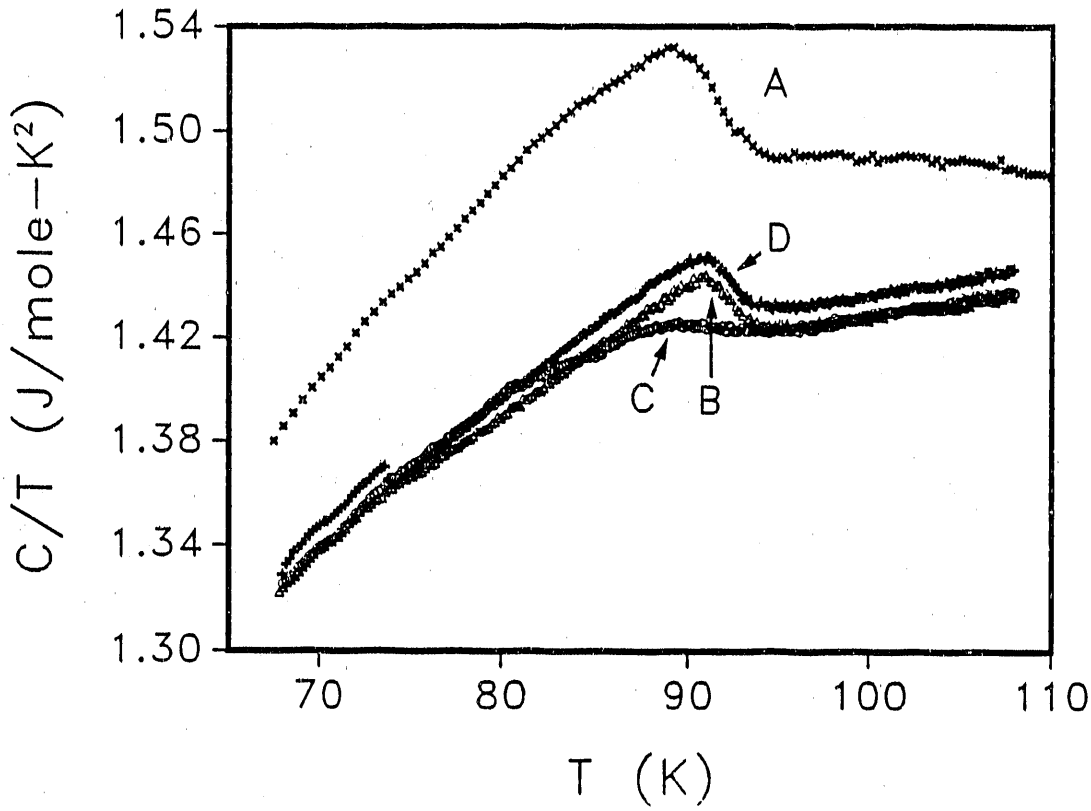

Fig. 26. Heat capacity divided by temperature C/T vs. T for $T \sim T_c$ measured at Berkeley using a continuous heating technique for the pellet sample of Figs. 24 and 25. The sequence was as follows. A: cooled from room temperature and held overnight at 65 K in zero applied magnetic field H before measurement; B: cooled from 110 K and held at 65 K overnight (H = 0); C: cooled from 110 K and held at 65 K overnight, then H = 70 kG applied; D: cooled from room temperature (H = 0) and held at 65 K overnight

peak near 89.5 K is clearly observed, associated with the onset of superconductivity. The sample was then cooled again to 65 K, held overnight, and the measurement repeated (labeled B in Fig. 26). The peak in C/T for B increased to 91.0 K from the value of 89.5 K found for A. From Fig. 26, large differences between the two measurements are seen in both the magnitude of C(T) and the size of the feature near T_c. Also, there is a hint of an anomaly near 102 K in B not evident in A, and of anomalies at ~ 74 K in both B and A. There were no differences obvious to us in the manner in which the data sets A and B were accumulated and analyzed.

Next, the sample was again cooled to 65 K and held overnight. A magnetic field of 70 kG was applied, and C(T) measured (curve C in Fig. 26) in the same manner as in the first two experiments. The feature at T_c is smeared out by the field as reported earlier [Fisher et al., 1988b; Salamon et al., 1988] and the temperature of the maximum in C/T has decreased to 88.5 K. There is a clear crossover of the data sets B and C near 85 K. Below 65 K and above 95 K, the B and C data sets coincide, and both show evidence of a feature at 102 K. After measurement C, the sample was warmed to room temperature, cooled to 65 K in zero field and held overnight, and a fourth data set obtained (set D in Fig. 26) using the same heating rate as before. Remarkably, the weak anomaly at

74 K in sets A and B appears now as a sharp mean-field-like second order transition in set D.

The results of the pulse C(T) measurements in zero field from 0.5 K to 10 K at Ames and at Berkeley are shown in Fig. 27. Fig. 28 shows the data obtained at Berkeley in both zero field and 70 kG. The zero field heat capacity measurements show a clear upturn in C/T below about 2 K. In H = 70 kG, a clear Schottky-like anomaly appears with a peak near 3 K; at very low T (< 0.5 K), a sharp upturn in C/T is observed.

An expanded plot of the DSC data for the pellet sample of $YBa_2Cu_3O_7$ in Fig. 24 from 120 K to 400 K taken with increasing T is shown in Fig. 29, where data for the same sample with decreasing T and for the powder sample with increasing T are also included. With increasing T, an anomaly near 330 K is seen for the pellet sample which is not obviously present in the measurement with decreasing T. From Fig. 29, there is no evidence of an anomaly near 220 - 240 K. There is also no evidence of any anomalies in C(T) for the powder sample upon increasing or decreasing (not shown) the temperature.

Magnetic susceptibility $\chi(T)$ data above T_c for the pellet and powder samples of $YBa_2Cu_3O_7$ in fields of 3 or 50 kG are shown in Figs. 7 and 13. The powder was aligned with the c-axis parallel and perpendicular to the field using a method described previously, whereas the grains in the pellet

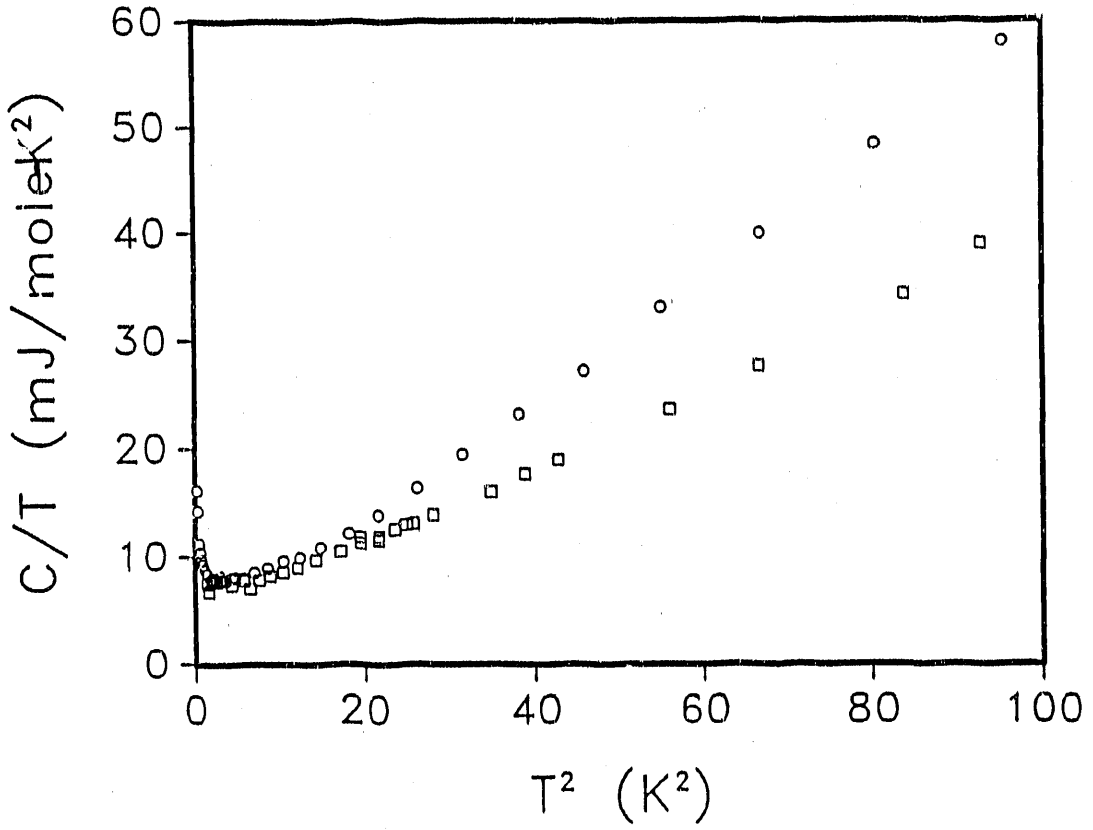

Fig. 27. Low temperature pulsed heat capacity divided by temperature C/T vs. T^2 in zero field measured at Ames (squares) and Berkeley (circles)

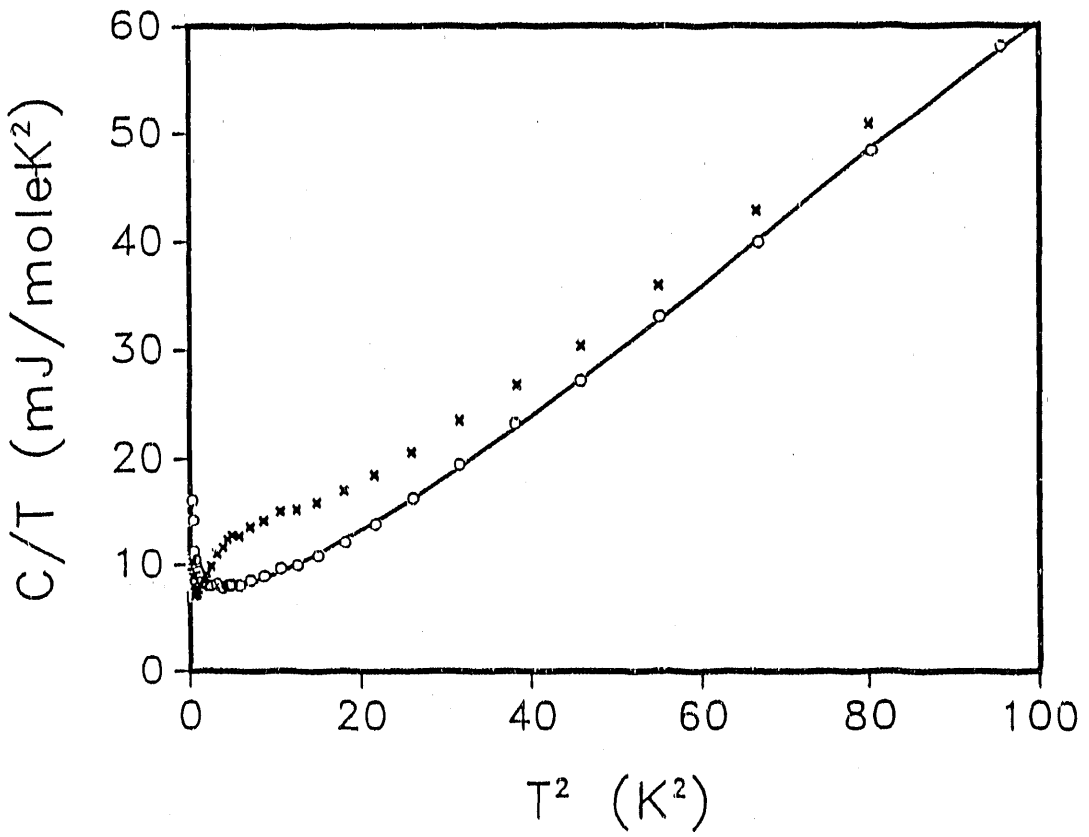

Fig. 28. Low temperature pulsed heat capacity divided by temperature C/T vs. T^2 measured at Berkeley with H = 0 (circles) and 70 kG (crosses); the zero-field data are the same as in Fig. 27 from Berkeley. The solid curve is a fit to the zero-field data (see text)

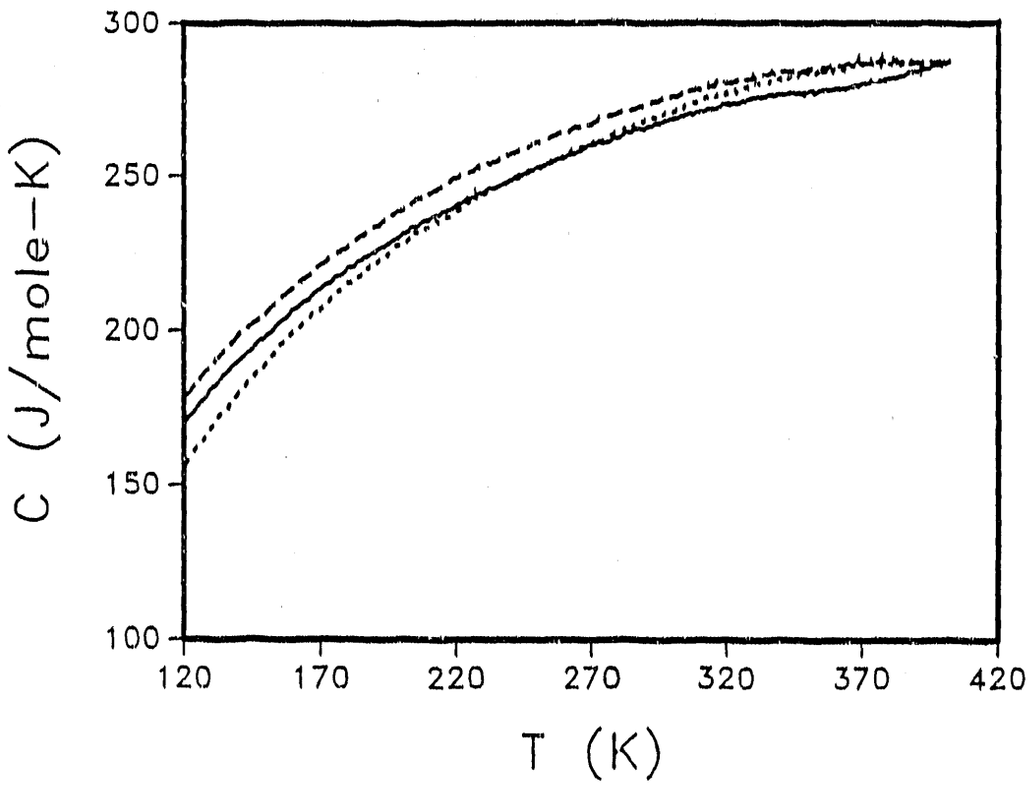

Fig. 29. Heat capacity C vs. temperature T measured at Ames using a differential scanning calorimeter with a temperature scanning rate of 10 °C/min. The solid data set was taken on heating the $YBa_2Cu_3O_7$ pellet sample, the long-dashed data on cooling the pellet sample, and the short-dashed data on heating the powder sample

were found using x-ray diffraction of the surface to be randomly aligned. The data for the pellet sample show a clear cusp at ≈ 320 K whereas the data for the powder exhibit no evidence of an anomaly above T_c. Because of the proximity of the cusp temperature for the pellet to that of the heat capacity anomaly observed above with the DSC on heating, the source of the anomalies in the two types of measurement may be the same.

Magnetization vs. temperature data below T_c for the pellet sample in fields of 50 G and 50 kG are shown in Fig. 9. The 50 kG data exhibit an anomaly near 74 K. This anomaly might be a manifestation of flux-pinning effects, although this appears unlikely because the magnetization is reversible with increasing and decreasing field at this field and temperature [Mitra et al., 1989]. Alternatively, it could be a reflection of some sort of phase transition occurring at this temperature as is suggested clearly in the C(T) data set D for the pellet in Fig. 26.

V. ANALYSIS AND DISCUSSION

A. Superconducting Fluctuation Diamagnetism above T_c

a. $YBa_2Cu_3O_{7-\delta}$

In order to compare grain aligned magnetic susceptibility (χ), results with theory, the modified Lawrence-Doniach model (see section II. B. b) was used, which was generalized to a magnetic field H at an arbitrary angle θ with respect to the c-axis of the unit cell, where the influence of local clean limit dynamics has also been accounted for [Klemm, 1990; Lee et al., 1989]. In that model, there are N conducting CuO_2 layers per unit cell, with N-1 equal interlayer spacings d and one different spacing d' (N = 2 for $YBa_2Cu_3O_7$), and one complex s-wave order parameter per layer; the c-axis unit cell edge $s = d' + (N - 1)d$. The layers are coupled by Josephson-like tunneling, with parameters ζ_1 and ζ_2, respectively. In twinned $YBa_2Cu_3O_7$, the intertwin distance is usually $\lesssim$ 1500 Å. We therefore take $v_F\tau_\phi$ to be $\lesssim$ 1 μm, which implies $H_o \gtrsim$ 17 kG, so our measurements are in the weak field regime. In addition, since there are numerous evidences [Fiory et al., 1988; Krusin-Elbaum et al., 1989; Mitra et al., 1989; Porch et al., 1988; Uemura et al., 1988] of BCS-type superconductivity for high T_c superconductors, we have changed the temperature-

dependent part $[(T-T_c)/T_c]$ in $\alpha(T)$ of equation (1) to $\ln(T/T_c)$ to coincide with that expected from BCS theory [Gorkov, 1959]. We note that in the theory [Klemm, 1990], we have neglected any coupling of the normal state $\chi(T)$ to the fluctuating superconducting order parameter.

In comparing our theory with the data in Fig. 14, it should be borne in mind that the $\chi(T)$ data contain possible temperature dependent contributions from normal state background antiferromagnetic spin correlations [Johnston, 1989] and crystallographic and/or electronic changes (see below), and from small amounts ($\approx$ 0.1 at. %; see section V. D. b. below) of magnetic impurity phases. Consider the anisotropy $\Delta\chi = \chi_{||c} - \chi_{\perp c}$ derived from Fig. 14 and shown in Fig. 15. The first (spin correlation) contribution should be absent in $\Delta\chi$, since it is essentially isotropic. From Fig. 15, $\Delta\chi = \Delta\chi_o = 2.32 \times 10^{-7}$ cm^3/gm is constant within experimental error above 250 K, suggesting that the anisotropy of the normal state background is independent of temperature. The quantity $\delta\chi(T) = \Delta\chi(T) - \Delta\chi_o$, plotted in Fig. 30, is thus expected to contain only the SFD contribution of present interest, and we therefore fit $\delta\chi(T)$ with the above theory. Heat capacity measurements on our sample gave $T_c = 90.8$ K, which is not an adjustable parameter in the fits below.

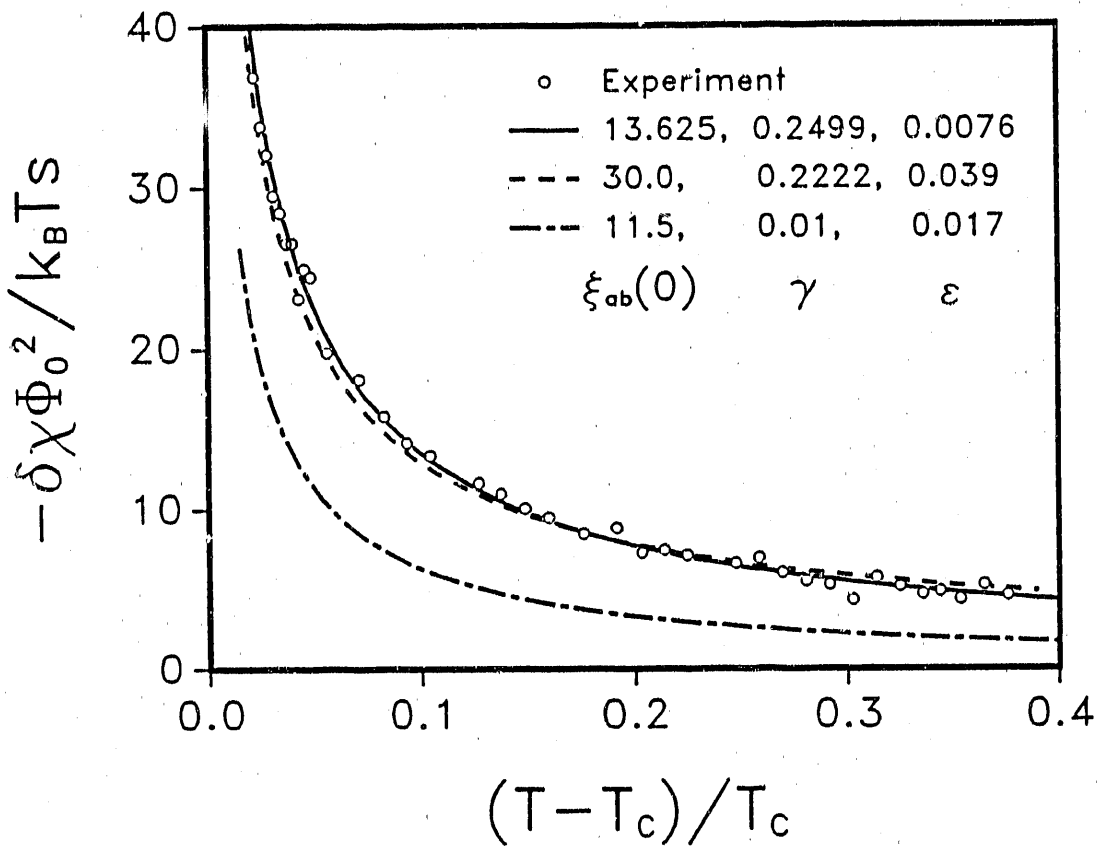

Fig. 30. Plot of $\delta\chi \equiv \Delta\chi - \Delta\chi_0$ vs. $(T-T_c)/T_c$; the solid curve is our optimum fit to the data and the other two curves are for nonoptimum fits

Theoretically predicted $\delta\chi(T)$ curves were computed numerically for γ values between 0.01 and 0.2499, ε values of 0.001 to 0.04 and $\xi_{ab}(0)$ values of 10 to 30 Å. The calculations were compared with the data on a plot of $\log_{10}[-\delta\chi/T]$ vs. $\log_{10}[\ln(T/T_c)]$ for $T < 126$ K, and the standard deviation σ for each set of parameter values was computed. At fixed $\xi_{ab}(0)$ and γ, ε was varied to give the minimum σ (Fig. 31). Fits with $\sigma \leqslant 0.035$ were judged acceptable; fits with $\sigma = 0.044$ were noticeably worse. For combinations of the three parameters yielding $\sigma > 0.035$, the fits showed systematic deviations from the data over appreciable ranges of temperature and were deemed unacceptable. The combinations of parameters which gave acceptable fits to the data in Fig. 30 are $\xi_{ab}(0) = (13.6 \pm 0.8)$ Å, $\gamma = 0.20 \pm 0.05$ and $\varepsilon = 0.0076 \pm 0.0015$. For these parameter ranges, both order parameter bands have nonzero T_c values [see Eq. (18)] and both therefore contribute to the SFD. Our optimum fit ($\sigma = 0.027$) is given by the solid curve in Fig. 30. Regions of $\xi_{ab}(0)$ values between 17 and ~ 25 Å and below 12 Å are clearly unacceptable ($\sigma > 0.07$). However, $\xi_{ab}(0)$ values near 30 Å are almost acceptable ($\sigma = 0.038$) if $\gamma \simeq 1/4$, as shown in the Fig. 30. Such large values of $\xi_{ab}(0)$ are, however, inconsistent with recent dc M(T) measurements [Welp et al., 1989] of dH_{c2}/dT at T_c for $\mathbf{H} \parallel \mathbf{c}$, which give $\xi_{ab}(0) \simeq 13.8$ Å. A further prediction of $\delta\chi(T)$ for $\xi_{ab}(0) = 11.5$ Å, $\xi_c(0)$

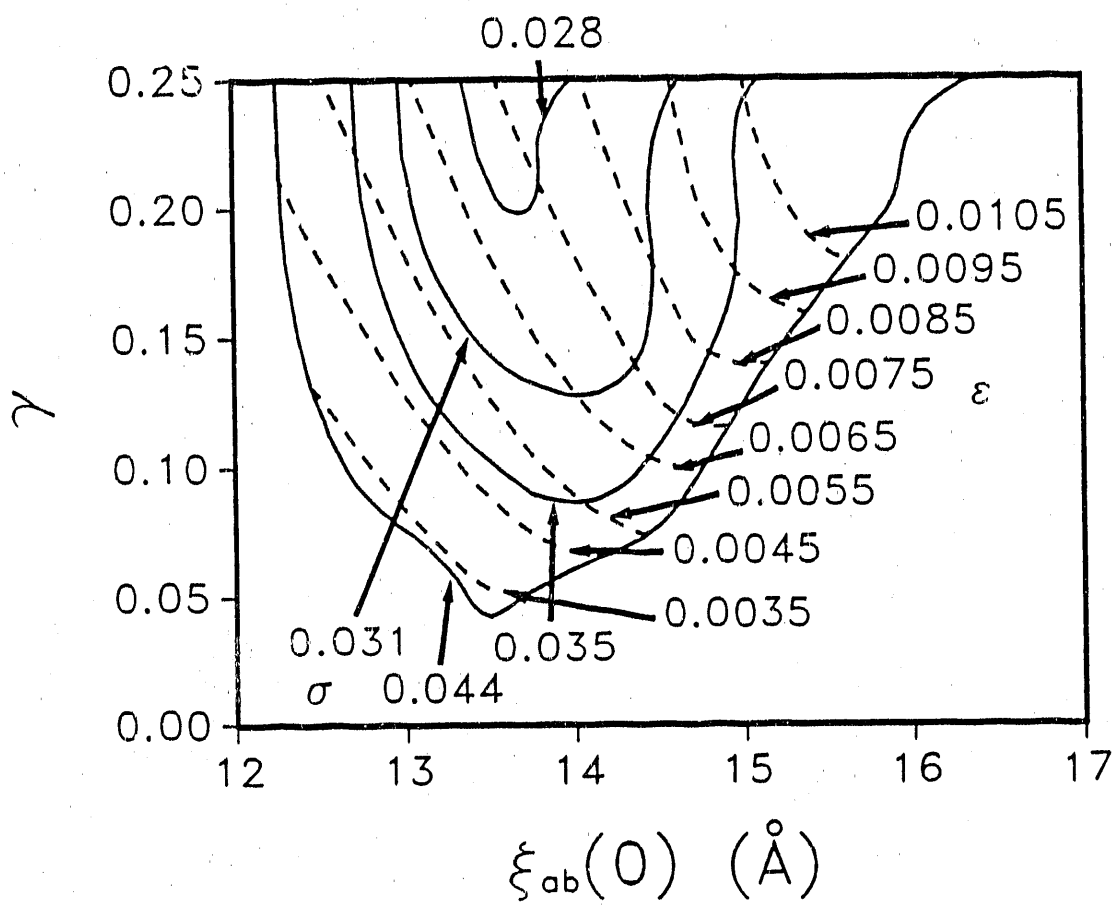

Fig. 31. γ vs. $\xi_{ab}(0)$, optimized with respect to ε, with contours of constant $\varepsilon = m/M$ and of constant standard deviation σ of the fit of theory from the data

= 1.5 Å and γ = 0.01, parameters derived [Aronov et al., 1989] from recent fits (excluding dynamics) to paraconductivity data, is shown in the Fig. 30; these parameters [Aronov et al., 1989] are obviously not consistent with our $\delta\chi(T)$ data.

From a log-log plot of the Fig. 30, the slope of which is ≈ -1/2 for the data points near to T_c (indicative of 3D behavior), we infer that the width of the critical region is less than 1 K, consistent with previous reports [Dubson et al., 1987; Freitas et al., 1987; Friedmann et al., 1989; Goldenfeld et al., 1988; Inderhees et al., 1988; Oh et al., 1988, Porch et al., 1988; Vidal et al., 1988]. While the slope on a log-log plot in the regime 110 K < T < 126 K is approximately -1, naively (i.e., in a static calculation) indicative of 2D behavior in that region, this interpretation is complicated by the dynamic effects present in the theory [Klemm, 1990]. Our ratio $1/\varepsilon = M/m \sim 100$ to 150 is consistent with some [Forro et al., 1988; Enomoto et al., 1987; Iye et al., 1987] H_{c2} anisotropy data near T_c which indicate $M/m \sim 70 - 120$. For these ε values, one would expect dimensional crossover in $\chi_c(T)$ [but not in $\chi_{ab}(T)$] to occur in the T regime pictured in the Fig. 30.

The background $\chi(T)$ for **H** || **c** and **H** $\perp$ **c** was determined by subtracting the above optimal SFD contributions from the data in Fig. 14, yielding the solid curves in Fig. 14. Both

backgrounds exhibit negative curvature below ~ 130 K; for H $\perp$ c, most of the observed curvature in the data arises from the temperature dependent background. This observation supports numerous other studies which indicate that some sort of structural, magnetic and/or electronic modification of $YBa_2Cu_3O_7$ occurs with decreasing T below ~ 130 K [Boolchand et al., 1988; Sharma et al., 1989; Sun et al., 1988; Warren et al., 1989; Yuen et al., 1988]. If the negative curvature in the normal state $\chi(T)$ background turns out to be anisotropic, then the parameters derived from our fits would have to be modified somewhat. Additionally, whatever sources are giving rise to the derived temperature-dependent background may also be causing the parameters of our model to be dependent on temperature.

b. $Bi_{2-x}Pb_xSr_2CaCu_2O_{8+\delta}$, $Bi_{2-x}Pb_xSr_2Ca_2Cu_3O_{10+\delta}$, and $La_{1.8}Sr_{0.2}CuO_{4-\delta}$

The structures of these Bi-based copper oxide superconductors are similar to $YBa_2Cu_3O_7$ in that they each contain CuO_2 layers. Therefore, we expected and found the magnitudes of the superconducting fluctuation diamagnetism (SFD) to be similar; in each case the region of negative curvature (attributed to the SFD) begins above ~ $2T_c$ as in $YBa_2Cu_3O_7$.

Our measurements were carried out on randomly oriented samples, so the measured susceptibilities are powder averages $\langle\chi\rangle$:

$$\langle\chi\rangle(T) = \frac{1}{3}\chi_c(T) + \frac{2}{3}\chi_{ab}(T) . \qquad (19)$$

The pair mass anisotropies in Bi2212 and Bi2223 are much larger than in $YBa_2Cu_3O_7$ [Farrell et al., 1989; Martin et al., 1989; Naughton et al., 1988]; according to the theory of Refs. [Klemm, 1990; Lawrence and Doniach, 1971; Lee et al., 1989], this means that the fluctuation contribution to $\chi_{ab}(T)$ is less than that to $\chi_c(T)$ by a factor of ~ 100. Many experiments [Beille et al., 1988; Farrell et al., 1989; Kang et al., 1988; Martin et al., 1989; Naughton et al., 1988; Palstra et al., 1988a] revealed essentially 2D behavior in various physical properties. We therefore neglect the fluctuation contribution to $\chi_{ab}(T)$. Neglecting also dynamic effects [Klemm, 1990], we fit the two dimensional LD model [Lawrence and Doniach, 1971] for the 2D regime to the data somewhat removed from T_c. From Eq. (19) and Ref. [Lawrence and Doniach, 1971], one obtains

$$\langle\chi\rangle(T) = \chi_o - \frac{1}{3} g_{eff} \frac{\pi k_B \xi_{ab}^2(0) T}{3\phi_0^2 s} \left[\frac{T_c}{T - T_c}\right] \qquad (20)$$

where χ_o contains the normal state contributions in the absence of fluctuations and is assumed to be independent of T. ϕ_o is the flux quantum hc/2e and g_{eff} is the effective number of complex s-wave order parameters in the repeat distance s discussed above; in the 2D regime, $g_{eff} = 2$ for Bi2212 and 3 for Bi2223 (see below).

$Bi_{1.8}Pb_{0.2}Sr_2CaCu_2O_{8+\delta}$ has two CuO_2 layers in the layer repeat distance s = 15.4 Å along the unit cell c-axis and is much more two-dimensional in the superconducting and normal states than is the case for $YBa_2Cu_3O_7$. In terms of the phenomenological model for the high T_c cuprates proposed in Refs. [Klemm, 1990; Lee et al., 1989], this translates to a larger superconducting pair mass anisotropy in the Bi-based compounds compared to Y123. Further, the two interlayer Josephson tunneling parameters ζ_2 and ζ_1 are expected to be much different from each other, whereas they are similar in Y123 [Lee et al., 1989; see above section]. For $\zeta_2 << \zeta_1$, the top of the n = 0 pair band is well below the higher n = 1 band, so the fluctuations in the three-dimensional (3D) temperature region are well-approximated by neglecting the contribution from the higher band [Klemm, 1990]. However, in the 2D region, even though the n = 1 band has a low T_c compared with the n = 0 band, the n = 1 band contributes significantly to the SFD in this region [Klemm, 1990]. Therefore, the effective number of complex s-wave order

parameters in the repeat distance s is taken to be one in the 3D region and two in the 2D region. Below, we fit the data in the 2D region only.

The observed $\chi(T)$ for $Bi_{1.8}Pb_{0.2}Sr_2CaCu_2O_{8+\delta}$ from Figs. 20 and 21 is replotted in Fig. 32. Our best fit of Eq. (20) to the data above ≈ 110 K is shown as the solid curve. Close to T_c, there is a deviation between experiment and theory. However, above ~ 110 K the fit is in good agreement with the data, implying that the system is in the 2D fluctuation regime above this temperature. The parameters of the fit are $\chi_o = 1.08(2) \times 10^{-7}$ cm^3/gm, $T_c = 91.1(1)$ K and $\xi_{ab}(0) = 20.4(2)$ Å. The value $T_c = 91.1$ K is lower than the observed onset temperature of 96 K from Fig. 17; this discrepancy is believed due to the presence of the higher T_c Bi2223 phase as an impurity. The diamagnetic behavior is further illustrated in a plot of $\log[-\chi_{dia}/T]$ versus $\log[(T-T_c)/T_c]$ in Fig. 33, where from Eq. (20) $\chi_{dia}(T) \equiv \langle\chi\rangle - \chi_o$; the slope above ~ 110 K is - 1, as expected. As in Fig. 32, we believe the deviation between experiment and theory in Fig. 33 below ~ 109 K is due to Bi2223 impurity phase. The value of $\xi_{ab}(0)$ is about 1.5 times that for $YBa_2Cu_3O_7$ [Lee et al., 1989] and somewhat less than values (23.5 to 27.1 Å) inferred from the results of upper critical field measurements on thin film [Kang et al., 1988] and single crystal [Beille et al., 1988; Martin et al., 1989; Palstra et al., 1988a] samples. Taking

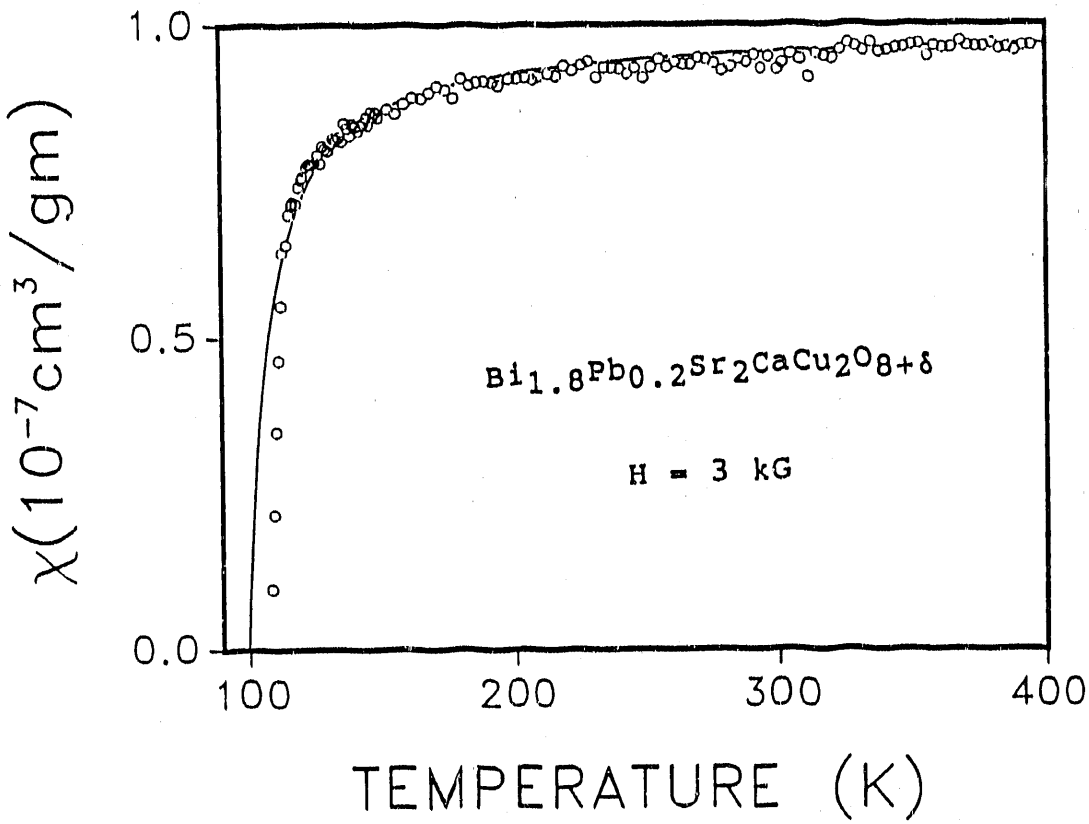

Fig. 32. Magnetic susceptibility χ vs. temperature of $Bi_{1.8}Pb_{0.2}Sr_2CaCu_2O_{8+\delta}$ in H = 3 kG. The solid curve is LD 2 dimensional theory

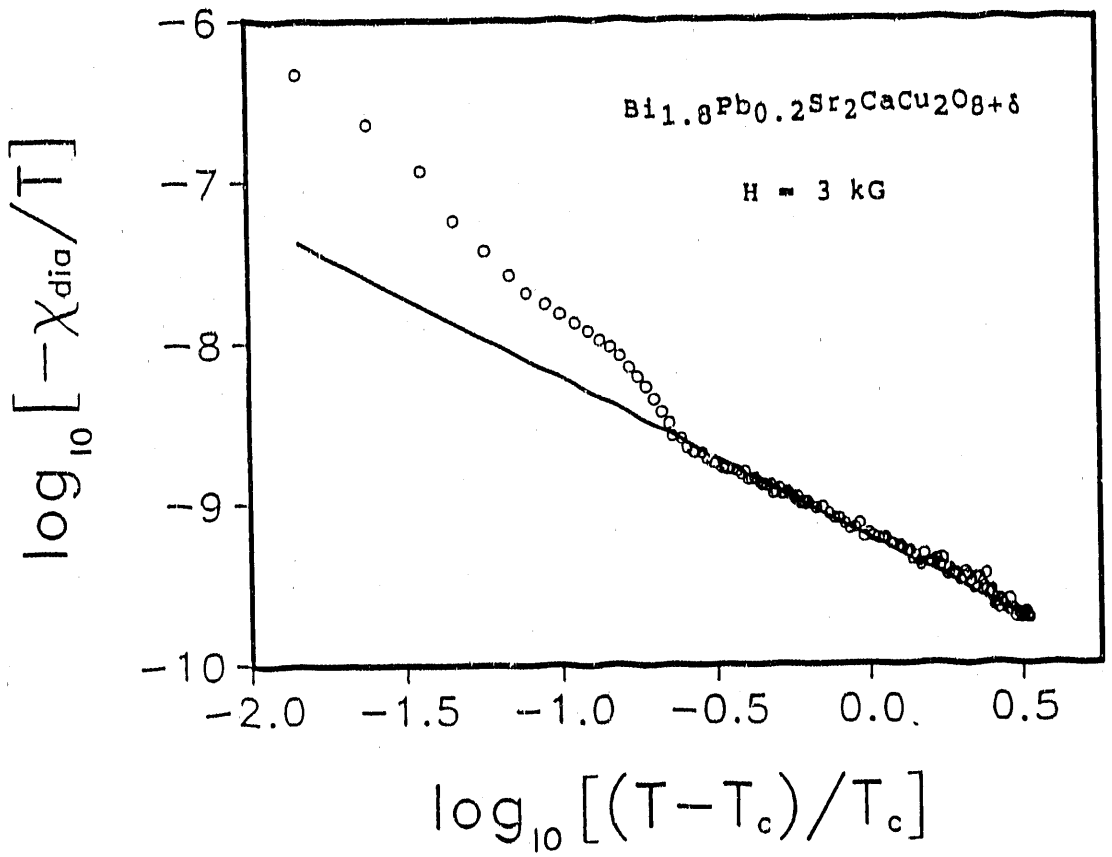

Fig. 33. log-log plot of the SFD divided by temperature χ_{dia}/T vs. reduced temperature $(T - T_c)/T_c$ from Fig. 32 for $Bi_{1.8}Pb_{0.2}Sr_2CaCu_2O_{8+\delta}$. Solid line is LD 2 dimensional theory

the pair mass anisotropy ratio $(M/m)^{1/2} \approx 50$ from Ref. [Naughton et al., 1988], one obtains $\xi_c(0) = \xi_{ab}(0)[m/M]^{1/2} \approx$ 0.4 Å. This very small $\xi_c(0)$ value is about 1/3 of that (1.2 Å) [Lee et al., 1989] for $YBa_2Cu_3O_7$, and both are of atomic dimensions.

For the $Bi_{2-x}Pb_xSr_2Ca_2Cu_3O_{10+\delta}$ system, there are three CuO_2 layers in the repeat distance s = 18.6 Å along the c-axis. Therefore, three interlayer Josephson tunneling parameters (ζ_1, ζ_2 and ζ_3) are present. As discussed above for Bi2212, if ζ_1, $\zeta_2 >> \zeta_3$ and $\zeta_1 \sim \zeta_2$, then in the 3D region the lower two bands dominate the fluctuations and g_{eff} = 2. However, in the 2D region all of the bands contribute to the fluctuation diamagnetism, and we take g_{eff} = 3 in this case. Fitting Eq. (20) to the data in Fig. 23a above 110 K for x = 0.20 yielded $\chi_o = 1.82(6) \times 10^{-7}$ cm^3/gm, T_c = 103(3) K and $\xi_{ab}(0)$ = 18.0(6) Å for g_{eff} = 3. A similar fit to the data in Fig. 23b for x = 0.25 gave $\chi_o = 2.32(5) \times 10^{-7}$ cm^3/gm, T_c = 107.8(3.2) K and $\xi_{ab}(0)$ = 11.8(4) Å. The fits are shown as the solid curves in Figs. 23a and 23b. Since ΔT_c is smaller for the x = 0.25 sample than for the x = 0.20 sample, the $\xi_{ab}(0)$ for the former sample is probably more reliable. This value of 11.8 Å is about half that for Bi2212 (x = 0.2), but similar to that (13.6 Å) [Lee et al., 1989] for $YBa_2Cu_3O_7$. Plots of $\log[-\chi_{dia}/T]$ vs. $\log[(T-T_c)/T_c]$ for the two Bi2223 samples are shown in Figs. 34a and 34b. As

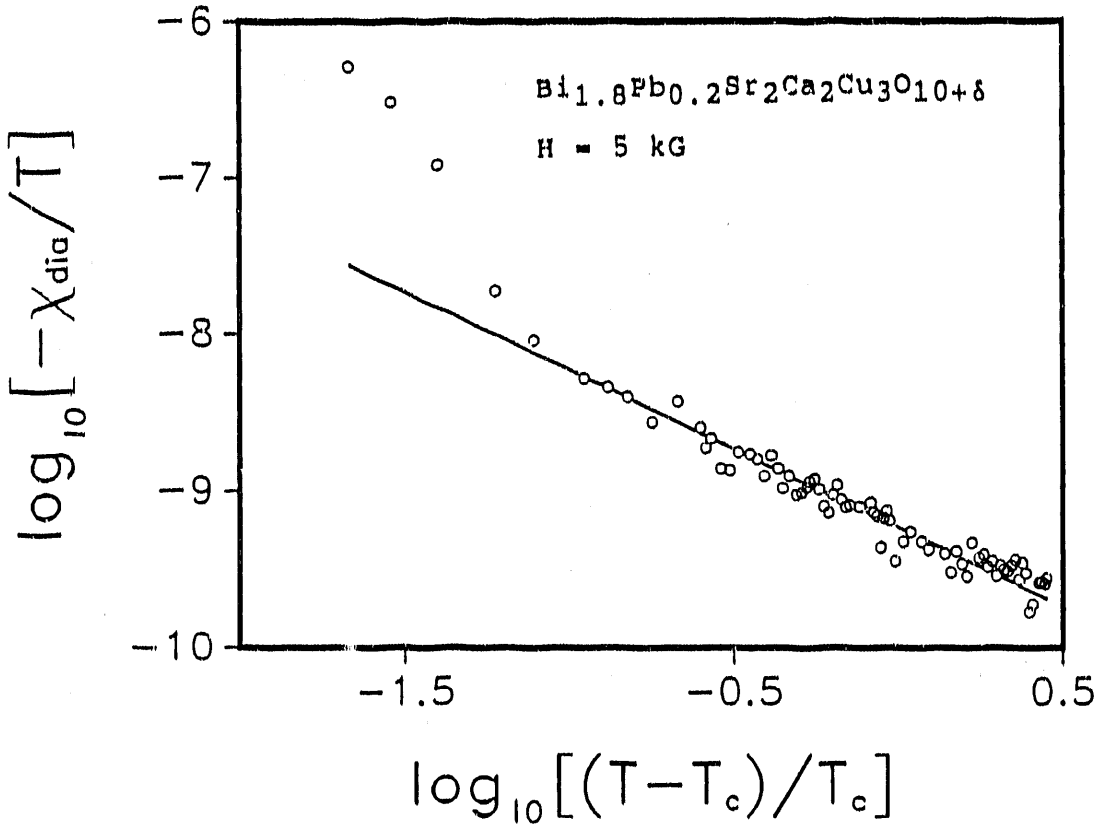

Fig. 34a. log-log plot of the SFD divided by temperature χ_{dia}/T vs. reduced temperature $(T - T_c)/T_c$ from Fig. 23a for $Bi_{1.8}Pb_{0.2}Sr_2Ca_2Cu_3O_{10+\delta}$. Solid line is LD 2 dimensional theory

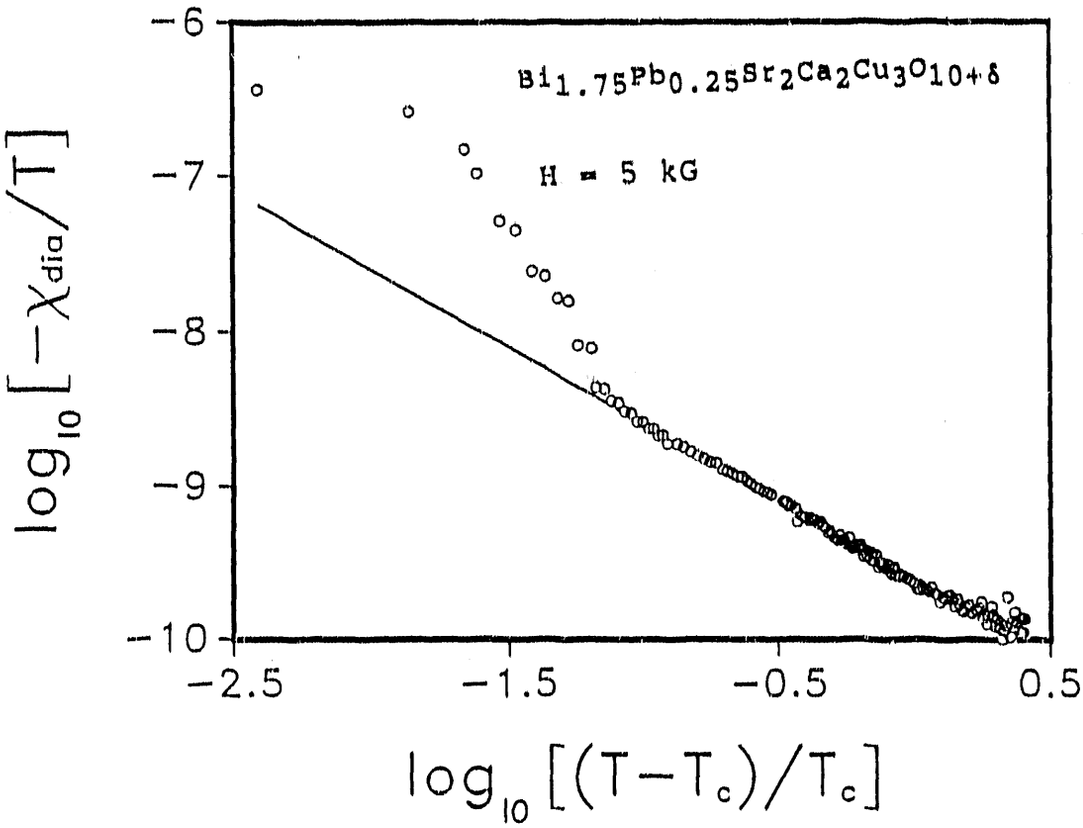

Fig. 34b. log-log plot of the SFD divided by temperature χ_{dia}/T vs. reduced temperature $(T - T_c)/T_c$ from Fig. 23b for $Bi_{1.75}Pb_{0.25}Sr_2Ca_2Cu_3O_{10+\delta}$. Solid line is LD 2 dimensional theory

for Bi2212, the deviations between theory (solid lines) and experiment below 110 K are believed to arise from the onset of bulk (nonfluctuating) superconductivity below this temperature, originating in these samples from the nonnegligible transition widths (see Figs. 22a and 22b).

We note that if $\zeta_1 \approx \zeta_2$, dynamic effects may be important in the fitted 2D regime, and the derived parameter values may be systematically in error by an unknown amount. A second consideration is that among the three CuO_2 layers in the layer repeat distance, one of the CuO_2 layers has no bridging oxygens, whereas the other two layers do. If the bridging oxygens turn out to have an important role in the superconductivity [Miller et al., 1990; Vaknin et al., 1989], then one might have $g_{eff} = 2$ rather than 3 in the 2D regime. In this case, the derived $\xi_{ab}(0)$ and $\xi_c(0)$ values would increase by a factor of 1.22. Finally, in a rigorous application of the theory to the data for Bi2223, one could compute numerically the fluctuation diamagnetism contributions from the three superpair bands in the 2D regime [Klemm, 1990].

Because of much stronger spin fluctuation contribution above T_c [Endoh et al., 1988; Shirane et al., 1987] in $La_{1.8}Sr_{0.2}CuO_{3.96}$ compared to the above other two systems, it is not easy to analyze the $\chi(T)$ data for $La_{1.8}Sr_{0.2}CuO_{3.96}$, in Fig. 35 which has $T_c \sim 31$ K [Johnston, 1989; Johnston et

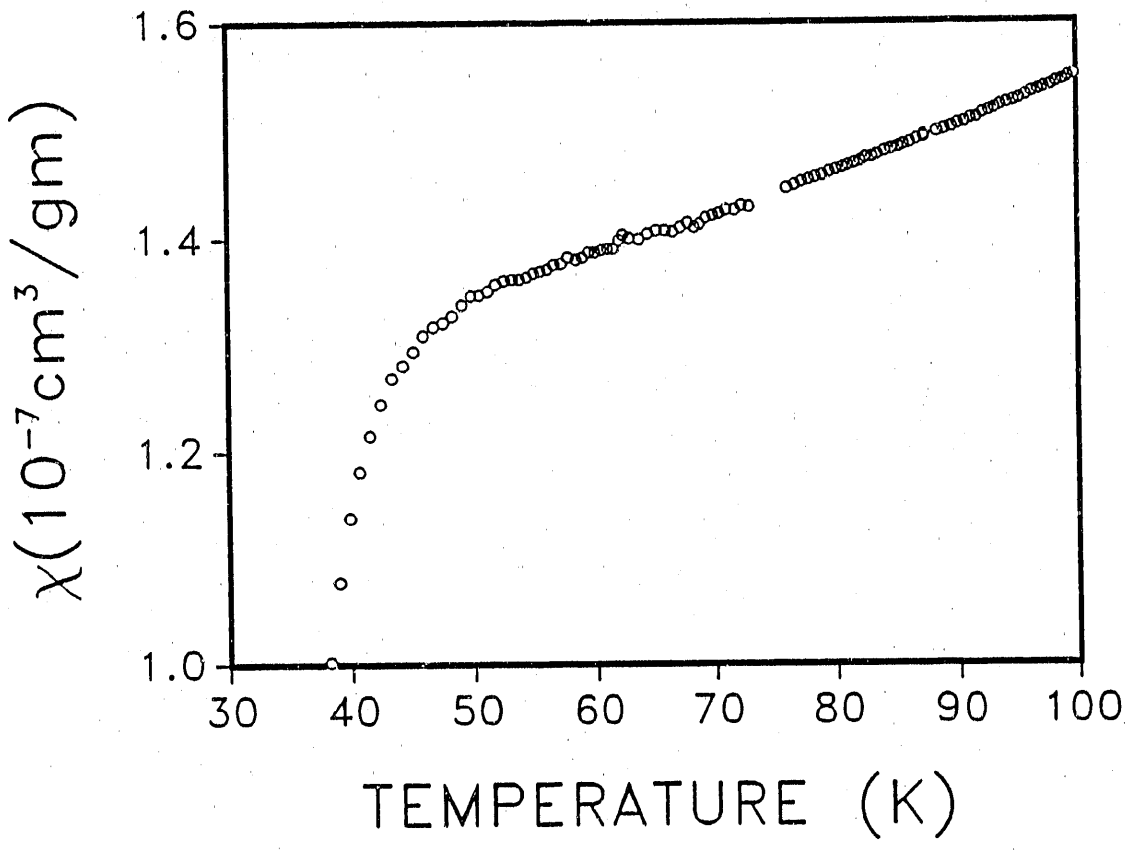

Fig. 35. Magnetic susceptibility χ vs. temperature of powder $La_{1.8}Sr_{0.2}CuO_{3.96}$ in H = 6 kG from references [Johnston, 1989; Johnston et al., 1988]

al., 1988]. The strong temperature dependent $\chi(T)$ above T_c is the superposition of contributions from spin fluctuations and superconducting fluctuations, but close to T_c we expect that the spin fluctuations will show smooth behavior. Therefore, the negative curvature close to T_c is dominated by the superconducting fluctuation effect as in the above other two systems.

B. Superconducting and Normal State Magnetic Susceptibility Anisotropy

We would first like to re-emphasize [Lee and Johnston, 1990b; Lee et al., 1989] that the **observed** susceptibility data for pellet and grain aligned powder $YBa_2Cu_3O_7$ in Fig. 7 and Fig. 13 exhibit no evidence for a Curie-Weiss contribution to $\chi(T)$. Herein, we will discuss the results from aligned $YBa_2Cu_3O_7$ samples. The data increase monotonically with temperature for both field orientations, exhibiting **negative** curvature below ~ 200 K. Between ≈ 200 K and 400 K, our data increase approximately linearly with temperature, confirming the intrinsic behavior deduced previously based on a study of the variation of $\chi(T)$ with oxygen content in this system [Johnston et al., 1988; see also Yamaguchi et al., 1989]. Other groups have also observed directly (without Curie-term correction) that $d\chi/dT$

> 0 above T_c [Kanoda et al., 1988a and 1988b; McGuire et al., 1987]. However, most published data are dominated by the presence of magnetic defects and/or impurity phases, yielding either nearly temperature independent $\chi(T)$ behavior or $d\chi/dT$ < 0 above T_c. The negative curvature in our data from T_c = 91 K to ≈ 200 K arises from a combination of superconducting fluctuation diamagnetism and a temperature dependent normal state background susceptibility [Johnston et al., 1988; Kanoda et al., 1988a and 1988b; Klemm, 1990; Lee et al., 1989]. Above ≈ 200 K, the superconducting fluctuation diamagnetism is negligible, and the temperature dependence of χ most likely arises from antiferromagnetic spin fluctuations [Johnston, 1989; Johnston et al., 1988].

Of particular interest here is the anisotropy in $\chi(T)$ in $YBa_2Cu_3O_7$ above ~ 200 K. For comparison with the present measurements, we list in Table I values of χ_c, χ_{ab} and $\Delta\chi$ for $YBa_2Cu_3O_7$ and for several other members of the high T_c cuprate family obtained from other studies [Cheong et al., 1987; Fukuda et al., 1988; Junod et al., 1988; Miljak et al., 1988 and 1989; Takigawa et al., 1989; Vaknin et al., 1990]. Because of the presence of variable amounts of paramagnetic and ferromagnetic impurities in various samples, which are sometimes not accounted for, perhaps the most reliable quantity to compare is $\Delta\chi$. Our value of $\Delta\chi$ for $YBa_2Cu_3O_7$ is slightly larger than those of Miljak et al. [1988 and 1989]

Table I. Experimental magnetic susceptibility data for H || c (χ_c) and H ⊥ c (χ_{ab}) at 300 K for $YBa_2Cu_3O_7$ and several other compounds. The χ data of 3, 4, 5, 6 and 9 are corrected for the contribution of paramagnetic impurities. The data for $Sr_2CuO_2Cl_2$ are for a temperature of 400 K

	Compound	T_c	χ_c	χ_{ab}	$\Delta\chi$	$\langle\chi\rangle$	Ref.
1	$YBa_2Cu_3O_7$	91	41.0	25.2	15.8	30.5	Lee and Johnston, 1990b
2	"	87	---	---	13.8	---	Miljak et al., 1988
3	"	87	41.3	28.5	12.8	32.8	Fukuda et al., 1988
4	"	92	33.9	25.0	8.9	28.0	Takigawa et al., 1989
5	"	90	---	---	---	29.3	Junod et al., 1988
6	"	92	---	---	---	27.7	Junod et al., 1988
7	La_2CuO_4	--	10.9	3.2	7.7	5.8	Cheong et al., 1987
8	$La_{1.9}Sr_{0.1}CuO_4$	31	19.7	13.1	6.6	15.3	Fukuda et al., 1988
9	$Sr_2CuO_2Cl_2$	--	9.1	1.8	7.3	4.2	Vaknin et al., 1990

T_c in K unit and χ in 10^{-5} cm^3/mole unit.

and Fukuda et al. [1988], obtained for single crystals with a somewhat lower T_c, and is about 80 % larger than recently reported [Takigawa et al., 1989] for a sample of $YBa_2Cu_3O_7$ grain-aligned powder in epoxy. From our large $\Delta\chi$ value, we conclude that the degree of grain-alignment achieved in our experiments is essentially 100 %; because our grain-aligned samples are free-flowing powders enclosed in quartz tubes, it was not possible to verify the degree of grain alignment using X-ray diffraction techniques. The reason that our value of $\Delta\chi$ is larger than observed [Fukuda et al., 1988; Miljak et al., 1988 and 1989] for the two single crystals may be that the substantial number of paramagnetic impurities present in those crystals have anisotropic susceptibilities that partially cancel the anisotropy intrinsic to $YBa_2Cu_3O_7$. A comparison of $\Delta\chi$ for a ceramic compact with our value and those in references [Miljak et al., 1988 and 1989] has been useful in estimating the degree of grain-alignment in the compact [Lusnikov et al., 1989]. It is noteworthy that the $\Delta\chi$ values for nonmetallic La_2CuO_4 and $Sr_2CuO_2Cl_2$ and for metallic $La_{1.88}Sr_{0.12}CuO_4$ in Table I are the same to within $\pm$ 7 %. This similarity suggests that the local electronic structure around the Cu ions in the CuO_2 planes is similar in these compounds.

To analyze our data in Table I, we separate χ for each field direction into orbital and spin contributions:

$$\chi(T) = \chi^{orb} + \chi^{spin}(T), \tag{21}$$

where χ^{orb} is assumed independent of temperature whereas χ^{spin} may depend on temperature. In the absence of superconducting fluctuation diamagnetism (i.e., above ≈ 200 K), we assume

$$\chi^{orb} = \chi^{dia} + \chi^{VV}, \tag{22}$$

which consists of the isotropic core diamagnetism χ^{dia} and the paramagnetic, and in general anisotropic, Van Vleck contribution χ^{VV} (we absorb possible contributions from Landau diamagnetism into χ^{spin}). From Eqs. (21) and (22),

$$\Delta\chi \equiv \chi_c - \chi_{ab} = \Delta\chi^{VV} + \Delta\chi^{spin} . \tag{23}$$

Estimates of χ^{spin} and χ^{VV} have been made previously for $YBa_2Cu_3O_7$. From the observed variation in the heat capacity jump at T_c with derived temperature independent susceptibility, Junod et al. [1988] derived the values in Table II. Analysis of the shifts from nuclear resonance experiments yielded other estimates, shown in Table II [Pennington et al., 1989; Takigawa et al., 1989; Walstedt et al., 1988]. Also shown in Table II are the predictions from

Table II. Derived contributions to the susceptibility, all in units of 10^{-5} cm^3/mole. Cu(2) and Cu(1) refer respectively to the Cu in the planes and chains of $YBa_2Cu_3O_7$

Entity	χ^{dia}	χ_c^{VV}	χ_b^{VV}	χ_a^{VV}	$\Delta\chi^{VV}$	$\langle\chi^{VV}\rangle$	χ^{spin}	Ref.
$YBa_2Cu_3O_7$	-17.5	---	---	---	---	14.5	32.5	a
"	-17.5	---	---	---	---	$\geq$22.9	$\leq$21.6	b
Cu(2)	---	12.7	2.9	2.9	9.8	6.2	18.8	c
Cu(2)	---	9.6(6)	1.7(2)	1.7(2)	7.9(7)	4.3(3)	---	d
Cu(1)	---	2.2(6)	3.0(2)	8.4(2)	-3.5(7)	4.5(3)	---	d
$YBa_2Cu_3O_7$	-17.5	21.3(10)	6.4(4)	11.8(4)	12.2(12)	13.2(12)	30.1	d
							H || c	
							33.4	
							H $\perp$ c	

$YBa_2Cu_3O_7$	"	"	"	"	"	"	37.2 H ∥ c 33.6 H ⊥ c	e
Sc_2CuO_4	-11	4.0	1.5	1.5	2.5	2.3	---	f

a = Junod et al., 1988.

b = Walstedt et al., 1988.

c = Pennington et al., 1989.

d = Takigawa et al., 1989.

e = Lee and Johnston, 1990b.

f = Leung et al., 1988.

band theory for χ^{dia} and χ^{VV} of hypothetical Sc_2CuO_4 [Leung et al., 1988]; the χ^{VV} values are smaller than inferred for Cu(2) ions in the CuO_2 planes in $YBa_2Cu_3O_7$.

Takigawa et al. [1989] derived their values of χ^{spin} using their anisotropic χ data in Table I. Since we find that the intrinsic anisotropy is much larger than reported in that reference, we have re-computed χ^{spin} using Eqs. (21) and (22), their values for χ^{dia} and χ^{VV}, and our χ anisotropy data, and the results are shown in Table II. The spin susceptibility is larger by about 10 % for **H** || **c** than for **H** $\perp$ **c**, rather than the reverse [Takigawa et al., 1989], consistent with the sign of $\Delta\chi^{spin}$ in $Sr_2CuO_2Cl_2$ [Vaknin et al., 1990]; the latter χ^{spin} anisotropy probably arises from anisotropy in the spectroscopic splitting factor g of the spin 1/2 Cu^{+2} ions [Vaknin et al., 1990]. We note that all the derived values of χ^{spin} for $YBa_2Cu_3O_7$ in Table II would shift upwards by 1.8×10^{-5} cm^3/mole if the value of χ^{dia} computed from reference [Selwood, 1956] (-19.3×10^{-5} cm^3/mole) were substituted for the value in Table II.

C. DC Resistivity

Unlike the almost temperature independent background in magnetic susceptibility, there is a strong temperature dependent background above T_c in resistance. Therefore to

separate the fluctuation part only from the measured resistance is not easy. But we can expect metallic property which shows linear temperature dependence in resistance far above T_c. In Fig. 5, there is an almost linear region between 150 K and 230 K and significant bending down behavior due to fluctuation effect can be seen below ~ 120 K, which is consistent with the result of magnetic susceptibility. Besides the fluctuation effect, the apparent anomaly around 250 K, which might be related with a structural phase transition [Calemczuk et al., 1988; Cheong et al., 1987; Johnston et al., 1987 and 1988; Laegreid et al., 1987; Miljak et al., 1988 and 1989], is, in a sense, consistent with those results. Even though there are some reports indicating the same anomaly in single crystal, polycrystalline pellet and powder samples, the origin of anomalies around 250 K needs further clarification (see below).

D. Heat Capacity

a. Near T_c

Here we will discuss the results in Fig. 26 of the set of four sequential C(T) measurements using the continuous heating method at Berkeley. The differences between the first data set A in zero field and the subsequent zero field sets B and D are striking. Near T_c, the heat capacity in B

is about 6% less than in A. Using the traditional method of entropy balance to estimate the heat capacity jump at T_c (but see below), one obtains $\Delta C/T_c$ = 32 mJ/K^2-mole $YBa_2Cu_3O_7$ for B, which is 42% less than the value of 55 mJ/mole-K^2 for A. These differences may be compared with the absolute accuracy of each measurement of 0.5% and with an expected reproducibility much better than this. Thus, these differences are real and must arise from a thermal history dependence of the heat capacity. Smaller differences are apparent between the data sets B and D. In D, a sharp anomaly at about 74 K is observed which appears to be smeared out in sets A and B; this anomaly occurs at about the same temperature as that seen in the magnetization data at 50 kG in Fig. 9. The origin of these anomalies is unknown.

In an applied field of 70 kG, the heat capacity in a plot of C/T vs. T (data set C) shows a smooth, broad peak at T_c and only a slight downward shift in the peak temperature compared with the zero field data, as previously reported [Fisher et al., 1988b; Salamon et al., 1988]. As noted above, a sharp anomaly was observed at 74 K in data set D; these data were taken in zero field after the high field set C was obtained. Thus, although it seems unlikely, the magnetic field history of the sample may be involved with the apparent irreproducibility of C(T) in Fig. 26, in addition to the above influence of the thermal history. The C/T data set

C in H = 70 kG is larger in magnitude than the zero field set B between ≈ 75 K and ≈ 85 K, whereas it is smaller between ≈ 85 K and ≈ 93 K. In the latter region, the entropy change $\Delta S = S(0) - S(70\ kG) \approx 83$ mJ/mole-K, and in the former it is -55 mJ/mole-K, yielding a net entropy change $\Delta S_{net} = 28$ mJ/mole-K. This apparent nonconservation of entropy is not yet understood; it could conceivably arise through the above thermal history dependence of C(T) or from the limited temperature range of the measurements in Fig. 26.

Due to lack of detailed knowledge of the dominant lattice contribution to the heat capacity of high T_c cuprate superconductors near T_c, it is not clear how to accurately separate the observed heat capacity into electronic and lattice parts. A further complication is that close to T_c, the thermodynamic and electronic transport properties of the cuprate superconductors are dominated by the influence of superconducting fluctuations [Klemm, 1990]. Therefore, without taking into account the fluctuation term carefully, one might infer an inaccurate mean-field heat capacity jump ΔC at T_c, which would then lead to an inaccurate estimate of the normal state Sommerfeld coefficient γ if one used, e.g., the BCS result relating γ to ΔC ($\Delta C/\gamma T_c = 1.43$).

We now consider the fluctuation contribution to the observed C(T) to lowest order. After references [Klemm, 1990; Lee et al., 1989], we utilize a model in which there

are two conducting layers per unit cell in $YBa_2Cu_3O_7$, each of which is assigned one complex s-wave order parameter; the layers are coupled by Josephson tunneling. Above T_c, the relationship between the superconducting fluctuation heat capacity $C_{fl}^{+}(T)$ and the superconducting fluctuation diamagnetism $\chi_c^{fl}(T)$ with $\mathbf{H} \parallel \mathbf{c}$ is given by [Klemm, 1990]

$$C_{fl}^{+}(T) = - \frac{3\phi_0^2 \, \chi_c^{fl}(T)}{4\pi^2 T \xi_{ab}^4(0)} \propto -\chi_c^{fl}(T)/T \, , \qquad (24)$$

where ϕ_0 is the flux quantum hc/2e and $\xi_{ab}(0)$ is the zero-temperature Ginzburg-Landau coherence length within a CuO_2 layer. Below T_c in the three-dimensional fluctuation region, the fluctuation heat capacity $C_{fl}^{-}(T)$ is reduced from $C_{fl}^{+}(T)$ by ~ $1/\sqrt{2}$ [Brand and Doria, 1988; Inderhees et al., 1988; Klemm, 1990; Muzikar, 1988].

Using Eq. (24), the measured $\chi_c^{fl}(T)$ and the derived $\xi_{ab}(0)$, one can estimate the contributions $C_{fl}^{+}(T)$ and $C_{fl}^{-}(T)$ to the measured C(T) above and below T_c, respectively. Then, by subtracting these contributions from C(T), an estimate of the sum of the lattice and electronic heat capacities in the absence of superconducting fluctuations (mean-field heat capacity C_{MF}) can be obtained. Here, we do not account for the superconducting transition width [Klemm, 1990; Sharifi et al., 1989] arising from chemical inhomogeneity in the sample. Therefore, the calculated fluctuation heat capacity diverges

close to T_c (Fig. 36), in contrast to our observations. For temperatures somewhat removed from the average T_c, we expect the calculated fluctuation contributions to more accurately apply to the observations.

In Fig. 37a, we replot the observed C/T vs. T data set D in Fig. 26 (crosses) and $C_{MF}(T)$ derived as described above (open circles) for the temperature ranges 81 - 85 K and 95 to 101 K, using $\xi_{ab}(0)$ = 13.6 Å and $\chi_c^{fl}(T)$ from reference [Lee et al., 1989]. For the temperature region closer to T_c, we linearly extrapolated $C_{MF}(T)$ on both sides of T_c to T_c (solid lines). T_c was taken to be 90.8 K, the temperature at which a pulsed C(T) data set taken at Ames over a limited temperature range spanning T_c (not presented here) showed a sharp cusp. This is also the temperature at which the magnetization data for H = 50 G in Fig. 9 showed a sharp onset, and is the average peak temperature of C(T)/T for data sets A, B and D in Fig. 26. From Fig. 37a, the mean-field heat capacity jump at T_c is inferred to be $\Delta C_{MF}(T_c)/T_c \approx 33$ mJ/mole-K^2, coincidentally nearly the same as the above value $\Delta C/T_c$ = 32 mJ/mole-K^2 obtained using conventional entropy balance near T_c. The value of ΔC_{MF} yields $\gamma_{MF} \approx 23$ mJ/mole-K^2 using the above BCS weak coupling mean-field result. This γ_{MF} value is less than most reported γ values [Fisher et al., 1988b; Junod et al., 1989; Stupp and Ginsberg, 1989]. However, this value is consistent with the value (26 mJ/mole-

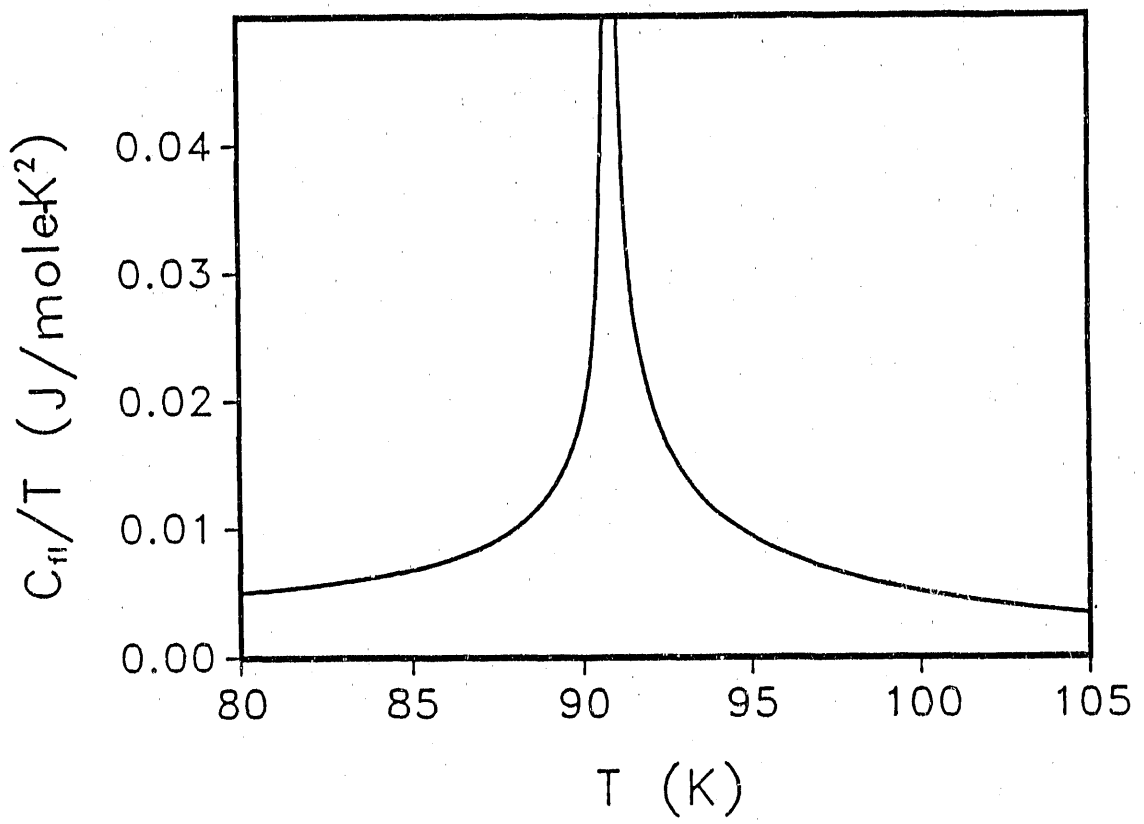

Fig. 36. Superconducting fluctuation heat capacity divided by temperature C_{fl}/T vs. T, calculated using the data and parameters from reference [Lee et al., 1989]

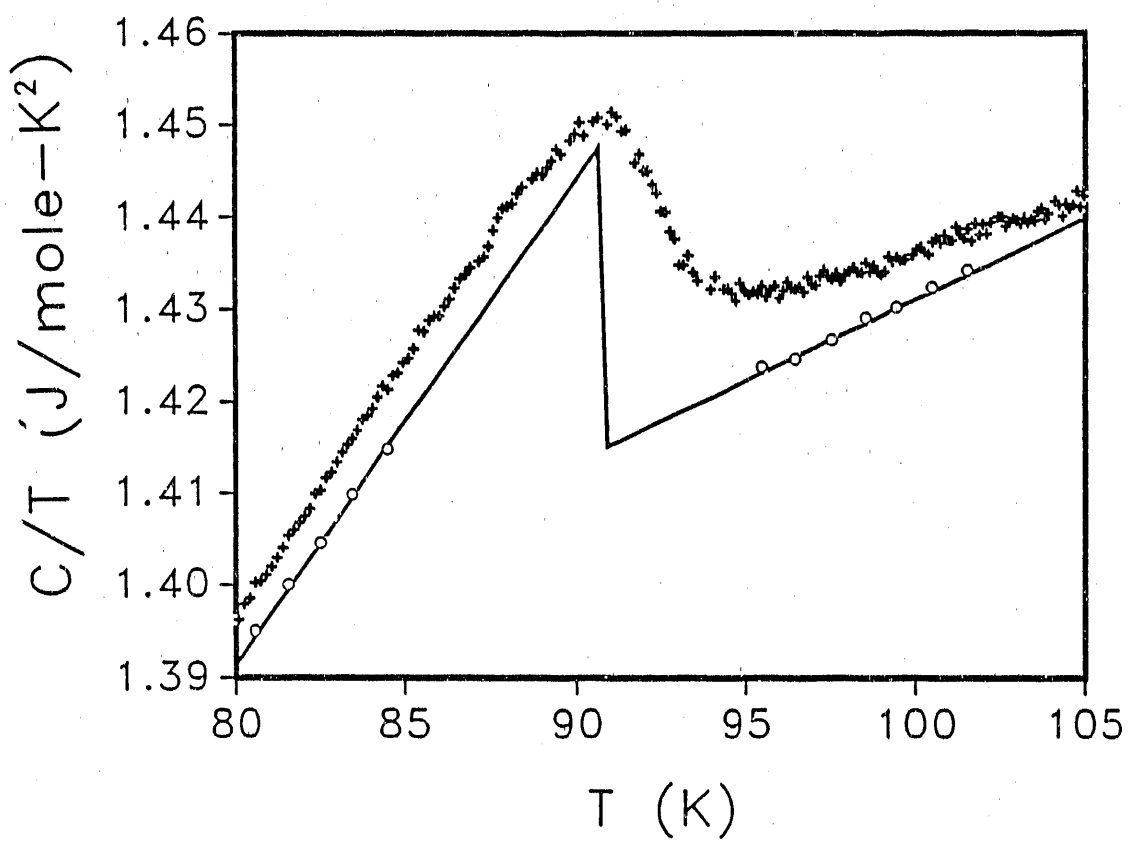

Fig. 37a. Observed heat capacity (plus symbols) from data set D in Fig. 26 compared with the sum of the estimated mean-field electronic and lattice heat capacities (solid lines)

K^2) obtained from a free electron gas analysis of the spin susceptibility [Lee and Johnston, 1990b] above T_c derived from $\chi(T)$ data as in Figs. 7 and 13. We estimate the density of states at the Fermi energy to be $D(E_F)$ = 3.3 states/eV-Cu atom using the relation $\gamma_{MF} = \pi^2\mu_B{}^2D(E_F)/3k_B$.

A similar analysis of the C(T) data set A in Fig. 26 is shown in Fig. 37b. Here, we find $\Delta C_{MF}/T_c$ = 64 mJ/mole-K^2, and γ_{MF} = 44 mJ/mole-K^2 in the BCS weak coupling limit. The $\Delta C_{MF}/T_c$ value is significantly larger than the above value $\Delta C/T_c$ = 55 mJ/mole-K^2 obtained using conventional entropy balance near T_c.

b. Between 0.4 K and 10 K

The Ames and Berkeley pulse calorimeter measurements are in agreement below ~ 5 K, as seen in Fig. 27. At higher temperatures, a large difference becomes apparent; both measurements are accurate to 1-2% below 30 K, so these differences are real. The source of this difference between the two C(T) data sets above 5 K is not known. This difference amounts to a difference in the lattice heat capacity apparently induced by change in the thermal and/or magnetic field history of the sample, as documented near T_c in Fig. 26 and above 120 K in Fig. 29. The two C(T) data sets in Fig. 27 yield Debye temperatures differing by more than 30 K (see below).

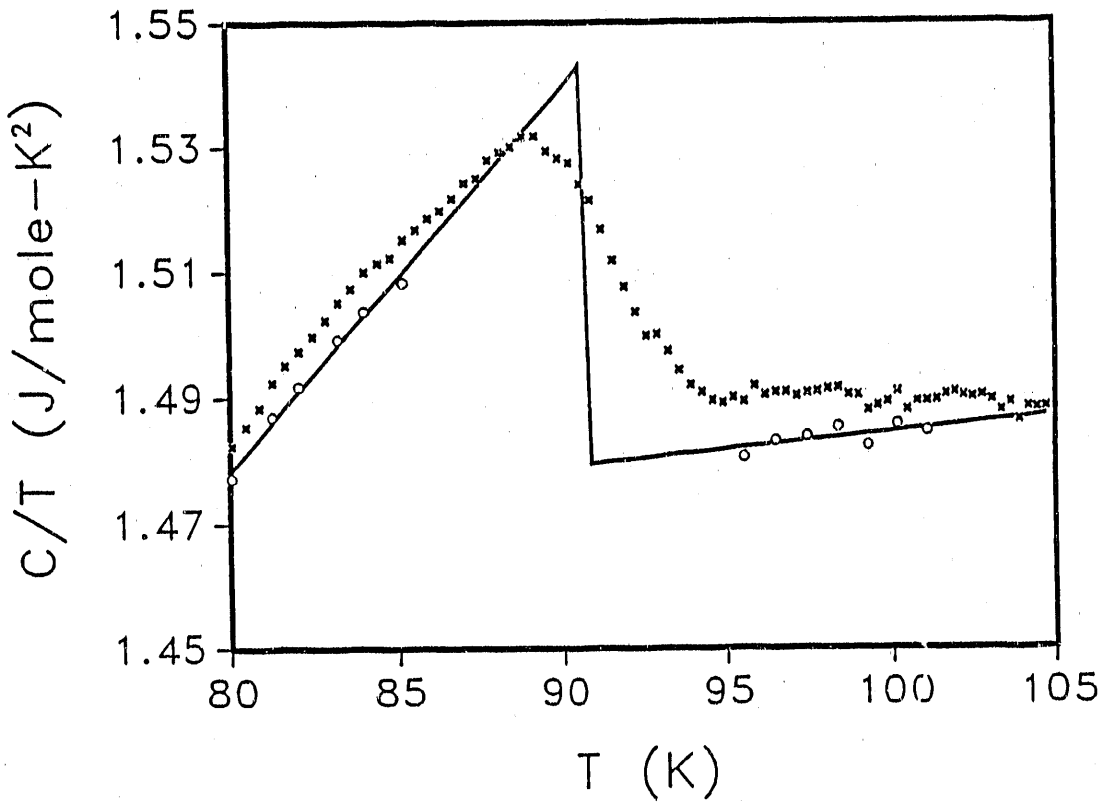

Fig. 37b. Same as Fig. 37a, but for data set A from Fig. 26

In Figs. 27 and 28, the low-temperature upturn in C(H = 0)/T starts near 2 K, arising primarily from magnetically isolated Cu^{+2} local magnetic moments. A common impurity in $YBa_2Cu_3O_7$ samples is $BaCuO_2$ [Eriksson et al., 1989; Kuentzler et al., 1988] and is one of the components of the eutectic impurity present in our samples as documented above. Some samples of $BaCuO_2$ exhibit C(T)/T behavior nearly independent of T at low T, while others show an upturn [Eckert et al., 1988; Kuentzler et al., 1988]. Considering the presence of this impurity phase as well as localized Cu^{+2} moments in our samples of $YBa_2Cu_3O_7$, we fit our zero-field C(T) data with the expression

$$C(T) = \frac{A_{-2}}{T^2} + \gamma^*(0)T + B_3T^3 + B_5T^5 + B_7T^7 \quad , \qquad (25)$$

where the first term accounts for the low T upturn, the second is a linear term of unknown origin, and the remaining terms are due to the lattice contribution. Fitting Eq. (25) to the zero-field data in Fig. 28 yields A_{-2} = 13.1(3) mJ-K/mole, $\gamma^*(0)$ = 5.0(1) mJ/mole-K^2, B_3 = 0.33(1) mJ/mole-K^4, B_5 = 4.22(8) x 10^{-3} mJ/mole-K^6, and B_7 = 2.02(4) x 10^{-5} mJ/mole-K^8. From the value of B_3, the calculated Debye temperature Θ_D = 422(8) K, which is similar to reported values [Fisher et al., 1988b; von Molnar et al., 1988; Swenson et al., 1989]. For the Ames C(T) data set in Fig.

27, $\gamma^*(T = 0) = 5.7(6)$ mJ/mole-K^2, which is equal within experimental error with the value from the Berkeley data, whereas $\Theta_D = 456$ K, about 30 K larger than the Berkeley value. The large difference between the Ames and Berkeley data sets between 5 K and 10 K is real, as noted above, and apparently arises from the different thermal histories of the sample in the two measurements.

It is known that a sufficiently high magnetic field can cause the C(T)/T upturn for H = 0 to become a Schottky-like anomaly [Gopal, 1966]. In Fig. 28 for H = 70 kG, there is indeed a broad maximum in C(T)/T near 3 K and there is a sharp upturn at much lower temperature. This sharp upturn is from the coupling between the magnetic field and the Cu nuclear moments [Gopal, 1966; Lounasmaa, 1962]. To analyze the H = 70 kG results, we used the expression

$$C(T) = \frac{A_{hf}}{T^2} + n_i C_{Sch}(T) + \gamma^*(H)T + C_{lattice} \quad , \qquad (26)$$

with

$$C_{Sch}(T) = R \frac{\delta^2}{T^2} \frac{e^{\delta/T}}{[1 + e^{\delta/T}]^2} \quad , \qquad (27)$$

where the first term in Eq. (26) is due to the hyperfine interaction, the next term is the Schottky anomaly due to n_i mole fraction of isolated Cu^{+2} defects, $C_{Sch}(T)$ is the heat capacity per mole of these defects, and $\gamma^*(H)T$ is the linear

contribution in the 70 kG magnetic field. In Eq. (27), R is the molar gas constant and δ is the energy splitting in K of the spin 1/2 Zeeman levels in the field H: $\delta = \mu_B H/k_B$, assuming a gyromagnetic factor g = 2. From a fit to the data on a CT^2 versus T^3 plot at low T, we find A_{hf} = 0.47(1) mJ-K/mole $YBa_2Cu_3O_7$, which is close to the theoretical value of 0.50 mJ-K/mole for the three moles of Cu, two of Ba and one of Y nuclei in one mole of $YBa_2Cu_3O_7$ [Ahrens et al., 1988; Fisher et al., 1988a and 1988b]. $\gamma^*(H = 70\ kG)$ is found to be 6.5(2) mJ/mole-K^2. From $\gamma^*(H = 0)$ and $\gamma^*(H = 70\ kG)$, we have $\partial\gamma^*/\partial H \sim 0.021$ mJ/mole-K^2-kG, which is similar to the reported value [Fisher et al., 1988a]. By subtracting the hyperfine, linear and lattice (from the H = 0 fit) terms from the observed C(T, H = 70 kG) data according to Eq. (25), the experimental isolated Cu^{+2} contribution to C(T, H = 70 kG) was computed and is plotted vs. T in Fig. 38 (open circles). Also shown is the theoretical Schottky contribution $n_i C_{Sch}(T)$ from Eq. (27) for n_i = 0.0044 (solid curve); the good agreement attests to the accuracy of applying Eq. (26) to fit the data.

The impurity mole fraction due to isolated Cu^{+2} defects, n_i, was found above to be 0.0044(1) mole Cu^{+2}/mole $YBa_2Cu_3O_7$. This could arise from isolated defects in the $YBa_2Cu_3O_7$ majority phase lattice itself and/or in the $BaCuO_2$ impurity lattice. The latter possibility is supported by the magnetic

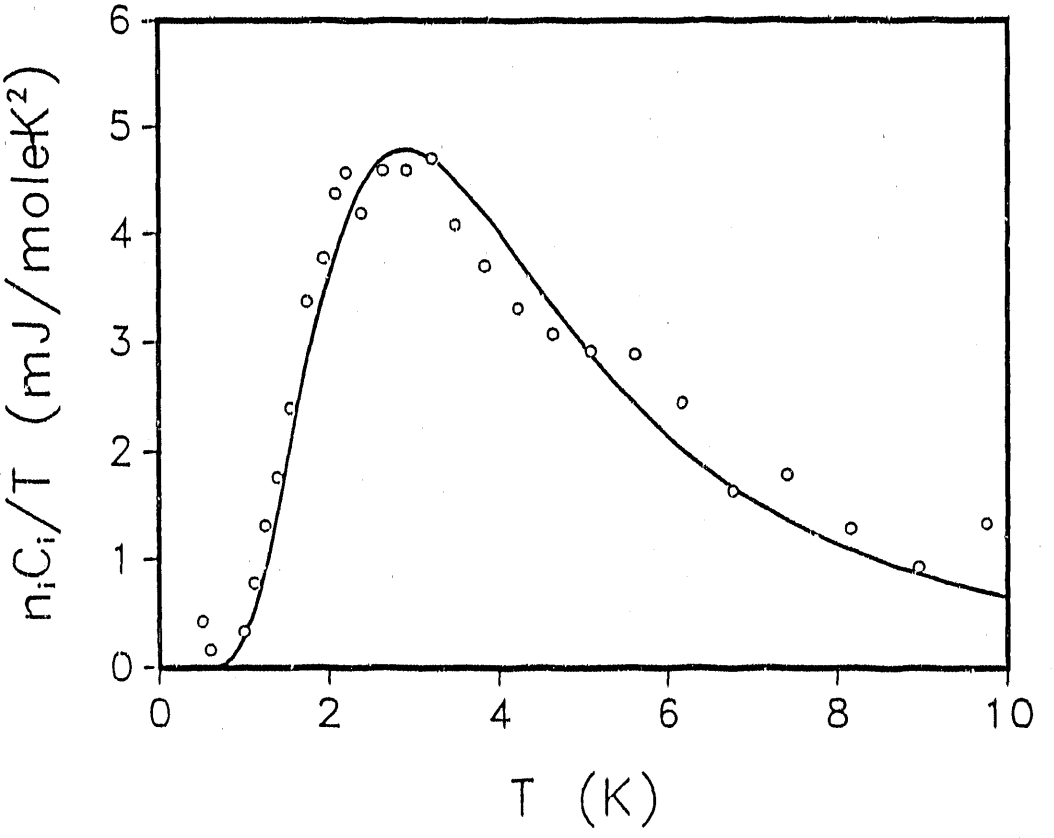

Fig. 38. Heat capacity of the magnetically isolated Cu^{+2} magnetic defects derived from the observed data divided by temperature n_iC_i/T vs. T for $YBa_2Cu_3O_7$ pellet sample in a field of 70 kG (open circles). The solid curve is the theoretical prediction for n_i = 0.0044 moles of spin 1/2 defects per mole of $YBa_2Cu_3O_7$

field dependence of C(T) for $BaCuO_{2+x}$ [Ahrens et al., 1988]. The DTA measurements revealed about 0.6 wt.% of Y-Ba-Cu-O eutectic impurity phase in our $YBa_2Cu_3O_7$ sample, corresponding to 0.3(1) wt.% $BaCuO_2$. If the upturn in the zero field C(T) and the Schottky-like anomaly in C(T, H=70 kG) are generated from all of the Cu^{+2} moments in this amount of $BaCuO_2$, one would expect n_i = 0.014(5) mole Cu^{+2}/mole $YBa_2Cu_3O_7$, significantly greater than the observed n_i value. Thus, the bulk of the Cu^{+2} ions in the $BaCuO_2$ impurity phase do not contribute to the zero-field low-temperature upturn in the observed C(T).

Our nonzero $\gamma^*(T = 0, H = 0) \equiv \gamma^*(0)$ value evidently arises from the $YBa_2Cu_3O_7$ phase and/or the bulk $BaCuO_2$ (BCO) impurity phase (the contribution to $\gamma^*(0)$ from CuO impurity is negligible). We consider first the second possibility. The above value of 0.3(1) wt.% $BaCuO_2$ corresponds to n_{BCO} = 0.014(5) moles $BaCuO_2$/mole $YBa_2Cu_3O_7$. For $BaCuO_2$ heat-treated in a way similar to the preparation of our sample of $YBa_2Cu_3O_7$, one expects γ_{BCO} < 80 mJ/mole $BaCuO_2$ from published heat capacity data [Kuentzler et al., 1988]. Thus, we expect the impurity contribution γ_i to our measured $\gamma^*(0)$ for $YBa_2Cu_3O_7$ to be given by $\gamma_i = n_{BCO}\gamma_{BCO}$ < 1.1(4) mJ/K^2-mole $YBa_2Cu_3O_7$. This value is much less than the above observed values $\gamma^*(0)$ = 5.0(1) and 5.7(6) mJ/mole-K^2. We conclude that the intrinsic $\gamma(0)$ associated with the

$YBa_2Cu_3O_7$ lattice itself in our pellet sample is $\gamma(0) \approx 4.0$ mJ/mole-K^2. A similar value was obtained by Reeves et al., [1989] based on a Raman scattering determination of the $BaCuO_2$ concentration, coupled with low temperature C(T) measurements.

The question now arises as to whether this $\gamma(0)$ is intrinsic to a perfectly ordered $YBa_2Cu_3O_7$ lattice, or whether it arises in some way from the presence of lattice disorder. One scenario presented recently is that lattice disorder and the presence of resultant localized Cu^{+2} magnetic moments produces normal (nonsuperconducting) regions in the sample, resulting in a nonzero $\gamma(0)$ and an upturn in the zero field C(T)/T associated with those regions [Phillips et al., 1989 and 1990].

c. Above 120 K

Our $\chi(T)$ data for the pellet sample in Fig. 29 partially confirm previous $\chi(T)$ measurements [Johnston et al., 1988; Miljak et al., 1988 and 1989] that anomalies sometimes occur at ~ 240 K, ~ 330 K, or both. The data for this sample show only the anomaly near 330-350 K with no obvious anomaly near 240 K. Our C(T) data for the pellet sample taken on warming show an anomaly at ~ 330 - 350 K, and therefore appear to confirm that the corresponding anomaly in $\chi(T)$ is a bulk effect and not due to impurity

phases. The origin of these anomalies is not known. However, the anomaly in the C(T) data for the pellet sample was not unambiguously observed on cooling, possibly due to the above thermal history dependence of C(T). χ(T) and C(T) data for our powder sample taken on warming from 120 K to 400 K and cooling from 400 K to 120 K showed no anomalies.

VI. CONCLUSIONS

We have presented $\chi(T)$ data for $YBa_2Cu_3O_7$, $Bi_{2-x}Pb_xSr_2CaCu_2O_{8+\delta}$ ($0.0 \leq x \leq 0.5$), and $Bi_{2-x}Pb_xSr_2Ca_2Cu_3O_{10+\delta}$ ($x = 0.2$ and 0.25) which show the lowest levels of paramagnetic impurities/defects reported to date.

In $YBa_2Cu_3O_7$, for $\mathbf{H} \parallel \mathbf{c}$ as well as $\mathbf{H} \perp \mathbf{c}$, χ increases monotonically with temperature from T_c up to at least 400 K. We find that part but not all of the negative curvature arises from superconducting fluctuation diamagnetism (SFD). The remainder arises from a temperature dependent background; this is likely reflected in the backgrounds of other properties such as the conductivity, which may significantly alter the interpretation of the influence of superconducting fluctuations on these properties. Our analysis is consistent with a superconducting order parameter with s-wave symmetry on each layer, as in the Lawrence-Doniach model. From fits of our new theory to the χ data of $YBa_2Cu_3O_7$, estimates of microscopic parameters were obtained.

By varying the Pb doping level in the $Bi_{2-x}Pb_xSr_2CaCu_2O_{8+\delta}$ ($0.0 \leq x \leq 0.5$) and $Bi_{2-x}Pb_xSr_2Ca_2Cu_3O_{10+\delta}$ ($x = 0.2$ and 0.25) systems, samples were obtained which showed no evidence for magnetic impurities in $\chi(T)$ measurements. For these samples, χ

increased monotonically from T_c up to at least 400 K, with strong negative curvature below ~ 200 K, as in $YBa_2Cu_3O_7$. By fitting the data in the two-dimensional regime with the Lawrence-Doniach theory as modified by Klemm [1990], the negative curvature in $\chi(T)$ for each of these samples is concluded to arise from superconducting fluctuation diamagnetism. The data are consistent with a superconducting order parameter with s-wave symmetry, and indicate that the Bi2212 and Bi2223 are highly two-dimensional, consistent with other measurements on thin films [Kang et al., 1988] and single crystals [Beille et al., 1988; Martin et al., 1989; Palstra et al., 1988a]. The in-plane Ginzburg-Landau coherence lengths $\xi_{ab}(0)$ for Bi2212 (20.4 Å) and Bi2223 (~ 11.8 Å) derived from the fits to the data are similar in magnitude to that (13.6 Å) previously inferred for $YBa_2Cu_3O_7$ [Lee et al., 1989]. Our $\xi_{ab}(0)$ values for Bi2212 and Bi2223 are tentative. The role of the out of plane oxygen ions in the superconductivity of the CuO_2 layers in Bi2223 is not yet clear. Additionally, the explicit fluctuation diamagnetism contributions from the superpair bands in the 2 D regime and the potentially important dynamic effects remain to be included in the theoretical fits to the data.

From the normal state $\chi(T)$ data of $YBa_2Cu_3O_7$, the spin susceptibility χ^{spin} was derived using the orbital susceptibility values for Cu^{+2} ions inferred from the nuclear

resonance measurements of Takigawa et al. [1989], and found to be nearly isotropic, in agreement with those authors. Thus, most of the large anisotropy in χ above ~ 200 K is of orbital origin, arising from the Cu d-orbitals. The anisotropy $\Delta\chi^{VV}$ in the orbital χ found for Cu(2) in the CuO_2 layers of $YBa_2Cu_3O_7$ is about the same as observed for nonmetallic La_2CuO_4 and $Sr_2CuO_2Cl_2$, and for superconducting metallic $La_{1.9}Sr_{0.1}CuO_4$, where the latter three compounds contain CuO_2 layers but no CuO chain layers. This similarity suggests that the local electronic environments around the Cu ions in the CuO_2 layers of all four compounds are similar, despite the fact that two of the compounds exhibit metallic character whereas the other two do not.

We have accomplished some of the goals of our heat capacity C(T) study of high purity $YBa_2Cu_3O_7$. From a determination of the $BaCuO_2$ magnetic impurity phase concentration in our batch of this compound from differential thermal analysis measurements, coupled with analysis of low (> 0.4 K) temperature C(T) measurements in zero and 70 kG applied magnetic fields, we conclude that the Sommerfeld heat capacity coefficient intrinsic to the $YBa_2Cu_3O_7$ phase in our pellet sample is $\gamma(0) \simeq 4.0$ mJ/mole-K^2. The origin of this $\gamma(0)$ is not yet clear. One possibility which is often considered is that this $\gamma(0)$ is an indication that part of the sample does not become superconducting; i.e., $\gamma(0)/\gamma$ is

the normal fraction, where γ is the normal state Sommerfeld coefficient.

It is clear that superconducting fluctuations have a dramatic influence on the thermodynamic and electronic transport properties of the high T_c cuprates in the vicinity of T_c. Heat capacity measurements on single crystals of $YBa_2Cu_3O_7$ near T_c show strong evidence for a nonmean-field shape, attributed to these fluctuations. However, even slight broadening of the superconducting transition, as in most polycrystalline samples of $YBa_2Cu_3O_7$, rapidly smooths out this shape to appear mean-field-like. Indeed, a mean-field-like shape was found for our pellet sample. Utilizing the data and theory, a quantitative estimate of the fluctuation heat capacity was made and found to be significant on the scale of the measurements. A lowest-order attempt was made to extract the mean-field heat capacity in the absence of the fluctuations. We find that the heat capacity jump at T_c, deduced from C(T) data using the conventional entropy balance technique, may be appreciably affected by the presence of the fluctuations.

There have been numerous reports in the literature of anomalies occurring at various temperatures in various measurements of $YBa_2Cu_3O_7$ which have not been confirmed as magnetic or structural transitions by neutron or x-ray scattering techniques. We presented calorimetric evidence

that one such anomaly in the magnetic susceptibility $\chi(T)$ at ~ 310-330 K is a bulk phase transition of some kind. The occurrence of these transitions is highly sample-dependent, and it is not known what characteristics of the samples control their occurrence. In our experiments, for example, we found that the powder sample of $YBa_2Cu_3O_7$ did not show the anomalies at ~ 330 K in C(T) and $\chi(T)$ seen for the pellet sample. Finally, and unexpectedly, our C(T) measurements on the pellet sample of $YBa_2Cu_3O_7$ revealed a surprisingly strong influence of the thermal and/or magnetic field history of the sample. The magnitude of C(T) in both the low (5 - 10 K) and higher (70 - 120 K) T regimes were strongly influenced by the thermal/magnetic field history. The heat capacity jump at T_c and Debye temperature (but not the $\gamma^*(0)$ value) derived from these data were quite different for different experiments, and the shape and size of the 74 K anomaly were also strongly history dependent. These types of effects have been observed in elastic measurements of various types, where it is found that such effects are highly sample dependent. Thus, for example, the heat capacities of some samples of $YBa_2Cu_3O_7$ are highly stable with time and thermal cycling.

The anomaly in C(T) near 74 K and an additional anomaly at 330-350 K are correlated with anomalies in the magnetic properties at similar temperatures. The origins of these anomalies are not known. A hint of a possible phase

transition near 102 K was also observed in our C(T) data. A detailed understanding of these anomalies must await further structural and other measurements.

VII. REFERENCES

R. Ahrens, T. Wolf, H. Wohl, H. Rietschel, and F. Steglish, Physica C 153-155, 1008 (1988).

P. W. Anderson, Science 235, 1196 (1987).

P. W. Anderson and Z. Zou, Phys. Rev. Lett. 60, 132 (1988).

A. G. Aronov, S. Hikami and A. I. Larkin, Phys. Rev. Lett. 62, 965 (1989). Note that these authors assumed N = 1 for Y123 (and hence $\gamma \ll 1$), and took the repeat distance s to be 12 Å (close to the value 11.7 Å used in our fits). While one could modify their theory to include both layers equally by letting $s \to s/2$, or roughly by letting $\gamma \to 1/4$, Fig. 30 shows that those modified parameter values would still be inconsistent with our data.

J. Bardeen, L. N. Cooper, and J. R. Schrieffer, Phys. Rev. 108, 1175 (1957).

W. Bauhofer, W. Biberracher, B. Gegenheimer, W. Joss, R. K. Kremer, Hj. Mattausch, A. Müller, and A. Simon, Phys. Rev. Lett. 63, 2520 (1989).

O. Beckman, L. Lundgren, P. Nordblad, L. Sandlund, P. Svedlindh, T. Lundström, and S. Rundqvist, Phys. Lett. A 125, 425 (1987).

J. G. Bednorz and K. A. Muller, Z. Phys. B 64, 189 (1986).

J. Beille, H. Dupendant, O. Laborde, Y. Lefur, M. Perroux, R. Tournier, Y. F. Yen, J. H. Wang, D. N. Zheng, and Z. Zhao, Physica C 156, 448 (1988).

R. Beyer, S. S. P. Parkin, V. Y. Lee A. I. Nazzal, R. Savoy G. Gorman, T. C. Huang, and S. La Placa, Appl. Phys. Lett. 53, 432 (1988).

S. Bhattacharya, M. J. Higgins, D. C. Johnston, A. J. Jacobson, J. P. Stokes, J. T. Lewandowski, and D. P. Gorshorn, Phys. Rev. B 37, 5901 (1988).

P. Boolchand, R. N. Enzweiler, I. Zitkovsky, J. Wells, W. Bresser, D. McDaniel, R. L. Meng, P. H. Hor, C. W. Chu, and C. Y. Huang, Phys. Rev. Lett. 37, 3766 (1988).

P. Bordet, C. Chaillout, J. Chenavas, J. L. Hodeau, M.

Marezio, J. Karpinski, and E. Kaldis, Nature 334, 596 (1988).

H. R. Brand and M. M. Doria, Phys. Rev. Lett. 61, 480 (1988).

R. A. Butera, Phys. Rev. B 37, 5909 (1988).

R. Calemczuk, E. Bonjour, J. Y. Henry, L. Forro, C. Ayache, M. J. M. Jurgens, J. Rossat-Mignod, B. Barbara, P. Burlet, M. Couach, A. F. Khoder, and B. Salce, Physica C, 153-155, 960 (1988).

R. Caspary, C. D. Bredl, H. Spille, M. Winkelmann, F. Steglich, H. Schmidt, T. Wolf, and R. Flükliger, Physica C 153-155, 876 (1988).

R. J. Cava, B. Batlogg, J. J. Krajewski, L. W. Rupp, L. F. Schneemeyer, T. Siegrist, R. B. VanDover, P. Marsh, W. F. Peck, P. K. Gallagher, S. H. Glarum, J. H. Marshall, R. C. Farrow, J. V. Waszczak, R. Hull, and P. Trevor, Nature 336, 211 (1988).

R. J. Cava, A. Santoro, D. W. Johnson, Jr., W. W. Rhodes, Phys. Rev. B 35, 6716 (1987).

G. Chen and W. A. Goddard III, Science 239, 899 (1988).

S-W. Cheong, S. E. Brown, Z. Fisk, R. S. Kwok, J. D. Thompson, E. Zirngiebl, G. Gruner, D. E. Peterson, G. L. Wells, R. B. Schwarz, and J. R. Cooper, Phys. Rev. B 36, 3913 (1987).

S-W. Cheong, Z. Fisk, J. D. Thompson, J. P. Remeika, and G. Gruner. New Mexico Section Material Research Society Conference, Santa Fe, NM, October (1987) (unpublished).

R. T. Collins, Z. Schlesinger, F. Holtzberg, and C. Feild, Phys. Rev. Lett. 63, 422 (1989).

M. F. Crommie, A. Zettl, T. W. Barbee III, and Marvin L. Cohen, Phys. Rev. B 37, 9734 (1988).

T. R. Dinger, T. K. Worthington, W. J. Gallagher, and R. L. Sandstrom, Phys. Rev. Lett. 58, 2687 (1987).

M. A. Dubson, J. J. Calabrese, S. T. Herbert, D. C. Harris, B. R. Patton, and J. C. Garland, in Novel Superconductivity, ed. S. A. Wolfe and V. Z. Kresin (Plenum, New York, 1987), p. 981.

D. Eckert, A. Junod, T. Graf, and J. Muller, Physica C 153-155, 1038 (1988).

Y. Endoh, K. Yamada, R. J. Birgeneau, D. R. Gabbe, H. P. Jessen, M. A. Kasner, C. J. Peters, P. J. Picone, T. R. Thurston, J. M. Tranquada, G. Shirane, Y. Hidaka, M. Oda, Y. Enomoto, M. Suzuki, and T. Muralami, Phys. Rev. B 37, 7443 (1988).

Y. Enomoto, M. Suzuki, M. Oda and T. Murakami Physica 148B, 408 (1987).

S. Eriksson, L. G. Johansson, L. Börjesson, and M. Kakihana, Physica C 162-164, 59 (1989).

D. E. Farrell, B. S. Chandrasekhar, M. R. DeGuire, M. M. Fang, V. G. Kogan, J. R. Clem, and D. K. Finnemore, Phys. Rev. B 36, 4025 (1987).

D. E. Farrell, S. Bonham, J. Foster, Y. C. Chang, P. Z. Jiang, K. G. Vandervoot, D. J. Lam, and V. G. Kogan, Phys. Rev. Lett. 63, 782 (1989).

A. T. Fiory, A. F. Hebard, P. M. Mankiewich, and R. E. Howard, Phys. Rev. Lett. 61, 1419 (1988).

R. A. Fisher, J. E. Gordon, S. Kim, N. E. Phillips, and A. M. Stacy, Physica C 153-155, 1092 (1988a).

R. A. Fisher, J. E. Gordon, and N. E. Phillips, J. Supercond. 1, 231 (1988b).

P. Fisher, J. Karpinski, E. Kaladis, E. Jilek, and S. Rusiecki, Solid State Commun. 69, 531 (1989).

L. Forro, J. Y. Henry, C. Ayache, and P. Stamp, Phys. Lett. A 128, 283 (1988).

K. Fossheim, O. M. Nes, T. Laegreid, C. N. W. Darlington, D. A. O'Connor, and C. E. Gough, Int. J. of Mod. Phys. B 5, 635 (1988).

P. P. Freitas, C. C. Tsuei, and T. S. Plaskett, Phys. Rev. B 36, 833 (1987).

T. A. Friedmann, J. P. Rice, J. Giapintzakis, and D. M. Ginsberg, Phys. Rev. B. 39, 4258 (1989).

K. Fukuda, S. Shamoto, M. Sato, and K. Oka, Solid State Commun. 65, 1323 (1988).

P. L. Gammel, L. F. Schneemeyer, J. V. Waszczak, and D. L. Bishop, Phys. Rev. Lett. 61, 1666 (1988).

V. L. Ginzburg and L. D. Landau, Zh. Eksperim. i Teor. Fiz. 20, 1064 (1950).

N. Goldenfeld, P. D. Olmsted, T. A. Friedmann, and D. M. Ginsberg, Solid State Commun. 65, 465 (1988).

J. P. Gollub, M. R. Beasley, R. S. Newbower, and M. Tinkham, Phys. Rev. Lett. 22, 1288 (1969).

E. S. R. Gopal, Specific heat at low temperatures (Plenum Press, New York, 1966) p. 102.

J. E. Gordon, M. L. Tan, R. A. Fisher, and N. E. Phillips, Solid State Commun. 69, 625 (1989).

L. P. Gorkov, Sov. Phys. JETP 9, 1364 (1959).

K. E. Gray, R. T. Kampwirth, and D. E. Farrell, Phy. Rev. B 41, 819 (1988).

S. J. Hagen, T. W. Jing, Z. Z. Wang, J. Horvath, and N. P. Ong, Phys. Rev. B 37, 7928 (1988a).

S. J. Hagen, Z. Z. Wang, and N. P. Ong, Phys. Rev. B 38, 7137 (1988b).

A. W. Hewat, E. A. Hewat, J. Brynestad, H. A. Mook, and E. D. Specht, Physica C 152, 438 (1988).

D. G. Hinks, B. Dabrowski, J. D. Jorgensen, A. W. Mitchell, D. R. Richards, S. Pei, and D. Shi, Nature 333, 836 (1988).

S. E. Inderhees, M. B. Salamon, N. Goldenfeld, J. P. Rice, B. G. Pazol, D. M. Ginsberg, J. Z. Liu, and G. W. Crabtree. Phys. Rev. Lett. 60, 1178 (1988); (Erratum) ibid. 60, 2445 (1988).

M. Ishikawa, Y. Nakazawa, T. Takabatake, A. Kishi, R. Kato, and A. Maesono, Solid State Commun. 66, 201 (1988).

Y. Iye, T. Tamegai, and T. Sakakibara, Physica C 153-155, 26 (1988).

Y. Iye, T. Tamegai, H. Takeya, and H. Takei, Jpn. J. Appl. Phys. 26, L1057 (1987).

D. C. Johnston, Phys. Rev. Lett. 62, 957 (1989).

D. C. Johnston, A. J. Jacobson, J. M. Newsam, J. T. Lewandowski, D. P. Goshorn, D. Xie, and W. B. Yelon, Chemistry Society Symposium Series, 351, Chapter 14, (American Chemical Society, Washington, D. C, 1987).

D. C. Johnston, S. K. Sinha, A. J. Jacobson, and J. M. Newsam, Physica C 153-155, 572 (1988).

A. Junod, D. Eckert, G. Triscone, V. Y. Lee, and J. Muller, Physica C 159, 215 (1989).

A. Junod, A. Bezinge, and J. Muller, Physica C 152, 50 (1988).

J. H. Kang, R. T. Kampwirth, and K. E. Gray, Appl. Phys. Lett. 52, 2080 (1988).

K. Kanoda, T. Kawagoe, M. Hasumi, T. Takahashi, S. Kagoshima, and T. Mizoguchi, J. Phys. Soc. Jpn. 57, 1554 (1988a).

K. Kanoda, T. Takahashi, T. Kawagoe, T. Mizoguchi, M. Hasumi, and S. Kagoshima, Physica C 153-155, 749 (1988b).

M. Kato, Y. Maeno, and T. Fujita, Physica C 152, 116 (1988).

R. A. Klemm, Ph. D. Thesis, Harvard University, unpublished (1974).

R. A. Klemm, Phys. Rev. B 41, 2073 (1990).

R. A. Klemm, M. R. Beasley, and A. Luther, Phys. Rev. B 8, 5072 (1973).

R. A. Klemm, A. Luther, and M. R. Beasley, Phys. Rev. B 12, 877 (1975).

S. Koyama, U. Endo, and T. Kawai, Jpn. J. Appl. Phys. 27, L1861 (1988).

V. Z. Kresin, Phys. Rev. B 35, 8716 (1987).

L. Krusin-Elbaum, R. L. Greene, F. Holtzberg, and A. P. Malozemoff, Phys. Rev. Lett. 62, 217 (1989).

R. Kuentzler, Y. Dossmann, S. Vilminot, and S. El Hadigui, Solid State Commun. 65, 1529 (1988).

J. Kurkijärvi, V. Ambegaokar, and G. Eilenberger, Phys. Rev. B 5, 868 (1972).

T. Laegreid, K. Fossheim, E. Sandvold, and S. Julsrud, Nature 330, 637 (1987).

T. Laegreid, K. Fossheim, O. Traetteberg, E. Sandvold, and S. Julsrud, Physica C 153-155, 1026 (1988).

T. Laegreid, P. Tuset, O. M. Nes, M. Slaski, and K. Fossheim, Physica C 162-164, 490 (1989).

W. E. Lawrence and S. Doniach, Proc. Twelfth Int. Conf. on Low Temp. Phys., Kyoto, ed. E. Kanda (Keigaku, Tokyo, 1971), p. 361.

P. A. Lee and M. G. Payne, Phys. Rev. Lett. 26, 1537 (1971).

W. C. Lee, J. H. Cho, and D. C. Johnston, unpublished (1990a).

W. C. Lee and D. C. Johnston, Phys. Rev. B 41, 1904 (1990b).

W. C. Lee and D. C. Johnston, unpublished (1990c).

W. C. Lee, R. A. Klemm, and D. C. Johnston, Phys. Rev. Lett. 63, 1012 (1989).

W. C. Lee, K. Sun, L. L. Miller, D. C. Johnston, C. A. Swenson, R. A. Klemm, S. Kim, R. A. Fisher, and N. E. Phillips, unpublished (1990d).

T. C. Leung, X. W. Wang, and B. N. Harmon, Phys. Rev. B 37, 384 (1988).

O. V. Lounasmaa, Phys. Rev. 128, 1136 (1962).

A. Lusnikov, L. L. Miller, R. W. McCallum, S. Mitra, W. C. Lee, and D. C. Johnston, J. Appl. Phys. 65, 3136 (1989).

Y. Maeno, T. Tomita, M. Kyogoku, S. Awaji, A. Aoki, K. Hoshino, A. Minami, and T. Fujita, Nature 328, 512 (1987).

K. Maki and H. Takayama, J. Low Temp. Phys. 5, 313 (1971).

B. Marosin, D. S. Ginley, P. F. Hiava, M. J. Carr, R. J. Baughman, J. E. Schirber, E. L. Venturini, and J. F. Kwak, Physica C 152, 413 (1988).

S. Martin, A. T. Fiory, R. M. Fleming, G. P. Espinosa, and A. S. Cooper, Phys. Rev. Lett. 62, 677 (1989).

Y. Matsui, S. Takekawa, H. Nozaki, A. Umezono, E. T. Muromachi, and S. Horiuchi, Jpn. J. Appl. Phys. 27, L1241 (1988).

R. W. McCallum, J. Metals, 41, 50 (1989).

T. R. McGuire, T. R. Dinger, P. J. P. Freitas, W. J. Gallagher, T. S. Plaskett, R. L. Sandstrom, and T. M. Shaw, Phys. Rev. B 36, 4032 (1987).

M. Miljak, G. Collin, and A. Hamzic, J. Mag. Mag. Mat. 76-77, 609 (1988).

M. Miljak, G. Collin, A. Hamzic and V. Zlatic, Europhys. Lett. 9, 723 (1989).

L. L. Miller, X. L. Wang, S. X. Wang, C. Stassis, D. C. Johnston, J. Faber, Jr., and C. K. Loong, Phys. Rev. B 41, 1921 (1990).

S. Mitra, J. H. Cho, W. C. Lee, D. C. Johnston, and V. G. Kogan, Phys. Rev. B 40, 2674 (1989).

P. Muzikar, Phys. Rev. Lett. 61, 479 (1988).

S. von Molnar, A. Torressen, D. Kaiser, F. Holtzberg, and T. Penny, Phys. Rev. B 37, 3762 (1988).

K. Nakao, N. Miura, K. Tatuhara, H. Takeya, and H. Takei, Phys. Rev. Lett. 63, 97 (1989).

M. J. Naughton, R. C. Yu, P. K. Davies, J. E. Fisher, R. V. Chamberlin, Z. Z. Wang, T. W. Jing, N. P. Ong, and P. M. Chaikin, Phys. Rev. B 38, 9280 (1988).

N. Nücker, J. Fink, J. C. Fuggle, P. J. Durham, and W. M. Temmerman, Phys. Rev. B 37, 5158 (1988).

B. Oh, K. Char, A. D. Kent, M. Naito, M. R. Beasley, T. H. Geballe, R. H. Hammond, A. Kapitulnik, and J. M. Graybeal, Phys. Rev. B 37, 7861 (1988).

N. P. Ong, Z. Z. Wang, S. Hagen, T. W. Jing, J. Clayhold, and J. Horvath, Physica C 153-155, 1072 (1988).

Y. Le Page, T. Siegrist, S. A. Sunshine, L. F. Schneemeyer, D. W. Murphy, S. M. Zahurak, J. V. Waszczak, W. R. McKinnon, J. M. Tarascon, G. W. Hull, and L. H. Greene, Phys. Rev. B 36, 3617 (1987).

T. T. M. Palstra, B. Batlogg, L. F. Schneemeyer, R. B. van Dover, and J. V. Waszczak. Phys. Rev. B 38, 5102 (1988a).

T. T. M. Palstra, B. Batlogg, L. F. Schneemeyer, and J. V. Waszczak, Phys. Rev. Lett. 61, 1662 (1988b).

B. Patton, V. Ambegaoker, and J. W. Wilkins, Solid State Commun. 7, 1287 (1969).

T. Penney, S. von Molnar, D. Kaiser, et al., Phys. Rev. B 38, 2918 (1988).

C. H. Pennington, D. J. Durand, C. P. Slichter, J. P. Rice, E. D. Bukowski, and D. M. Ginsberg, Phys. Rev. B 39, 2902 (1989).

Norman E. Phillips, R. A. Fisher, J. E. Gordon, and S. Kim, Physica C 162-164, 1651 (1989).

Norman E. Phillips, R. A. Fisher, J. E. Gordon, S. Kim, and A. M. Stacy, unpublished (1990).

N. E. Phillips, R. A. Fisher, S. E. Lacy, C. Marcenat, J. A. Olsen, W. K. Ham, A. M. Stacy, J. E. Gordon, and M. L. Tan, Physica 148B, 360 (1987).

A. Porch, J. R. Waldram, and L. Cohen, J. Phys. F 18, 1547 (1988).

R. E. Prange, Phys. Rev. B 1, 2349 (1970).

P. Prelovsek, T. M. Rice, and F. C. Zhang, J. Phys. C 20, L229 (1987).

M. E. Reeves, S. E. Stupp, T. A. Friedmann, F. Slakey, D. M. Ginsberg, and M. V. Klein, Phys. Rev. B 40 4573 (1989).

J. P. Rice, B. G. Pazol, D. M. Ginsberg, T. J. Moran, and M. B. Weissman, J. Low Temp. Phys. 72, 345 (1988).

M. B. Salamon, S. E. Inderhees, J. P. Rice, B. G. Pazol, D. M. Ginsberg, and N. Goldenfeld, Phys. Rev. B 38, 885 (1988).

A. Schmid, Phys. Rev. 180, 527 (1969).

J. R. Schrieffer, X. G. Wen, and S. C. Zhang, Mod. Phys. Lett. B 2, 935 (1988).

P. W. Selwood, Magnetochemistry (Interscience, New York, 1956), 2nd edition, p. 78.

F. Sharifi, J. Giapintzakis, D. M. Ginsberg, and D.J. Van Harlingen, Physica C 161, 555 (1989).

R. P. Sharma, L. E. Rehn, P. M. Baldo, and J. Z. Liu, Phys. Rev. Lett. 62, 2869 (1989).

G. Shirane, Y. Endoh, R. J. Birgeneau, M. A. Kasner, Y. Hidaka, M. Oda, M. Suzuki, and T. Murakami, Phys. Rev. Lett. 59, 1613 (1987).

S. Solin, N. Garcia, S. Vieira, and M. Hortal, Phys.Rev. Lett. 60, 744 (1988).

C. Stassis, B. N. Harmon, T. Freltoft, G. Shirane, S. K. Sinha, K. Yamada, Y. Endoh, Y. Hidaka, and T. Murakami, Phys. Rev. B 38, 9291 (1988).

E. Stupp and D. M. Ginsberg, Physica C 158, 299 (1989).

M. A. Subramanian, J. B. Parise, J. C. Calabrese, C. C. Torardi, J. Gopalakrishnan, and A. W. Sleight, J. Solid State Chem. 77, 192 (1988).

K. Sun, L. L. Miller, and D. C. Johnston, unpublished (1990).

L. Sun, Y. Wang, H. Shen, and X. Cheng, Phys. Rev. Lett. 38, 5114 (1988).

J. Z. Sun, D. J. Webb, M. Naito, K. Char, M. R. Beasley, R. H. Hammond, and Kapitulnik, Phys. Rev. Lett. 58, 1574 (1987).

C. A. Swenson, R. W. McCallum, and K. No, Phys. Rev. B 40, 8861 (1989).

M. Takigawa, P. C. Hammel, R. H. Heffner, Z. Fisk, J. L. Smith, and R. B. Schwarz, Phys. Rev. B 39, 300 (1989).

J. M. Tarascon, P. Barboux, P. F. Miceli, L. H. Greene, G. W. Hull, M. Elibschutz, and S. A. Sunshine, Phys. Rev. B 37, 7458 (1988a).

J. M. Tarascon, Y. Le Page, P. Barboux, B. G. Bagley, L. H. Greene, W. R. McKinnon, G. W. Hull, M. Giroud, and D. M. Hwang, Phys. Rev. B 37, 9382 (1988b).

J. M. Tarascon, W. R. McKinnon, L. H. Greene, G. W. Hull, and E. M. Vogel, Phys. Rev. B 36, 226 (1987).

M. Tinkham, Introduction to superconductivity (McCraw - Hill, Tokyo, Japan, 1975) p. 37.

Y. Tokura, H. Takagi, and S. Uchida, Nature 337, 345 (1989).

Y. Tokura, J. B. Torrance, T. C. Huang, and A. I. Nazzal, Phys. Rev. B 38, 7156 (1988).

C. C. Torardi, M. A. Subramanian, J. C. Calabrese, J. Gopalakrishinan, E. M. McCarron, K. J. Morrissey, T. R. Askew, R. B. Flippen, U. Chowdhry, and A. W. Sleight, Phys. Rev. B 38, 225 (1988a).

C. C. Torardi, M. A. Subramanian, J. C. Calabrese, J. Gopalakrishinan, E. M. McCarron, K. J. Morrissey, T. R. Askew, R. B. Flippen, U. Chowdhry, and A. W. Sleight, Science 240, 631 (1988b).

J. B. Torrance, Y. Tokura, S. J. LaPlaca, T. C. Huang, R. J. Savoy, and A. I. Nazzal, Solid State Commun. 66, 703 (1988).

S. W. Tozer, A. W. Kleinsasser, T. Penny, D.Kaiser, and F. Holtzberg, Phys. Rev. Lett. 59, 1768 (1987).

J. M. Tranquada, A. I. Goldman, A. R. Moodenbaugh, G. Shirane, S. K. Sinha, A. J. Jacobson, and J. T. Lewandowski, Phys. Rev. B 37, 519 (1988).

Y. J. Uemura, V. J. Emery, A. R. Moodenbaugh, M. Suenaga, D. C. Johnston, A. J. Jacobson, J. T. Lewandowski, J. H. Brewer, R. F. Kiefl, S. R. Kreitzman, G. M. Luke, T. Riseman, C. E. Stronach, W. J. Kossler, J. R. Kempton, X. H. Yu, D. Opie, and H. E. Schone, Phys. Rev. B 36, 909 (1988).

D. Vaknin, E. Caignol, P. K. Davies, J. E. Fisher, D. C. Johnston, and D. P. Goshorn, Phys. Rev. B 39, 9122 (1989).

D. Vaknin, S. K. Sinha, C. Stassis, L. L. Miller, and D. C. Johnston, Phy. Rev. B 41, 1926 (1990).

C. M. Varma, S. Schmitt-Rink, and E. Abrahams, Solid State Commun. 62, 681 (1987).

F. Vidal, J. A. Veira, J. Maza, F. Miguelez, E. Moran, and M. A. Alario, Solid State Commun. 66, 421 (1988).

R. E. Walstedt, W. W. Warren, Jr., R. F. Bell, G. F. Brennert, G. P. Espinosa, R. J. Cava, L. F. Schneemeyer, and J. V. Waszczak, Phys. Rev. B 38, 9299 (1988).

Z. Z. Wang, J. Clayhold, N. P. Ong, J. M. Tarascon, L. H. Greene, W. R. McKinnon, and G. W. Hull, Phys. Rev. B 36, 7222 (1987).

W. W. Warren, Jr., R. E. Walstedt, G. F. Brennert, R. J. Cava, R. Tycko, R. F. Bell, and G. Dabbagh, Phys. Rev. Lett. 62, 1193 (1989).

U. Welp, W. K. Kwok, G. W. Crabtree, K. G. Vandervoot, and J. Z. Liu, Phys. Rev. Lett. 62, 1908 (1989).

M. K. Wu, J. R. Ashburn, C. J. Torng, P. H. Hor, R. L. Meng, L. Gao, Z. J. Huang, Y. Q. Wang, and C. W. Chu, Phys. Rev. Lett. 58, 908 (1987).

G. Xiao, M. Z. Cieplak, D. Musser, A. Gavrin, F. H. Streitz, C. L. Chien, J. H. Rhyne, and J. A. Gottas, Nature 332, 238 (1988).

Y. Yamaguchi, M. Tokumoto, S. Waki, Y. Nakagawa, and Y. Kimura, J. Phys. Soc. Jpn. 58, 2256 (1989).

Y. Yeshurun and A. P. Malozemoff, Phys. Rev. Lett. 60, 2202 (1988).

T. Yuen, C. L. Lin, J. E. Crow, G. N. Myer, R. E. Salamon, P. Schlottman, N. Bykovetz, and W. N. Herman, Phys. Rev. Lett. 37, 3770 (1988).

J. M. Ziman, Principles of the Theory of Solids (Cambridge university press, England, 1972), 2nd edition, Chap. 9.6 and 9.7.

VIII. APPENDIX

Compound	Space Group and Lattice Parameters(Å)	T_c(K)	Reference
$Ba_{0.6}K_{0.4}BiO_3$	$Pm\bar{3}m$ a = b = c = 4.293	27	Hinks et al., 1988
$La_{1.85}Sr_{0.15}CuO_4$	I4/mmm a = 3.779 c = 13.226	37	Cava et al., 1987
$Nd_{1.85}Ce_{0.15}CuO_4$	I4/mmm a = 3.95 c = 12.07	24	Tokura et al., 1989
$YBa_2Cu_3O_7$	Pmmm a = 3.827 b = 3.877 c = 11.708	91	Le Page et al., 1987
$YBa_2Cu_4O_8$	Cmmm a = 3.841 b = 3.872 c = 27.240	80	Fisher et al., 1989
$Y_2Ba_4Cu_7O_{14}$	Cmmm a = 3.851 b = 3.869 c = 50.290	40	Bordet et al., 1988
$Pb_2Sr_2(Ca,Y)Cu_3O_8$	Cmmm a = 5.435 b = 5.463 c = 15.817	80	Cava et al., 1988

$Bi_2Sr_2CuO_6$	I4/mmm a = 3.810 c = 24.607	6	Torrance et al., 1988
$Bi_2Sr_2CaCu_2O_8$	I4/mmm a = 3.812 c = 30.66	85	Tarascon et al., 1988b
$Bi_2Sr_2Ca_2Cu_3O_{10}$	P4/mmm a = 5.396 c = 37.180	110	Koyama et al., 1988
$TlBa_2CuO_5$	P4/mmm a = 3.869 c = 9.694	-	Beyer et al., 1988
$TlBa_2CaCu_2O_7$	P4/mmm a = 3.857 c = 12.754	103	Marosin et al., 1988
$TlBa_2Ca_2Cu_3O_9$	P4/mmm a = 3.853 c = 15.913	110	Subramanian et al., 1988
$Tl_2Ba_2CuO_6$	I4/mmm a = 3.866 c = 11.620	90	Torardi et al., 1988a
$Tl_2Ba_2CaCu_2O_8$	I4/mmm a = 3.856 c = 29.260	99	Hewat et al., 1988
$Tl_2Ba_2Ca_2Cu_3O_{10}$	I4/mmm a = 3.850 c = 35.880	125	Torardi et al., 1988b

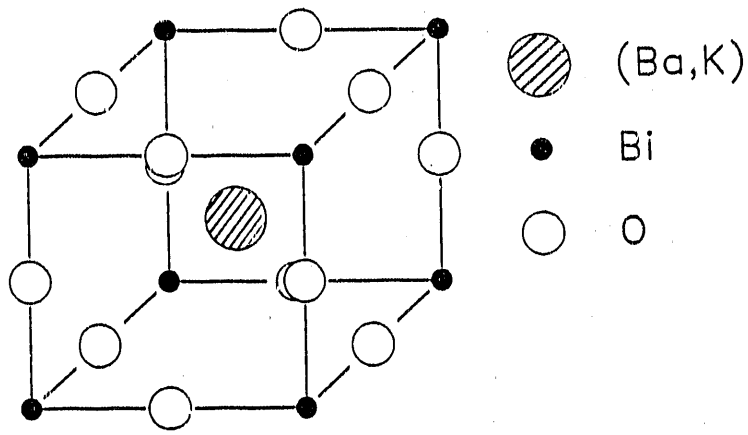

$Ba_{0.6}K_{0.4}BiO_3$

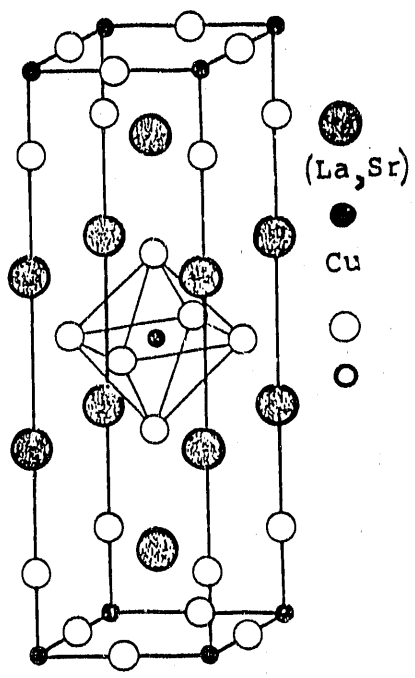

$La_{1.85}Sr_{0.15}CuO_4$

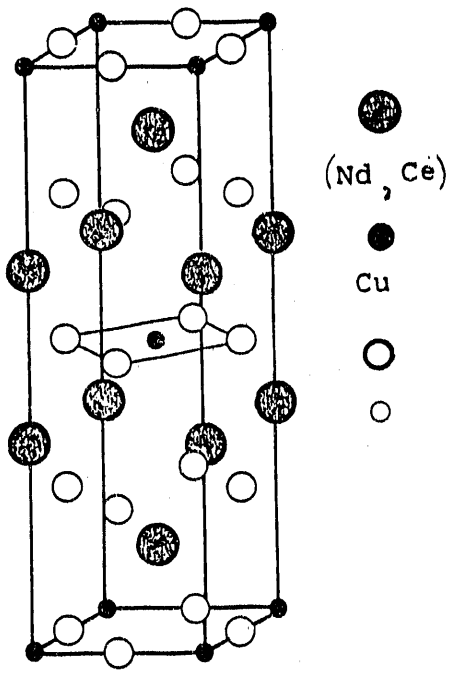

$Nd_{1.85}Ce_{0.15}CuO_4$

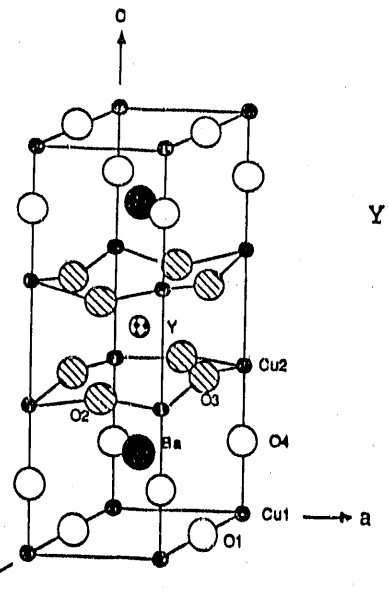

$YBa_2Cu_3O_7$

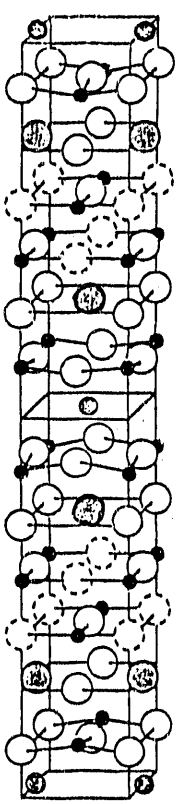

Ba
Y
Cu
O
vacancy

$YBa_2Cu_4O_8$

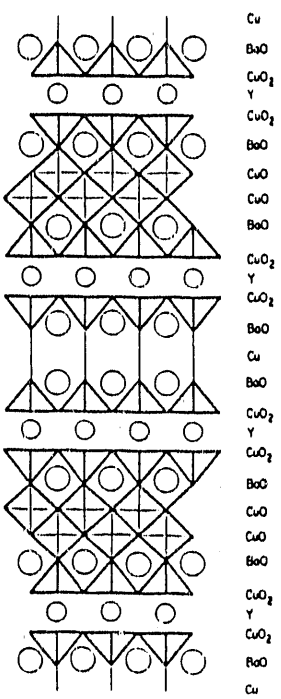

$Y_2Ba_4Cu_7O_{14}$

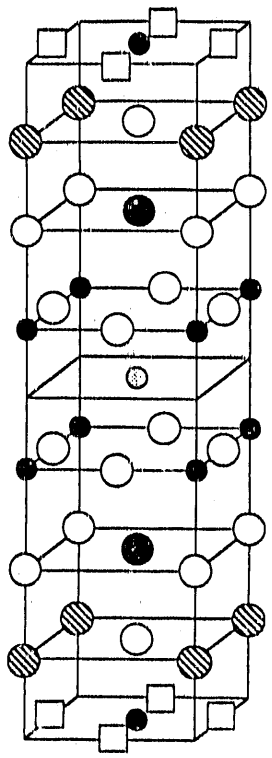

Pb Cu
Sr O
Ca,Y vacancy

$Pb_2Sr_2(Ca,Y)Cu_3O_8$

Bi Ca
Sr Cu O

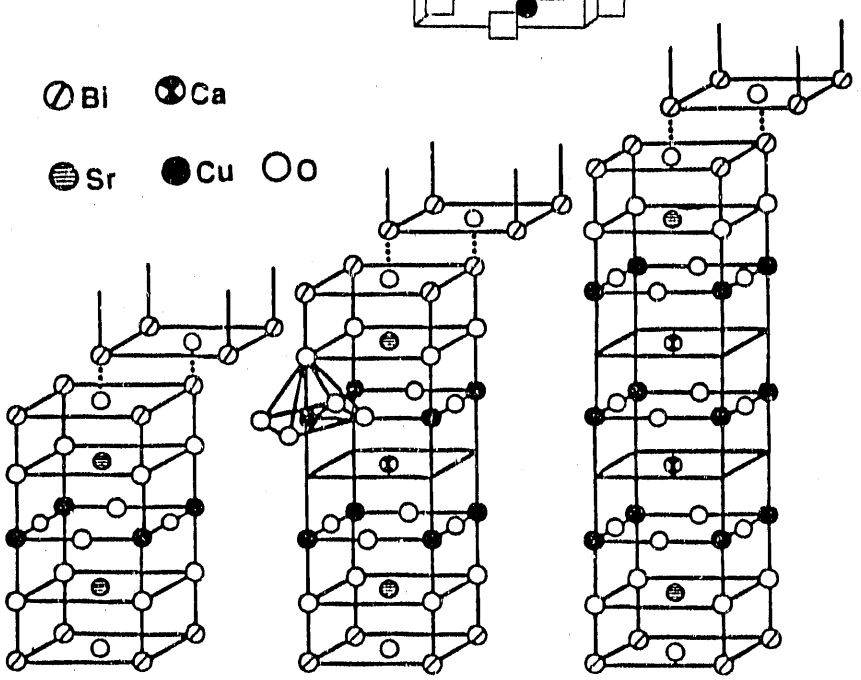

$Bi_2Sr_2CuO_6$ $Bi_2Sr_2CaCu_2O_8$ $Bi_2Sr_2Ca_2Cu_3O_{10}$

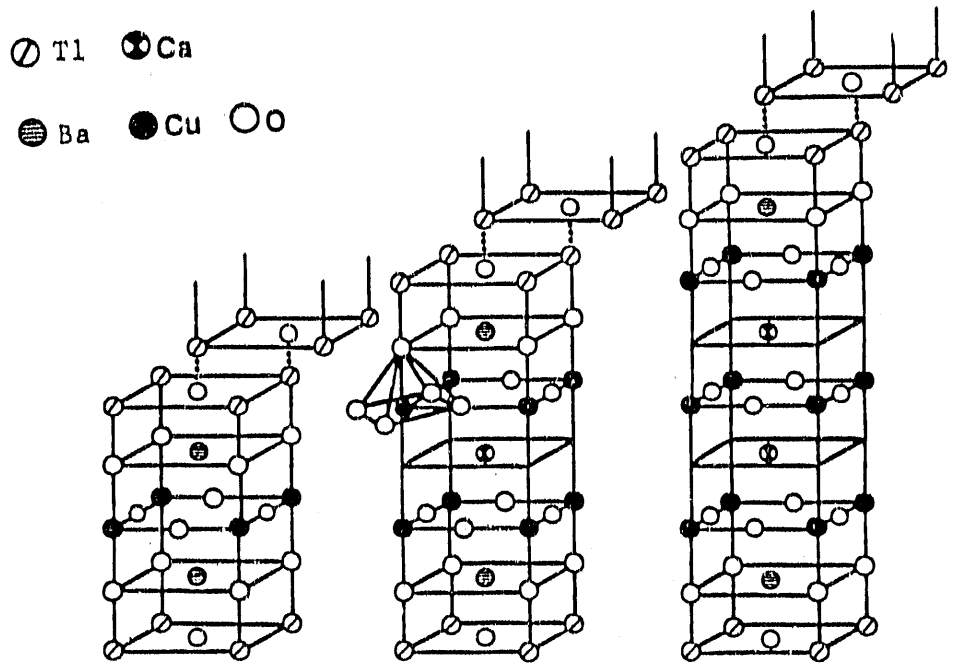

$Tl_2Ba_2CuO_6$ $Tl_2Ba_2CaCu_2O_8$ $Tl_2Ba_2Ca_2Cu_3O_{10}$

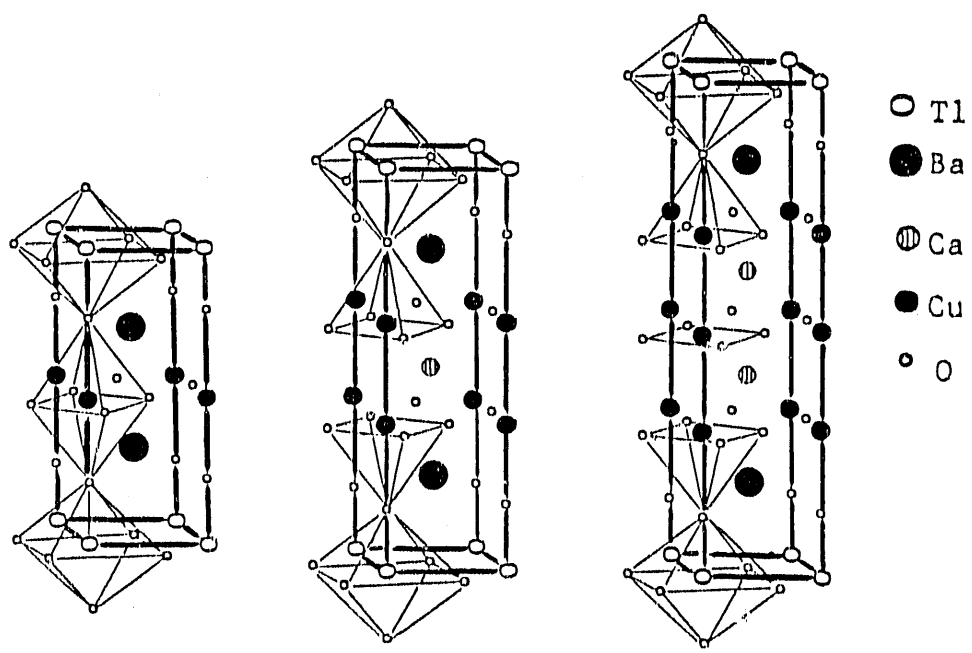

$TlBa_2CuO_5$ $TlBa_2CaCu_2O_7$ $TlBa_2Ca_2Cu_3O_9$

IX. ACKNOWLEDGMENTS

I would like to express my deepest appreciation to my advisor Prof. David C. Johnston for his guidance, encouragements throughout this work.

I also extend my thanks to Dr. Richard A. Klemm for his theoretical contributions and helpful discussions; to Prof. Douglas K. Finnemore and Prof. Bruce N. Harmon for their encouragements throughout this research; to Prof. Clayton A. Swenson for numerous advices and discussions throughout specific heat measurements in Ames; to Dr. Norman E. Phillips and Dr. Robert A. Fisher for arranging me to do the specific heat measurements at Berkeley; J. H. Cho for providing one of the Bi2223 samples.

Finally, I would like to extend many thanks to my wife Moonja Jeong, who stayed too far away throughout my and her whole graduate careers, for her patience. Without her consistent encouragement and patience this work could never have been possible.

This work was performed at Ames Laboratory under contract no. W-7405-Eng-82 with the U. S. Department of Energy. The United States government has assigned the DOE report number IS-T 1448 to this thesis.

THIS THESIS IS DEDICATED TO MY WIFE AND OUR FIRST BABY.

END

DATE FILMED

11 / 1 / 90